INVESTIGATING THE VARIATIONS IN DEPOSITIONAL FACIES BY INVESTIGATING THE ACCURACY OF THE NEURAL NETWORK MODEL WITHIN THE ST. LOUIS LIMESTONE, KEARNY COUNTY, KANSAS

By

CHANCE REECE

B.S., Kansas State University, 2014

A THESIS

Submitted in partial fulfillment of the requirements for the degree

MASTER OF SCIENCE

Department of Geology
College of Arts and Sciences

KANSAS STATE UNIVERSITY
Manhattan, Kansas

2016

Approved by:

Major Professor
Dr. Matt Totten

Copyright

Abstract

The Mississippian-aged St. Louis Limestone has been a major producer of oil, and natural gas for years in Kearny County, Kansas. Since 1966 two major fields in the County, the Lakin, and Lakin South fields, have produced over 4,405,800 bbls of oil. The St. Louis can be subdivided into six different depositional facies, all with varying lithologies and porosities. Only one of these facies is productive, and the challenge of exploration in this area is the prediction of the productive facies distribution.

A previous study by Martin (2015) used a neural network model using well log data, calibrated with established facies distributed within a cored well, to predict the presence of these facies in adjacent wells without core. It was assumed that the model's prediction accuracy would be strongest near the cored wells, with increasing inaccuracy as you move further from the cored wells used for the neural network model.

The aim of this study was to investigate the accuracy of the neural network model predictions. Additionally, is the greater accuracy closest to the cored wells used to calibrate the model, with a corresponding decrease in predictive accuracy as you move further away? Most importantly, how well did the model predict the primary producing unit (porous ooid grainstone) within the St. Louis Limestone? The results showed that the neural network was not completely reliable in predicting total facies distribution. This can be attributed to many different inefficiencies in the data, including different resolutions between cuttings data and well logs, limited well cuttings available, and missing cuttings from the wells that were observed. Relating the neural network predictions to actual well productivity validates the neural network's ability to predict the producing facies. There are also instances of the productive facies being present

when not predicted. This is likely a function of different facies thickness in these wells from the cored wells used to calibrate the model, rather than distance from the cored well.

Table of Contents

List of Figures

List of Tables

Acknowledgements

I would first like to thank my committee members Dr. Chaudhuri, and Dr. Raef. Their help in answering my various questions along with giving great advice has been much appreciated and beneficial.

Secondly I would like to thank the Kansas Geologic Survey for making available all the necessary items I needed to complete my research. Also the Kansas State University Geology department for providing all the resources needed to conduct this research.

A lot of thanks to my parents for all of the support, and encouragement they have given me over the years. Lastly I would like to thank my advisor Dr. Totten. I could never have asked for a better mentor, and teacher who has always been there to help with anything when I needed it.

Chapter 1 - Introduction

The early beginnings of the Kansas petroleum industry can be traced back to the early 1850's (Skelton, 2015). During this time oil was recovered from crevices seen in sandstone outcrops in the eastern portion of the state. Since then the industry has grown tremendously from oozing outcrops to deeply drilled reservoirs and even horizontally targeted thin shale beds. Despite the fact that exploration for petroleum has been around for many years there still remains a tremendous amount of reserves yet to be discovered. Approximately 400 million barrels in proven reserves exist in Kansas according to the Kansas Crude Oil Proved Reserves (2015). That ranks Kansas 12th in the U.S. in proven reserves. Many of these reserves along with much of the petroleum that has already been extracted have come from the carbonate reservoirs of the Mississippian aged system. This Mississippian system is a major target in petroleum drilling around the state, especially in Kearny County, Kansas. In Kearny County there is one unit within the Mississippian that has been an important producer of oil, and natural gas for years, the St. Louis Limestone

Study Area

Kearny County is located in the southwestern portion of Kansas. The county lays within the south-central portion of the Hugoton Embayment lying west of the Central Kansas Uplift, and north of the Anadarko Basin (Figure 1).

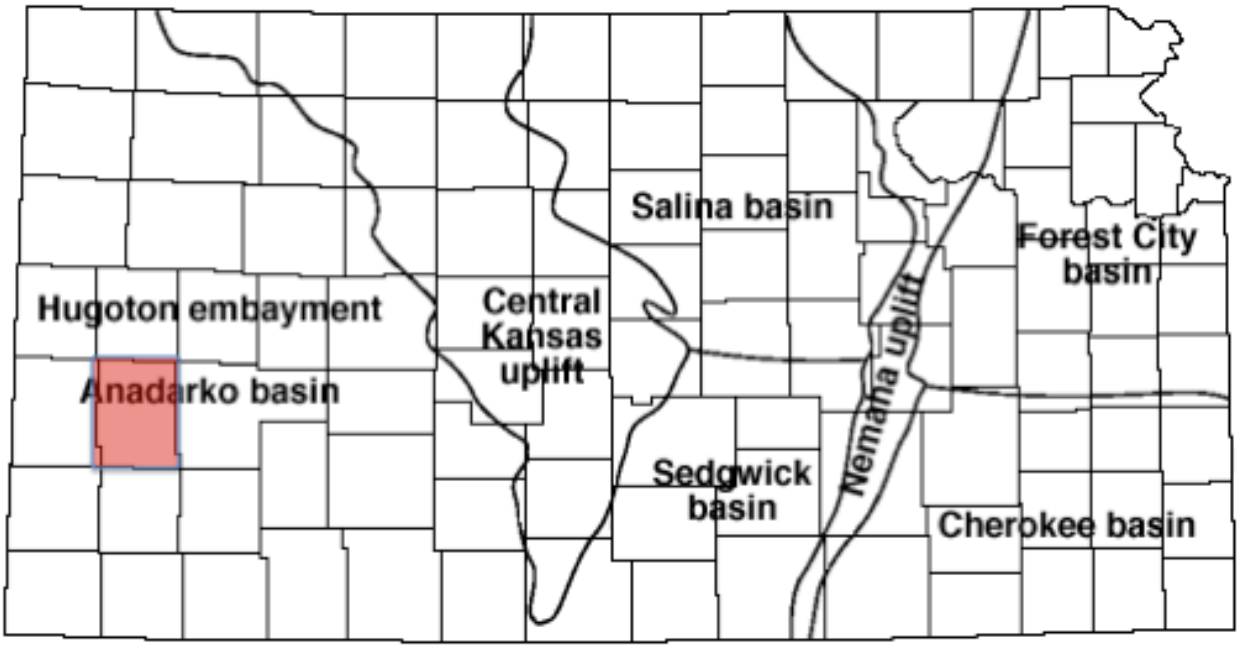

Figure 1. Kearny County in red (Modified from Baars et al, 1989).

The Central Kansas uplift separates the Hugoton embayment from the two other major basins in Kansas, the Salina and Sedgwick basins (Goebel, 1968).

The main focus of this study concentrates on two fields located within the southernmost portion of Kearny County. Kearny is part of the large Hugoton shallow gas area, with various scattered fields that have primarily produced oil over the years. The two fields that will be investigated in this study are the Lakin, and Lakin South fields in the southernmost part of the county (Figure 2).

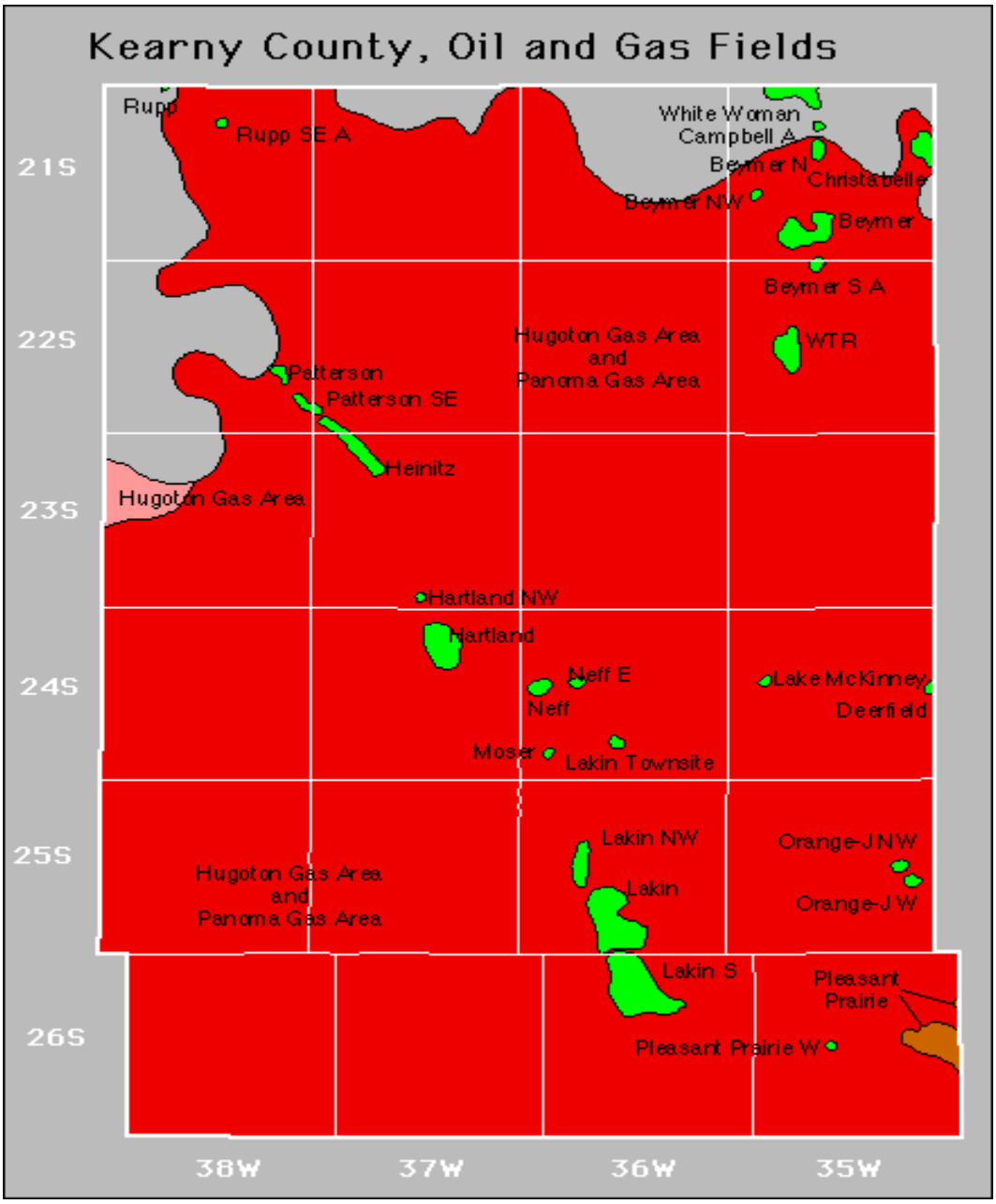

Figure 2. Showing the Lakin, and Lakin South fields located in the southern portion of Kearny County (Kearny County, Oil and Gas Fields, Kansas Geologic Survey, 2015).

These two fields have been active since 1966, producing a lucrative 4,405,741 (bbls), although they have experienced a significant decline in production within the past two years. The main unit that these fields produce from is the carbonate-rich Mississippian, found at depths of around 4,800 feet.

Geologic Setting

During Mississippian time period Kansas was mostly covered by a shallow inland sea with shoreline to the north-northeast, and open ocean to the south towards the Oklahoma pan handle and west Texas (Figure 3).

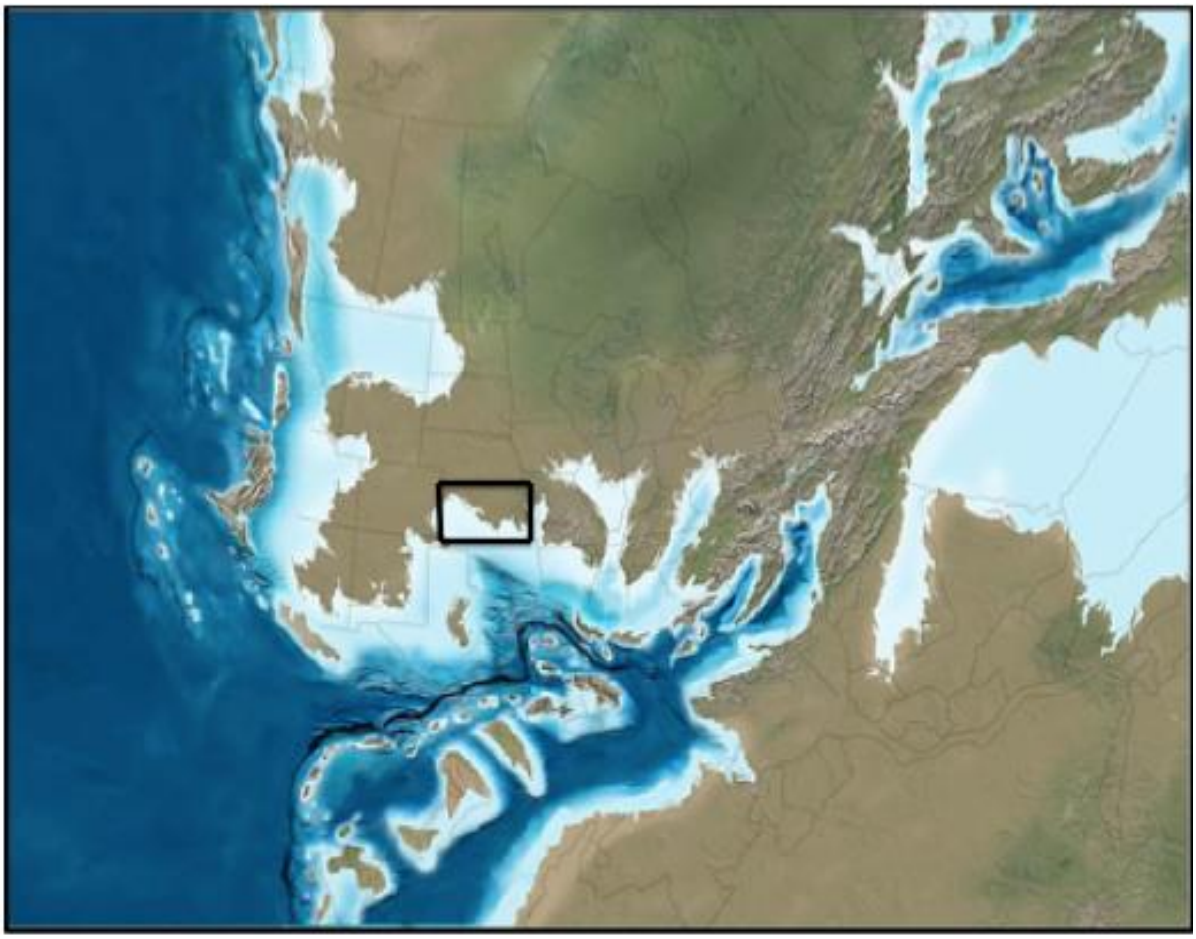

Figure 3. View of Kansas, outlined in black, during the Mississippian time period (Modified from Evans and Newell, 2013).

During this time, Mississippian sediments were deposited, creating shallow-marine limestones, cherts, and cherty limestones (Evans and Newell, 2013). The upper most portion of the Mississippian is an erosional karst unit overlain by the regional sub-Pennsylvanian unconformity according to Montgomery and Frans (2000). During the Mississippian period, a combination of

numerous factors such as global paleoclimate, global sea level change, and geochemical influences, along with the best possible regional paleogeographic and tectonic conditions, resulted in extensive deposition of marine oolitic limestones across the continent of North America (Lianshuang and Carr, 2005).

Stratigraphy

Mississippian rocks are found in the subsurface throughout Kansas, with the exceptions of the Central Kansas uplift, the Nemaha anticline, and parts of the Cambridge arch. In Kansas, the Upper Mississippian Series is primarily composed of limestone and dolomite beds, with interbedded shales and sandstones, and minor amounts of chert (Goebel, 1968). The maximum thickness of the Mississippian-aged rocks found in the Kearney County region of the Hugoton embayment can be up to 1,700 feet thick. The stratigraphy of the upper Mississippian section is illustrated in Figure 4.

The Meramecian Stage of the Mississippian lies disconformably on Osagian rocks, but in northeastern and southwestern Kansas the disconformity is obscure. The upper formations consist mostly of granular, sandy, oolitic and fossiliferous limestone, but lower formations contain interbedded dolomite or are mainly dolomite and silty, dolomitic limestone containing variable quantities of chert (Goebel, 1968).

The Ste. Genevieve Limestone, which lies disconformably beneath Chesteran rocks, but seemingly conformable on the St. Louis Limestone, is widespread in the Hugoton embayment, but is not recognized in the Salina basin. It consists mainly of silty and sandy white fossiliferous limestone interbedded with fine-textured oolitic limestone and calcarenite. Beds in the Ste. Genevieve cannot be differentiated in areas in which they overlie finely oolitic limestone beds of the St. Louis Limestone. The thickness is more than 200 feet in the Hugoton embayment, where

the formation maintains a constant thickness except where it is beveled by pre-Chesteran or later erosion on the crests and flanks of uplifted areas (Goebel, 1968).

The St. Louis contains noncherty lithographic and sub lithographic limestone, but also includes remarkably widespread beds of oolitic limestone and calcarenite. Traces of translucent chert contained in semi-granular limestone occur locally. In the deeper part of the Hugoton embayment the St. Louis contains coarsely crystalline fossiliferous limestone and dolomitic limestone. Locally intraformational beds of limestone breccia, chert breccia, and anhydrite are preserved. The St. Louis Limestone in the Hugoton Embayment is often divided into 4 zones, being the A, B, C, and D zones. These zones can be further subdivided into six distinct depositional facies. The variations and occurrence of these depositional facies will be the main focus of this study. Although restricted to basin areas, the St. Louis is more widely distributed than the Ste. Genevieve. The maximum thickness in Hugoton the embayment for the St. Louis is about 200 feet (Goebel, 1968).

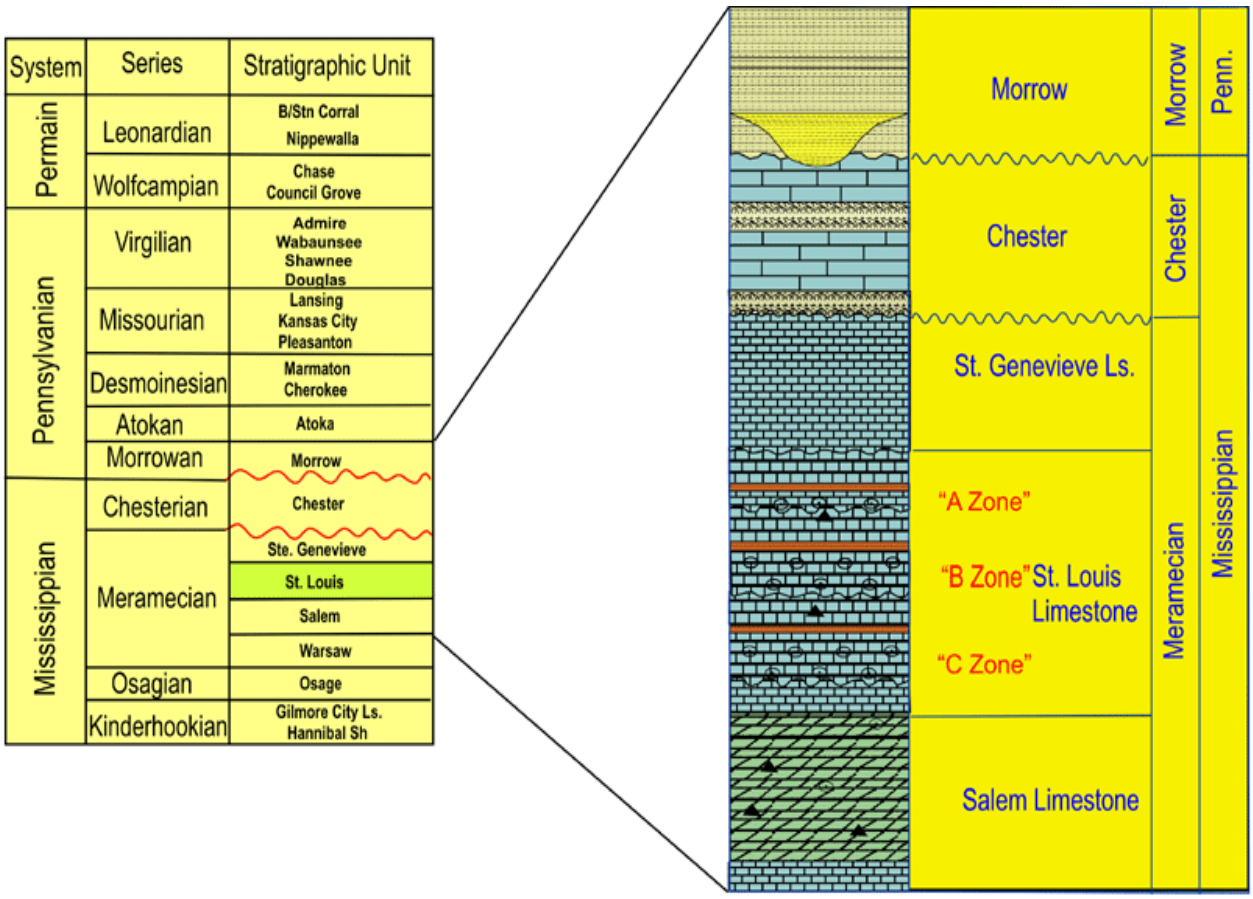

Figure 4. Upper Mississippian stratigraphy including the zonation of the St. Louis Limestone (Reservoir Characterization of the Mississippian St. Louis Carbonate Reservoir System in Kansas, Stratigraphic Facies Architecture Modeling, 2003).

The St. Louis Limestone

In Kearny County the majority of oil and gas production has come from the St. Louis Limestone. The St. Louis can be broken down into four different zones with varying lithologies and reservoir characteristics (Reservoir Characterization of Mississippian St. Louis Carbonate Reservoir System in Kansas, Stratigraphic and Facies Architecture Modeling, 2003). Within these four zones are six different lithofacies that affect the oil and gas production due to abrupt changes in porosity between facies. For the purpose of this study I will be focusing mainly on the

porous ooid grainstone, cemented ooid grainstone, and skeletal packstone facies of the St. Louis, due to their hydrocarbon reservoir qualities.

The primary lithofacies in the St. Louis that controls reservoir quality is the porous ooid grainstone (Martin, 2015). This facies is the primary target for drilling in the St. Louis. This porous ooid grainstone can be characterized by a medium to coarse, moderately-sorted ooids that have a radial concentric structure with skeletal grains, peloids, and detrital quartz nuclei (Lianshuang and Carr 2005). Also present are minor amounts of peloids along with occasional large skeletal grains. Commonly these skeletal grains are echinoderms, bryozoans, and brachiopods. In well cuttings the porous ooid facies is very apparent. Another example of this lithofacies can also be seen in thin-section in Figure 5.

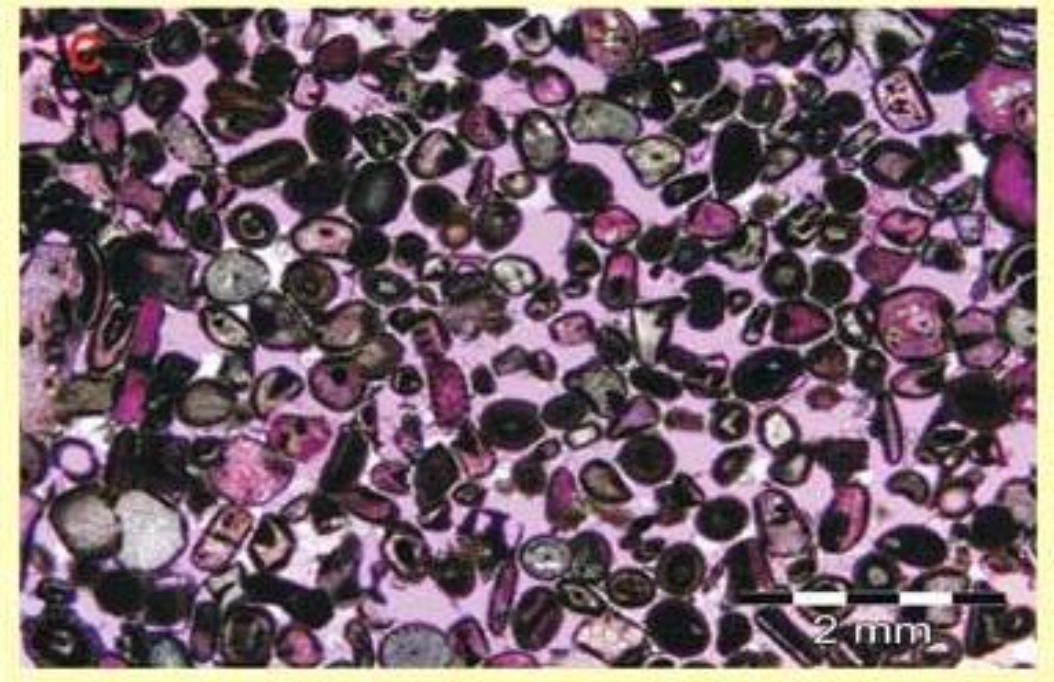

Figure 5. Thin-section of porous ooid grainstone with skeletal grains (Lianshuang and Carr, 2005).

The primary reason this lithofacies is so productive is the great porosity it exhibits. This facies has excellent reservoir qualities, including a porosity ranging from 3 to around 20 percent

with the potential for localized seals within the St. Louis. The thickness of the lithofacies is relatively thin and can range anywhere from 1.5 feet to 15 feet.

The second lithofacies within the St. Louis is the cemented ooid grainstone, which is important because it creates a fluid barrier that distinguishes it from the porous ooid grainstone. This facies is comparable to the porous ooid grainstone with some minor differences. As far as skeletal grains and ooid structure go it is similar to the porous lithofacies including things like ooids and peloids, but is not a reservoir quality rock (Figure 6). The skeletal grains are held together with micritic cement reducing its porosity to around 1 to 3 percent, and has a thickness range of 0.5 to 5.5 feet.

Figure 6. Example of the cemented ooid grainstone (Lianshuang and Carr, 2005).

The third lithofacies found within the St. Louis is the quartz-rich carbonate grainstone. This lithofacies can contain well-sorted ooid, skeletal fragments, peloidal carbonate grains mixed with very-fine siliciclastic sand and silts (Lianshuang and Carr, 2005). The silts found in this facies are ultrafine to medium-sized quartz grains, with similar sized grains of peloids, skeletal fragments, and ooids. These quartz grains often occur in amounts ranging from 20-36% (Martin, 2015). The facies is held together by a micritic and calcite spar cement (Figure 7). This unit can range widely in thickness from 1 to 50 feet thick.

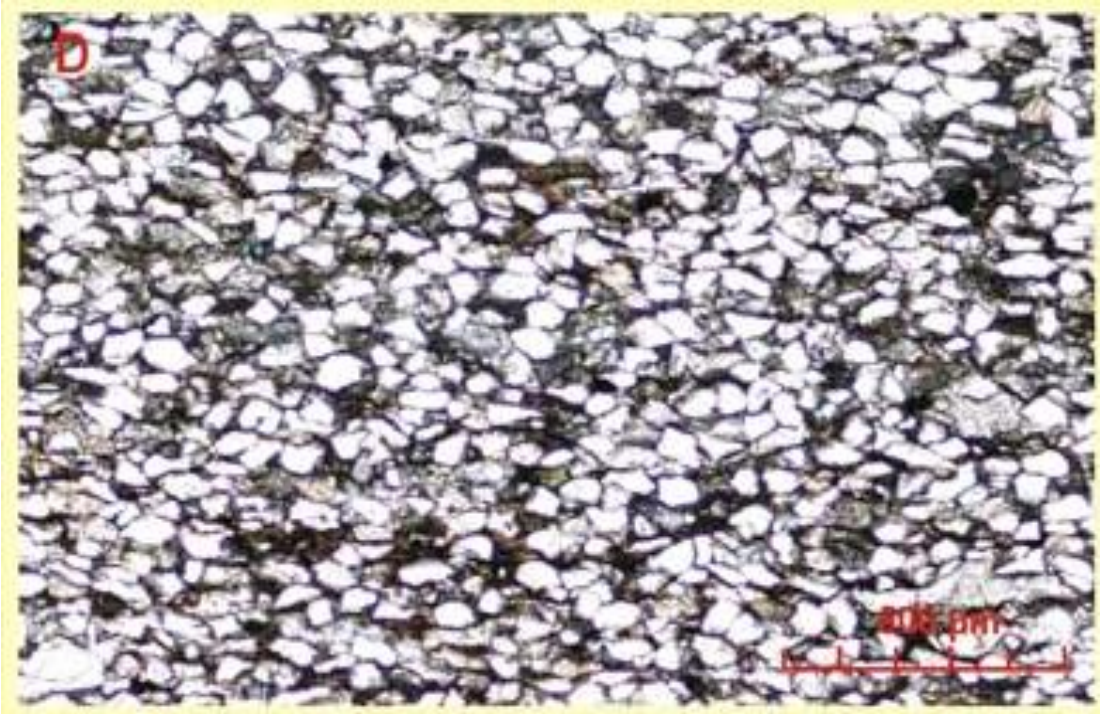

Figure 7. Example of the quartz-rich carbonate grainstone (Lianshuang and Carr, 2005).

The fourth lithofacies in the St. Louis is the peloidal packstone. This facies contains skeletal remains with a large amount of peloidal grains with fine ooid and quartz grains. The unit is green to dark yellow-brown in color with variable skeletal fragment. Crinoids and bryozoans are abundant with echinoderms, brachiopods, gastropods, and foraminifera also present (Figure

8). Bioturbation, algae lamination, mud intraclast, stromatolites, and chert replacement are a common characteristic structures of the peloidal packstone lithofacies, and indicate deposition in an intertidal to supratidal environment. Large vugs, filled with anhydrite or replaced with chert or calcite spar can be seen (Lianshuang and Carr, 2005). The thickness of this lithofacies can range from half a foot to 5 feet.

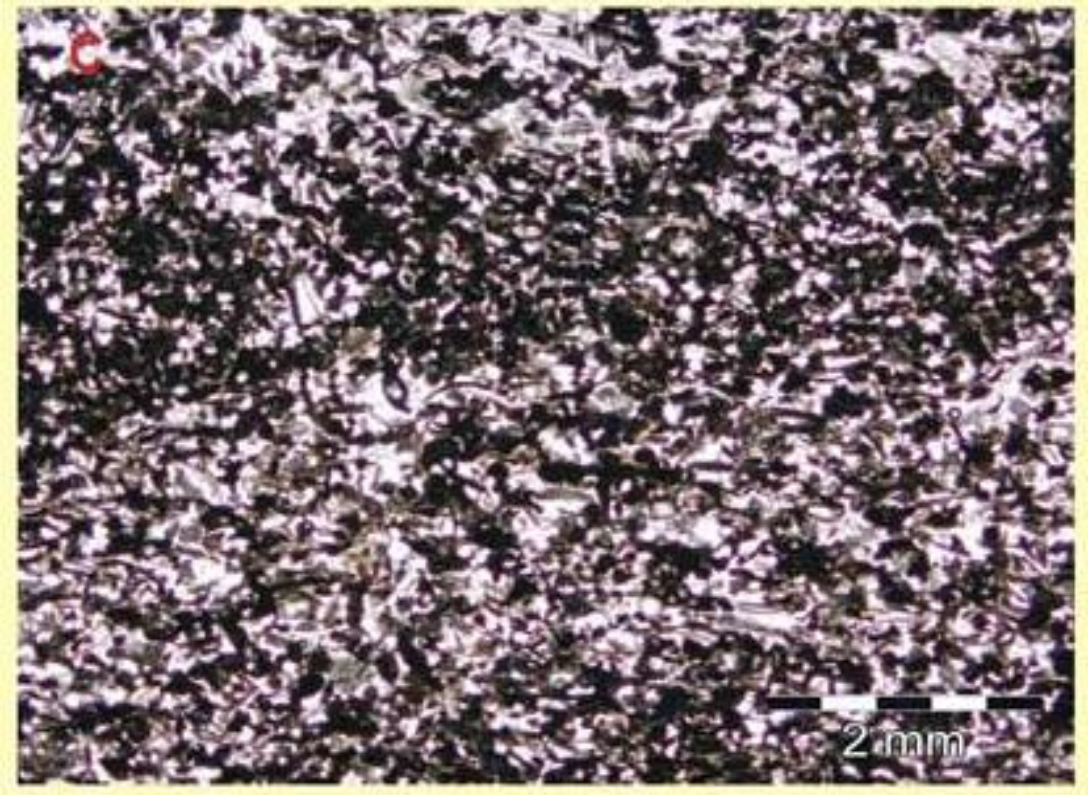

Figure 8. Example of the peloidal packstone (Lianshuang and Carr, 2005).

The fifth lithofacies in the St. Louis is a clay-rich mudstone. This facies is characterized as a grayish black, very fine grained, highly microtized interval. There is very little fossil content but can have highly microtized peloid grains (Figure 9). The clay-rich mudstone commonly has a green tint indicating high amounts of glauconite as seen in cuttings. This facies is relatively thin ranging from 3 to 9 feet.

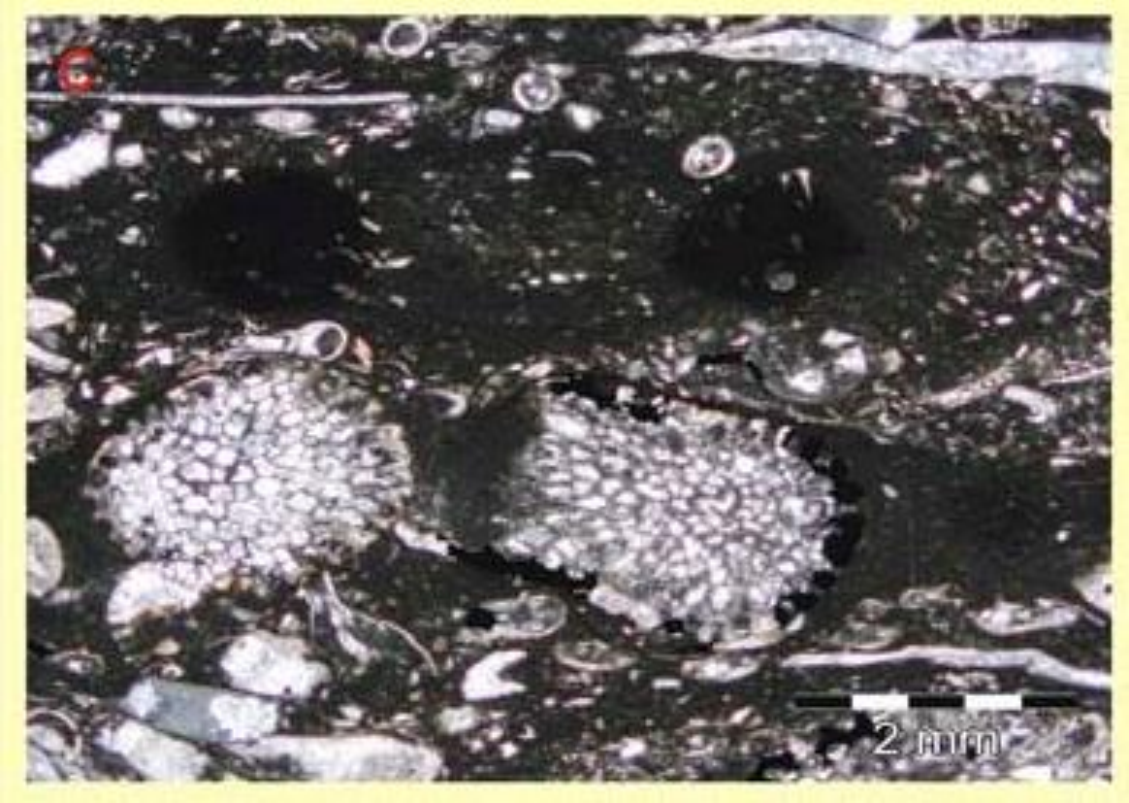

Figure 9. Example of the clay-rich mudstone (Lianshuang and Carr, 2005).

The sixth lithofacies in the St. Louis is the skeletal wackestone. This facies is a poorly sorted primarily mud-supported and green to dark yellow-brown in color. The sedimentary structures in the facies have been completely obliterated by bioturbation (Lianshuang and Carr, 2005). The skeletal fragments in this facies are generally large consisting of crinoids, bryozoans, brachiopods, and gastropods which are seen while looking through well cuttings (Figure 10). The skeletal fragments can be found within a micritic matrix and the facies ranges from a thickness of half a foot to 7 feet.

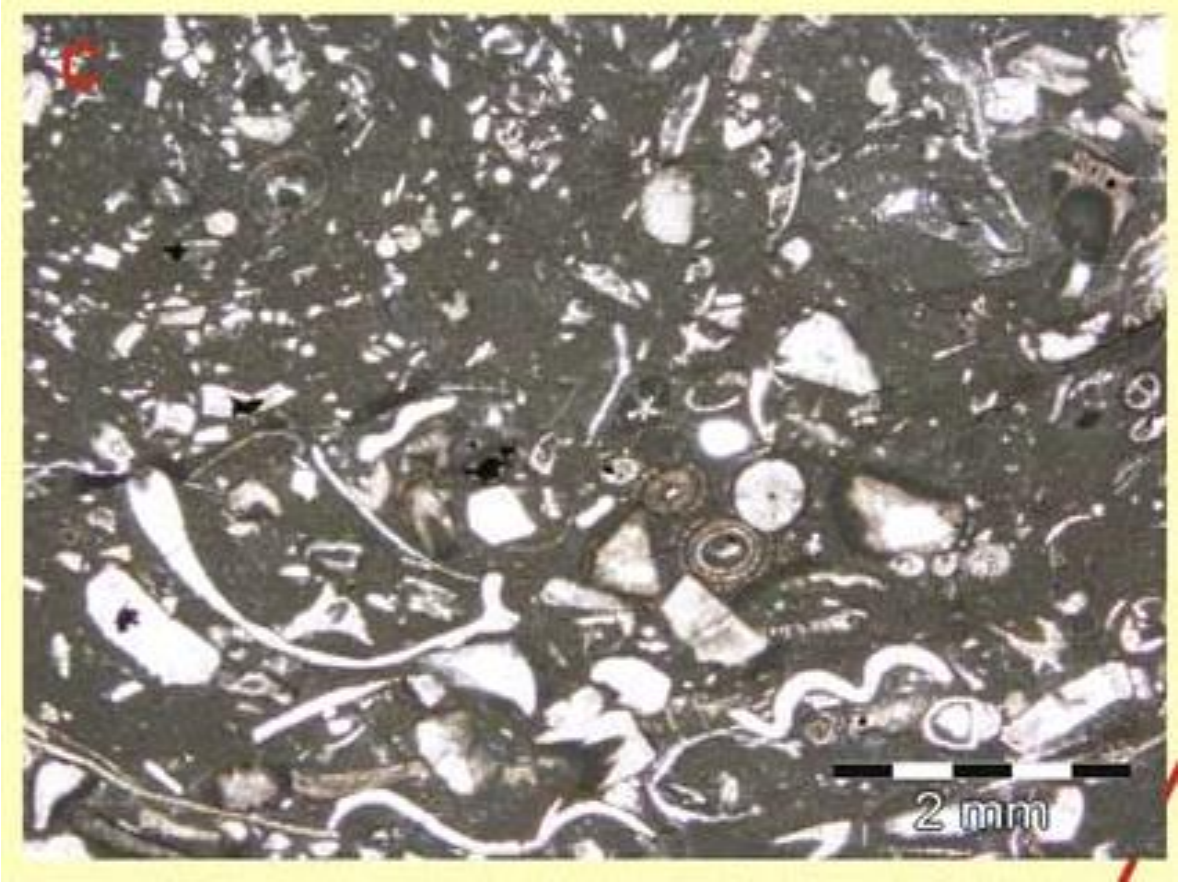

Figure 10. Example of the skeletal wackestone (Lianshuang and Carr, 2005).

Chapter 2 - Carbonate Porosities

One of the most important characteristics when evaluating a potential reservoir is the porosity of that reservoir. Porosity is the volume of voided space within a rock. Permeability is also an extremely important factor when controlling reservoir quality. The permeability refers to the ability for any sort of fluid, such as oil or gas, to move through the reservoir (Dikkers, 1985). Identifying various types of porosity is very important when determining reservoir quality. This is because porosity and permeability are generally dependent upon each other. Depending on the type of porosity present in the reservoir, you can often estimate the permeability of the reservoir.

Carbonate porosity is a function the depositional environment, as modified by diagenetic processes during burial (Flenthrope, 2007). These diagenetic processes can include the filling of pores by carbonate cement, or by the leaching of grains within the rock. Figure 11 shows the various types of carbonate porosities that can be seen in a carbonate rock.

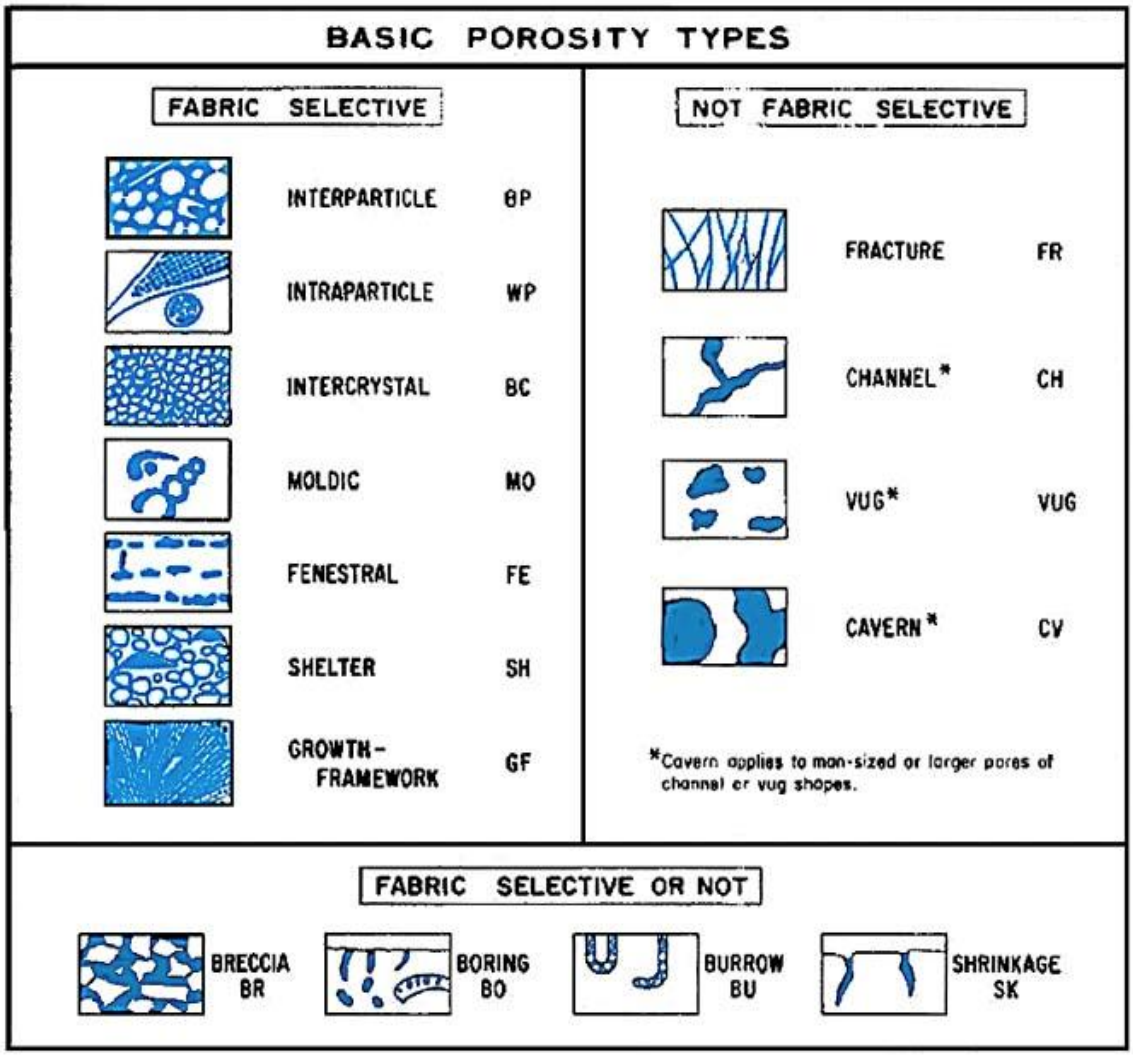

Figure 11. Carbonate porosity types (Wilson, 1975).

Interparticle porosity is defined as pore space around the grains. These grains can be any sort of organism or abiotic grain such as ooids or peloids. Interparticle porosity usually occurs within highly grain-supported rock with a great amount of porosity between the grains. This

porosity generally comes from high-energy environments such as ooid shoals and can be seen in Figure 6.

Intraparticle porosity is defined as pore space within the grains of the rock. This porosity originates from the living chambers of organisms such as gastropods, foraminifera, bryozoans, or brachiopods. Once deposited these now empty living chambers go through the process of maceration (Scoffin, 1987). Abiotic ooids can also give intraparticle porosity when the center of the ooid goes through dissolution before, during, or after deposition (Moore, 1989). The intraparticle porosity type can typically be found in reef environments, but generally gives poor permeability because the pore connectivity is poor.

With intercrystaline porosity crystals of similar sizes are formed either by recrystallization or by dolimitization (Scoffin, 1987). In Kearny County, it is due to recrystallization not by dolomitization (Martin, 2015). This occurs due to chemical changes either from hydrocarbon maturation or because the reservoir has been influenced by meteoric water from an unconformity (Moore, 1989). Permeability of this porosity type is largely influenced by the size of crystals usually yielding low porosities. The quartz-carbonate grainstone as well as the highly cemented ooid grainstone exhibit this type of porosity with little to no porosity connectivity as seen in Figure 7.

Vuggy porosity occurs as holes within grains as well as cement boundaries in the rock. Vuggy porosity can be due to karstic weathering and the presence of flowing freshwater, which result in dissolution of calcite. A high-energy environment can result in a vuggy porosity in the cases of porous ooid facies as well as the peloidal packstone facies.

Carbonate Classifications

Classification of carbonate rocks from well cuttings is sometimes difficult. When combining a petrographic microscope with descriptions from a binocular microscope, an enhanced classification can be made. With these tools it becomes possible to identify individual grains that comprise the rock. There were two classification schemes used during this study, developed by Folk (1959), and Dunham (1962). These two classification schemes subdivide limestones based upon the limestones matrix, content, and then on skeletal frameworks present (Flenthrope, 2007).

In the Folk classification scheme limestones are classified by their allochemical content as long as the rock contains more than 10% allochems. Allochems can be any sort of transported carbonate grain including things such as ooids, and pellets. Based upon interstitial material the rock can be further divided into either sparry calcite cements, or a microcrystalline calcite matrix. Further subdivision is based on allochems present as well as the ratios of the allochems. For this study the Folk classification scheme was used because of its ability to be used in identifying thin-sections of limestones by seeing the matrix as well as allochems comprising the limestone (Figures 12, 13).

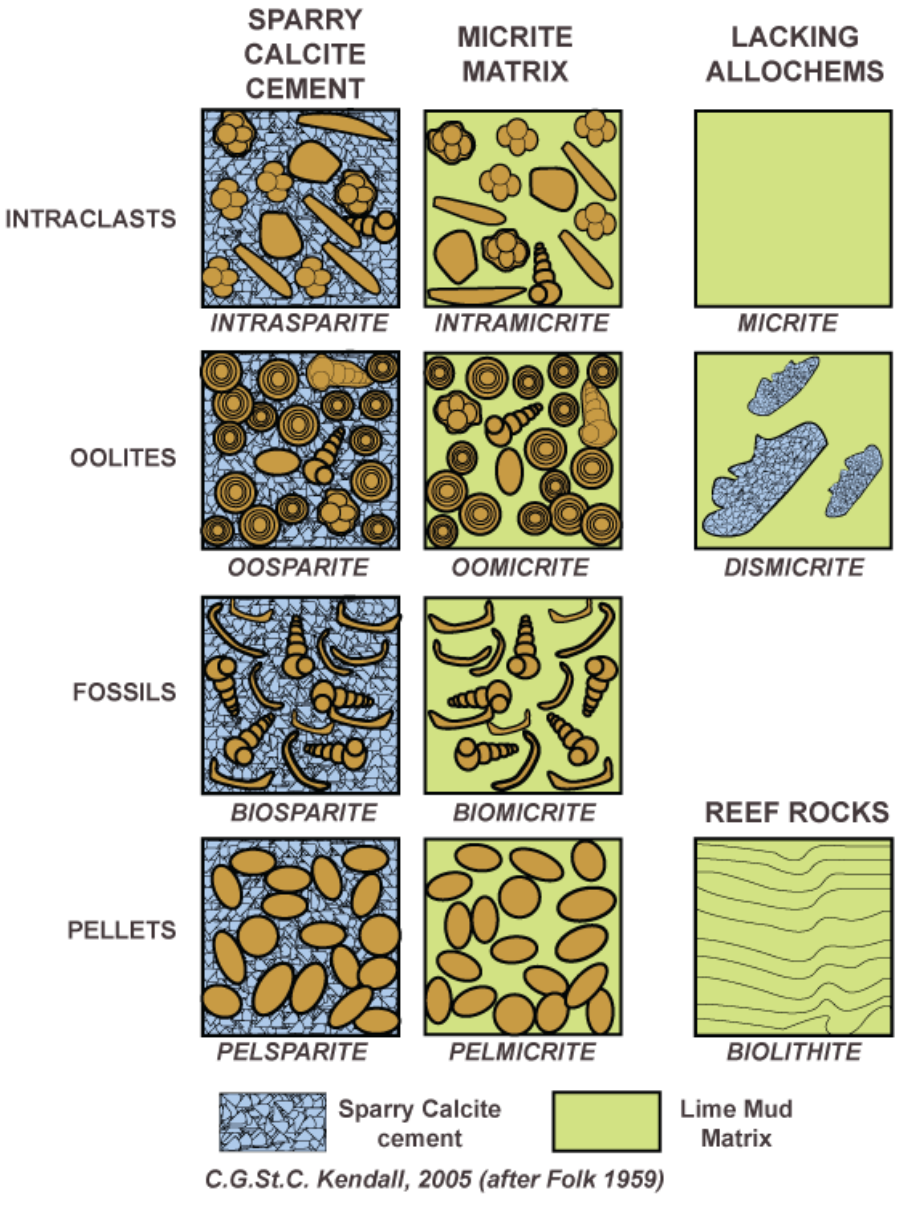

\

Figure 12. Folk classification schematic (Folk, 1959).

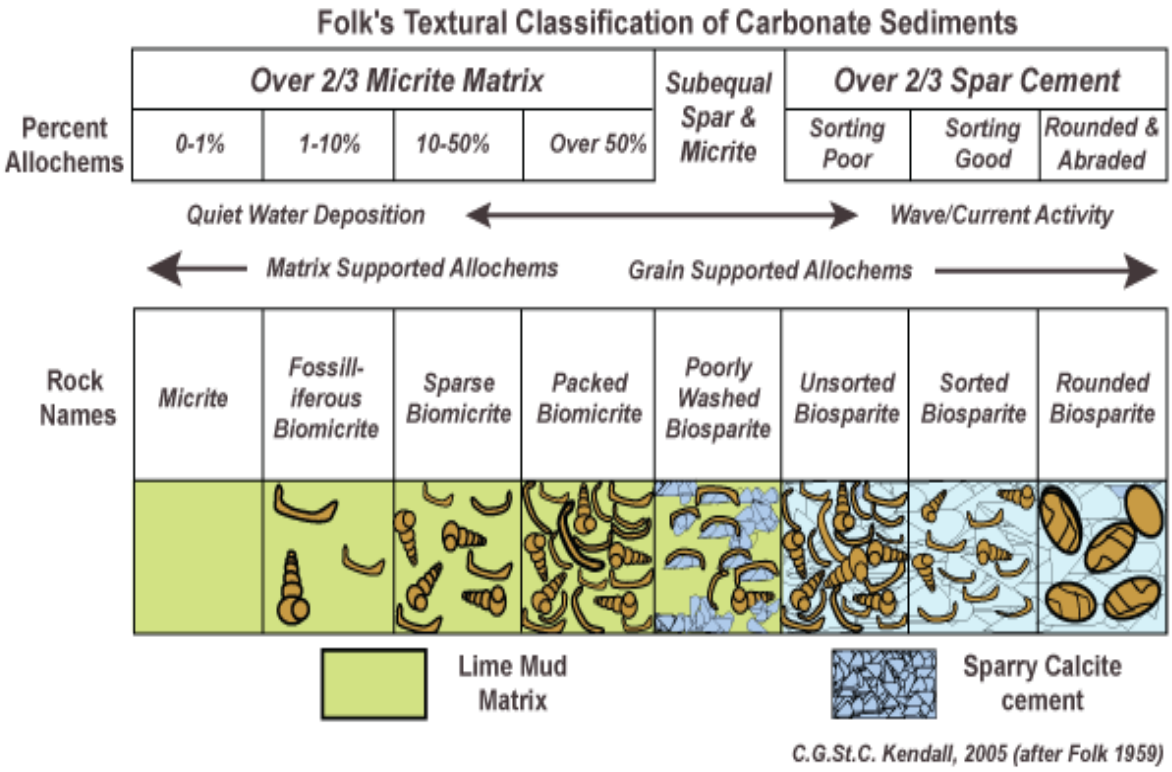

Figure 13. Folk Classification Schematic (Folk, 1959).

The Dunham classification of limestone differs from Folk because it is focused primarily upon the texture of the rock. This classification is simpler, and observing the rock with a binocular microscope is often sufficient to name the rock. For instance if a limestone has an abundance of allochems touching each other with little to no mud then the rock would be termed a grainstone (Figure 14).

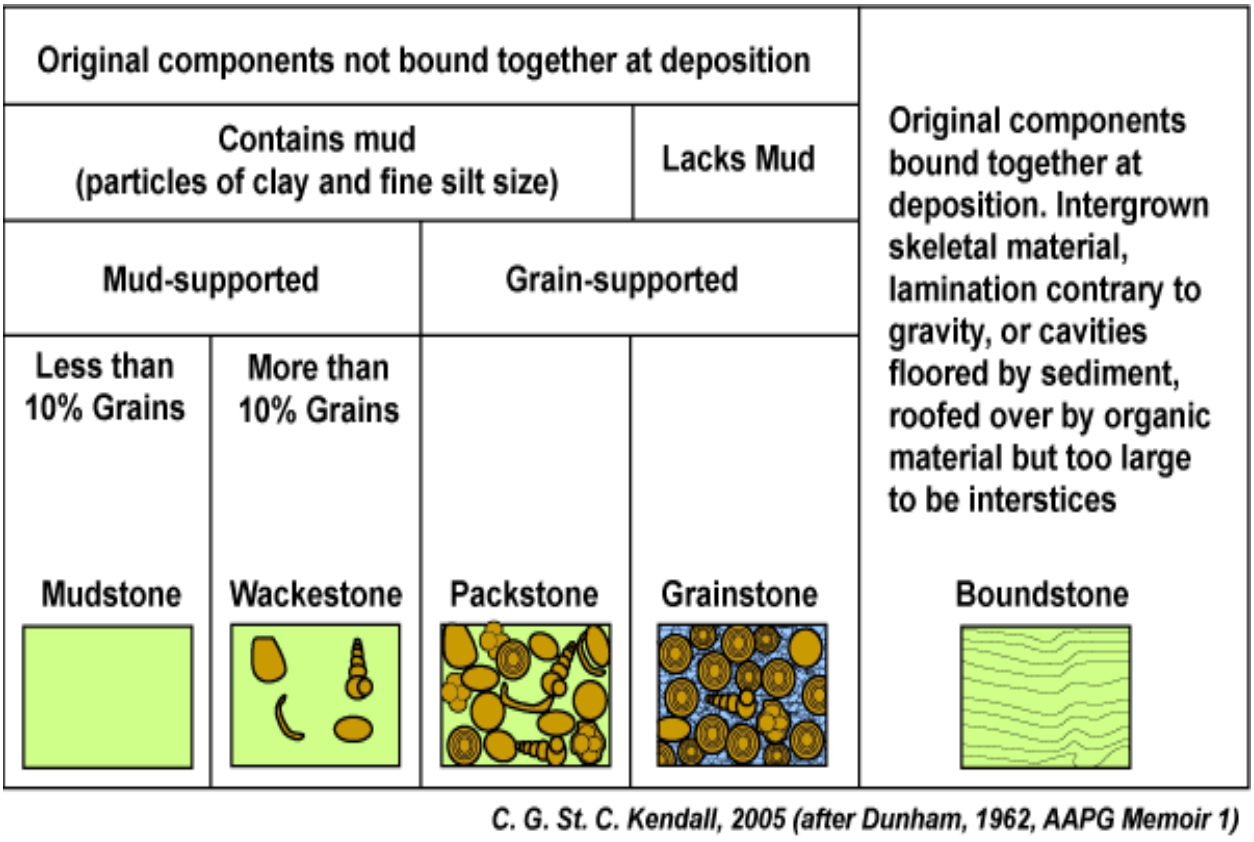

Figure 14. Dunham classification schematic (Dunham, 1962).

For this study both schemes were used to combine observations using the binocular microscope with those of a petrographic microscope. Comparing the two classifications, a rock rich in carbonate mud would be termed a micrite by the Folk classification, but a mudstone by the Dunham. A rock containing little matrix is termed a sparite by the Folk and a grainstone by the Dunham (Embry and Klovan, 1971). This difference helps in truly knowing what is being observed.

Previous Study

Martin (2015) conducted a previous study in the same area of Kearny County, Kansas of facies distribution within the St. Louis Limestone. The St. Louis in Kearny County was identified by Martin as an ooid shoal based on the geometry of the St. Louis C zone (the porous

ooid grainstone) and is analogous to that of Great Bahama Banks marine sand shoals identified by Handford (1998) as seen in Figure 15.

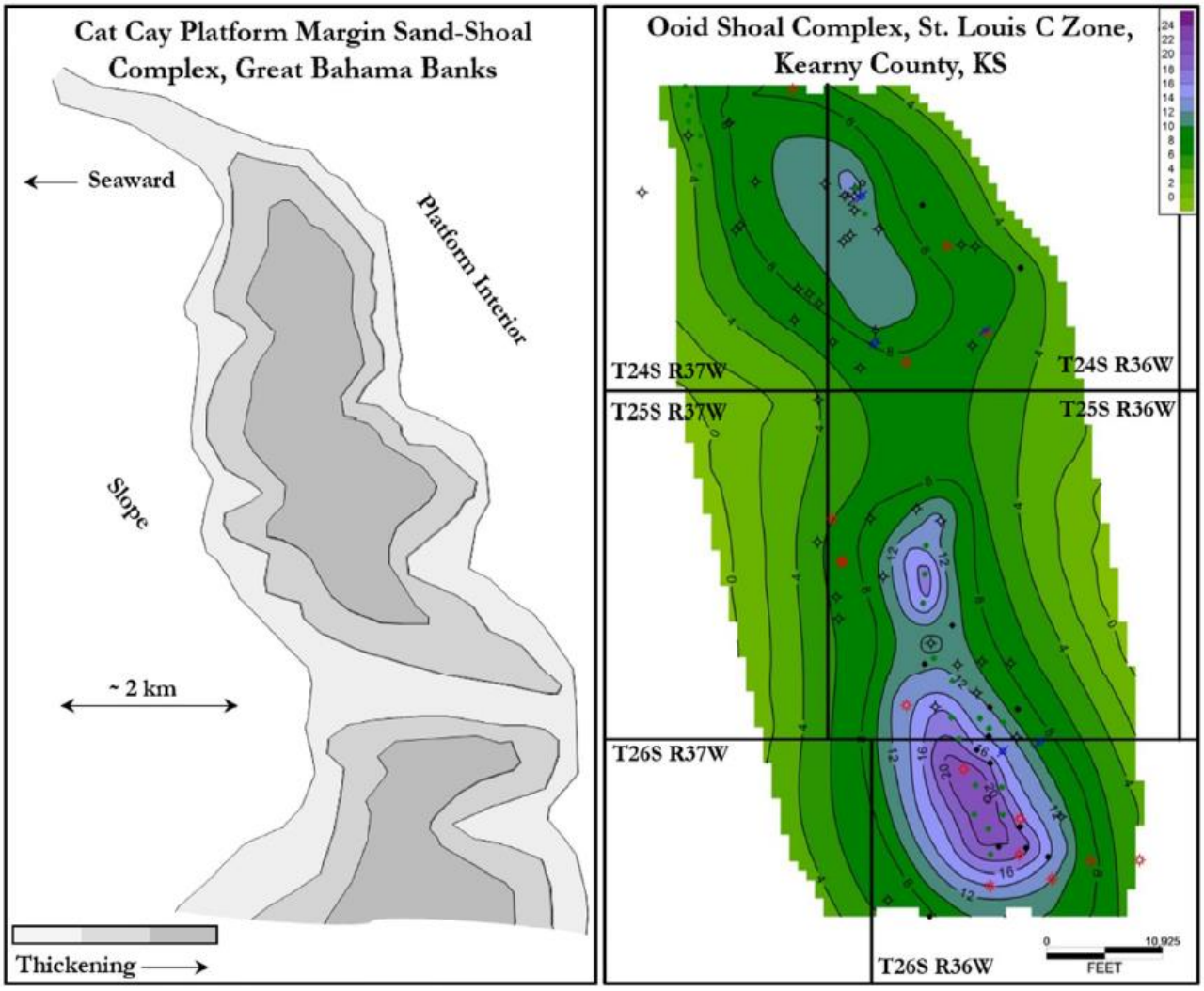

Figure 15. Great Bahama Banks Cat Cay platform margin sand-shoal geometry. Geometry of the ooid shoal within the St. Louis C zone with similar geometry identified by Martin (Martin, 2015).

This study initially described approximately 400 feet of core in the upper Mississippian portion of three wells in close proximity to each other. The core was described using textural changes within the core relating to the six depositional facies. The changes in core intervals were noted and thin-sections were made where any distinct changes took place. Thin-sections, handheld X-

ray fluorescence, and well log characteristics were used to divide the core into six distinct depositional facies, referred to as the St. Louis facies 1 through 6.

The information observed by the well logs in the cored wells were then used to calibrate a neural network as a single hidden-layer feed-forward network. The neural network program provided an output of probabilities of each facies (Figure 16).

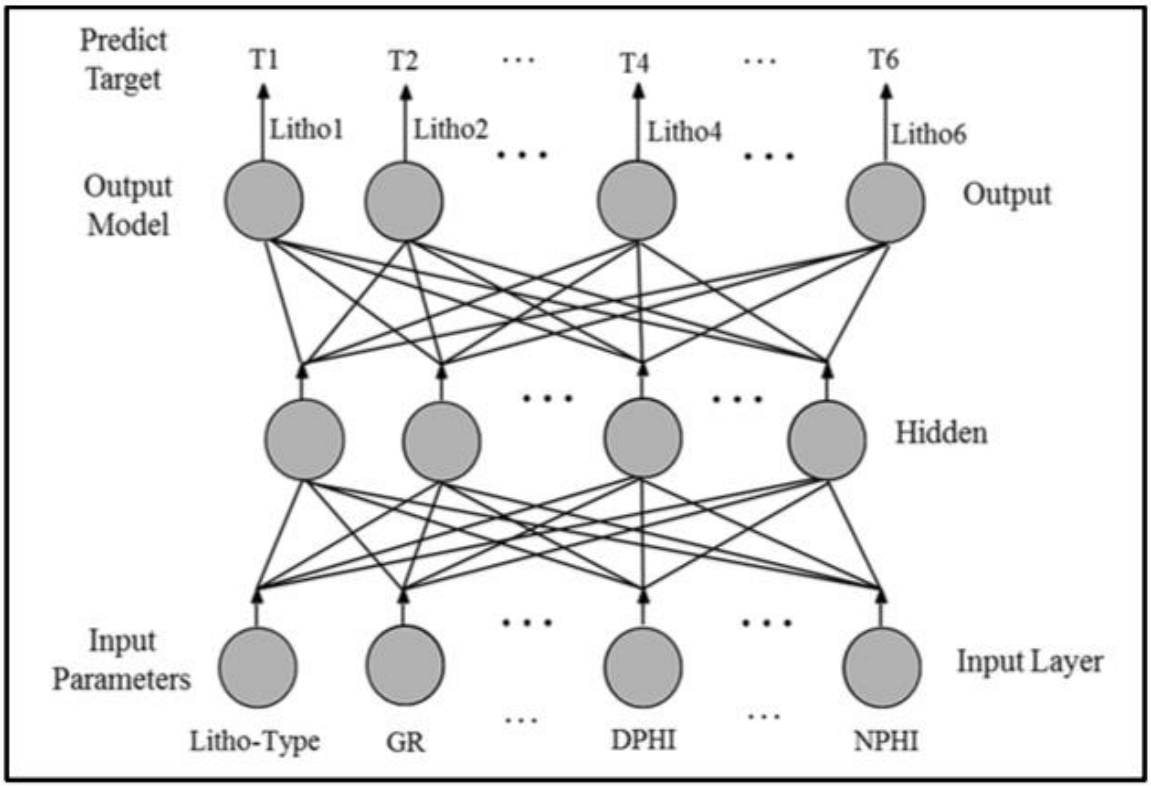

Figure 16. Generalization of the neural network workflow (Martin, 2015).

These computed probabilities were then matched with predicted facies that closely match the facies observed in the core, the result of this process can be seen in Figure 17.

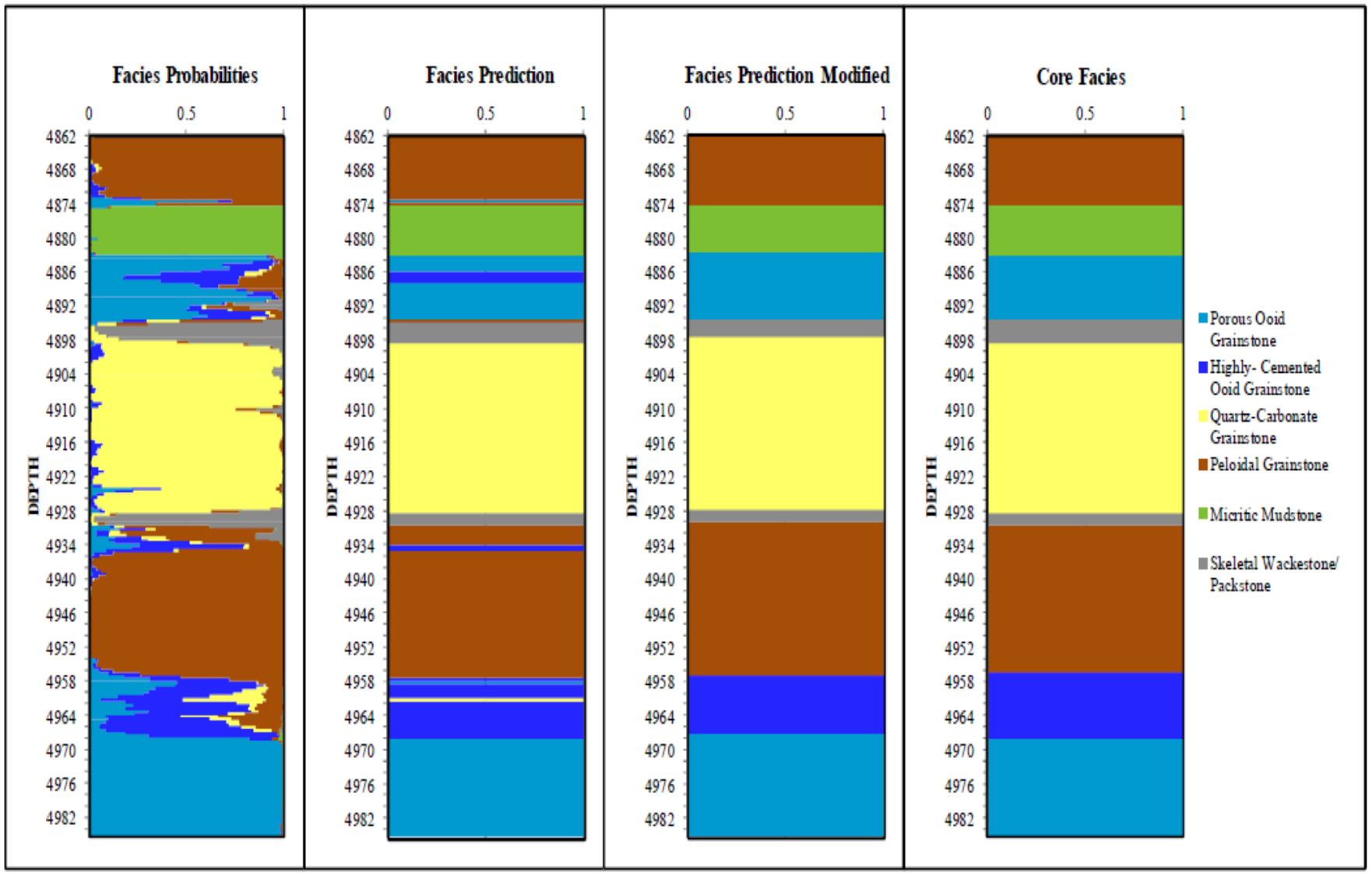

Figure 17. Four plots of the facies probability, facies prediction, facies prediction modified, and core facies (actual facies) that illustrate the neural network models predictions (Martin, 2015).

The general purpose of the neural network programming is that once the facies are matched with the continuous well log measurements over the cored interval, then these facies can be predicted laterally in the subsurface using only well log data with some degree of accuracy. Predicted facies, once computed, were then organized into spreadsheets that can be seen in Appendix C. With these predictions Martin created cross sections to show the distribution of the predicted facies (Figures 18, 19). Martin (2015) assumed that the predictions were accurate nearest the cored interval, and that the further from the cored model well the predictions lost some degree of accuracy.

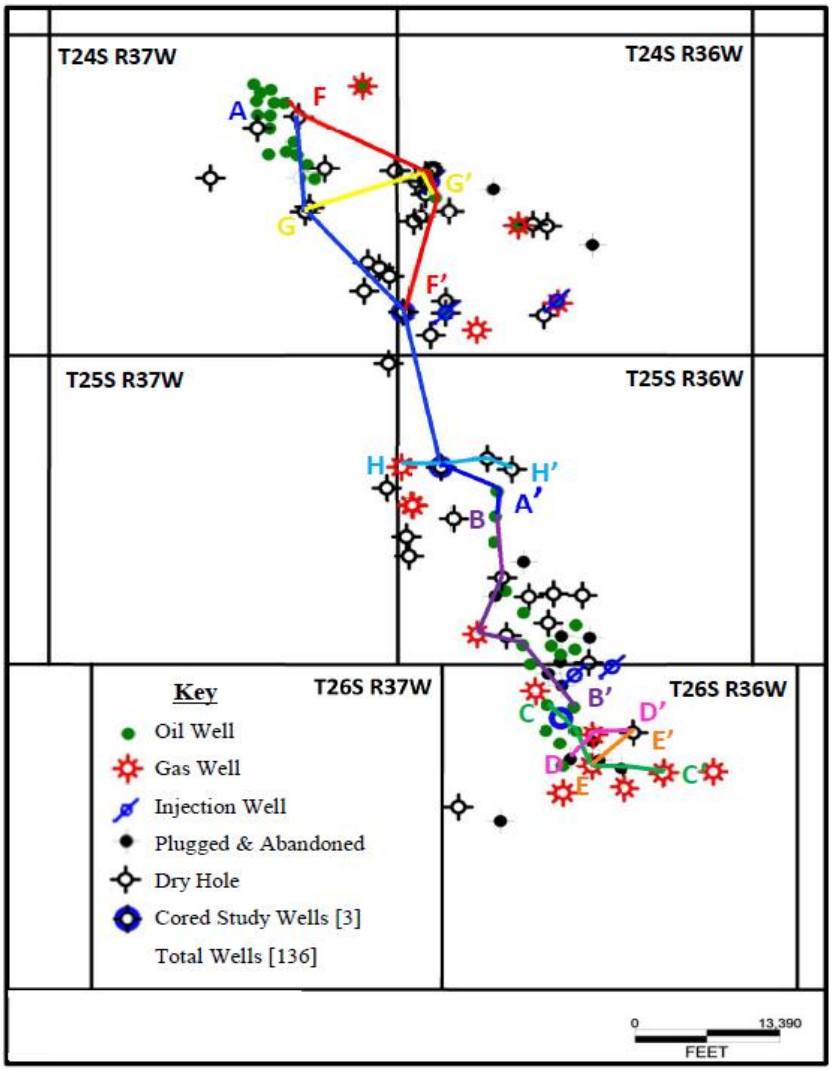

Figure 18. Base map with color coded cross section (Martin, 2015).

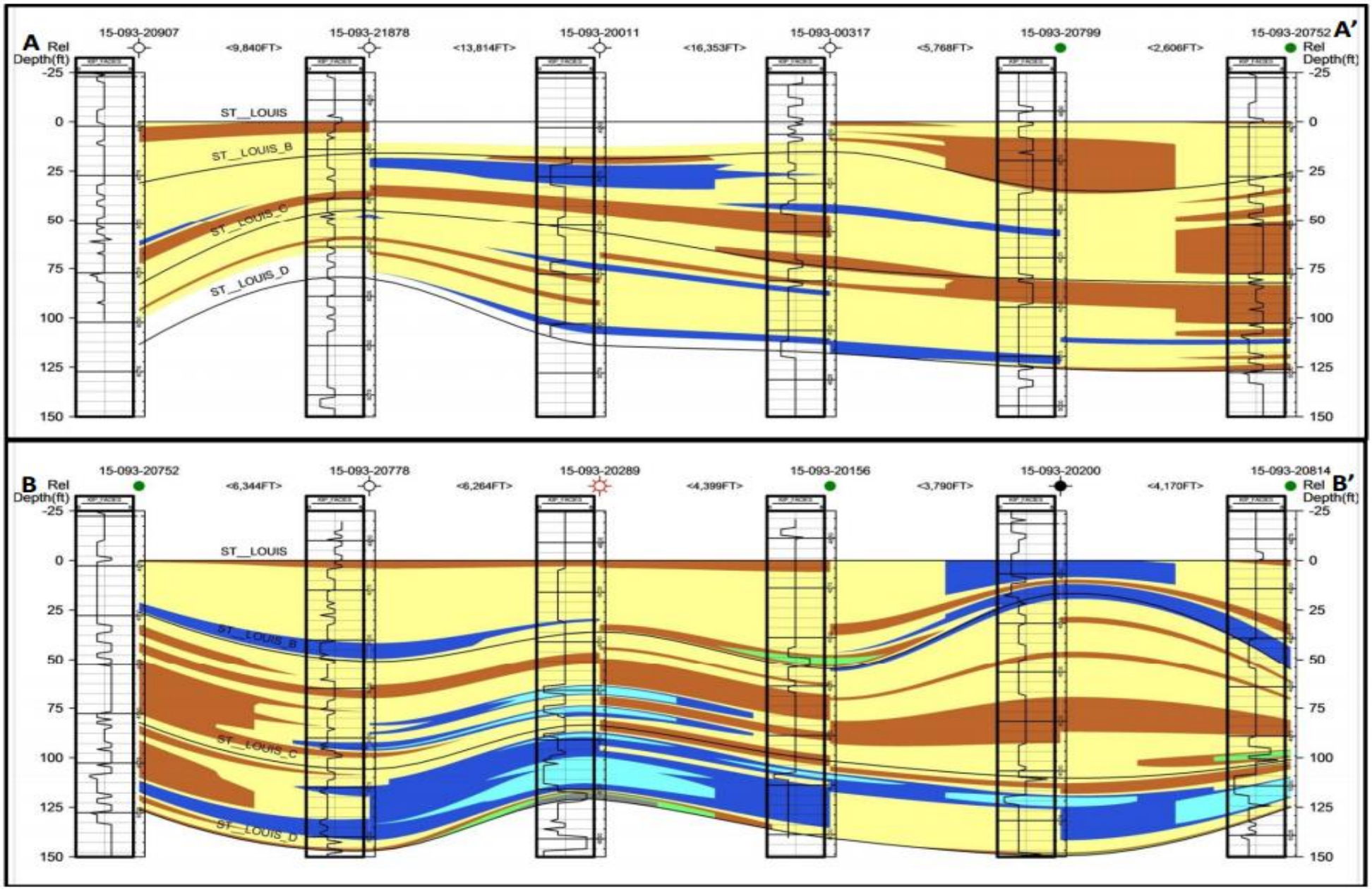
A
A'
Rel Depth(ft)
15-093-20907
15-093-21878
15-093-20011
15-093-00317
15-093-20799
15-093-20752
<9,840FT>
<13,814FT>
<16,353FT>
<5,768FT>
<2,606FT>
ST__LOUIS
ST__LOUIS_B
ST__LOUIS_C
ST__LOUIS_D
-25
0
25
50
75
100
125
150
B
B'
15-093-20752
15-093-20778
15-093-20289
15-093-20156
15-093-20200
15-093-20814
<6,344FT>
<6,264FT>
<4,399FT>
<3,790FT>
<4,170FT>

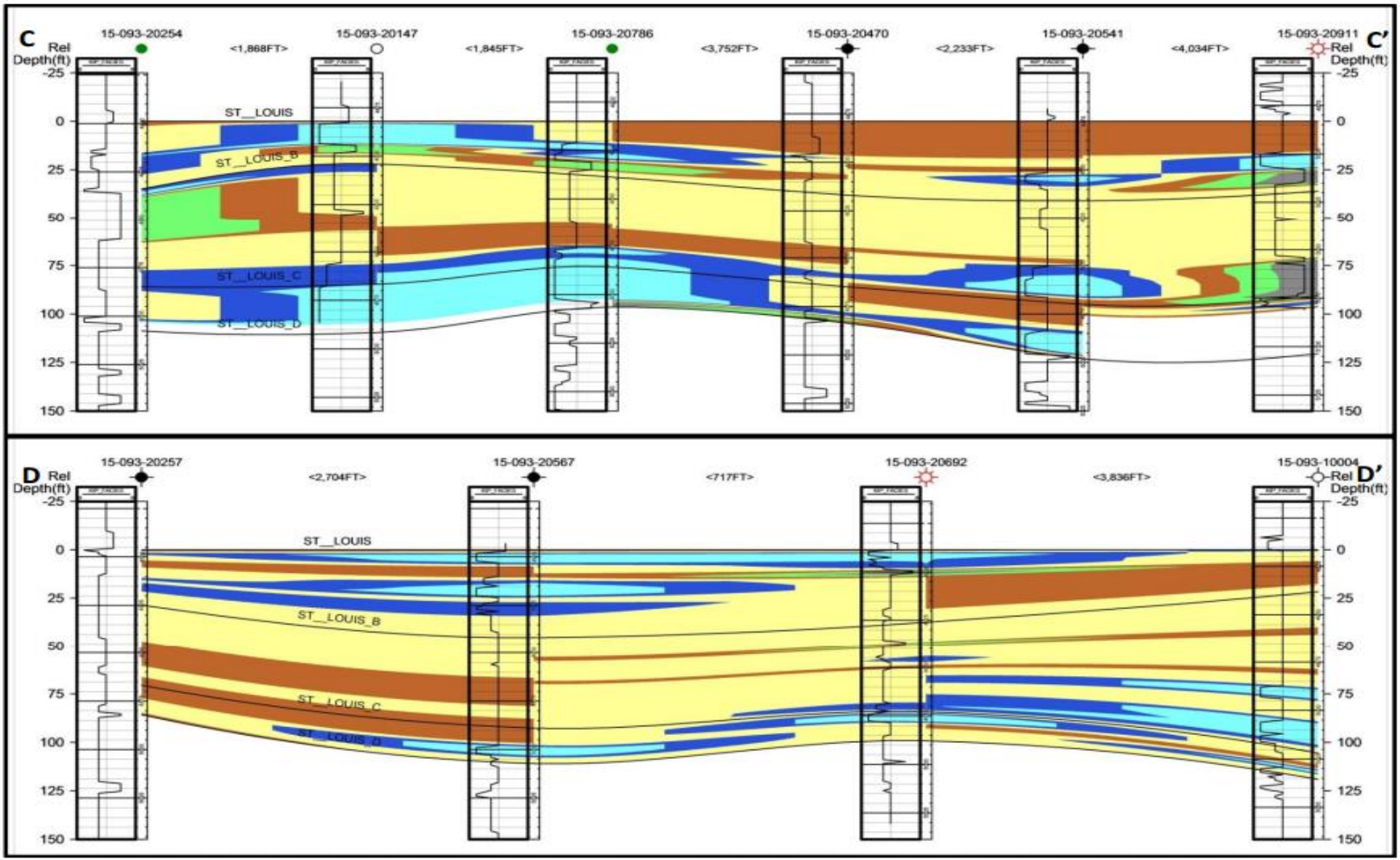

Figure 19. Cross sections of A, B, C, and (Martin, 2015)

Chapter 3 - Methods

Well Cuttings

The neural network model was used to predict facies in 16 wells within proximity to the three cored wells. Of these wells, five were picked based on whether or not the porous ooid facies was predicted, the availability of cuttings, and the distances from the cored wells used in the neural network program. Locations of the wells, and locations of the neural network model well can be seen in Figure 20, and Figure 21. Cuttings were obtained from the Kansas Geologic Survey Well Sample Library located in Wichita, Kansas. Lag times to match cuttings with actual drilling depths were estimated from well log data to accurately predict sample depths of the St. Louis limestone. While drilling, samples from the location of the drill bit take some amount of time before reaching the surface. When samples come up at ten-foot intervals the actual depth of the drill bit is lower than where the actual sample came from, and this is why lag time must be taken into account. The cuttings were then observed at ten-foot foot intervals using a binocular microscope at 20X power carefully identifying porosity, and allochems present. Cuttings were picked based on what facies was present, the facies predicted by the neural network model, and where the well site geologist and the KGS named specific tops. Once cuttings were thoroughly described these picked cuttings were then made into thin-sections.

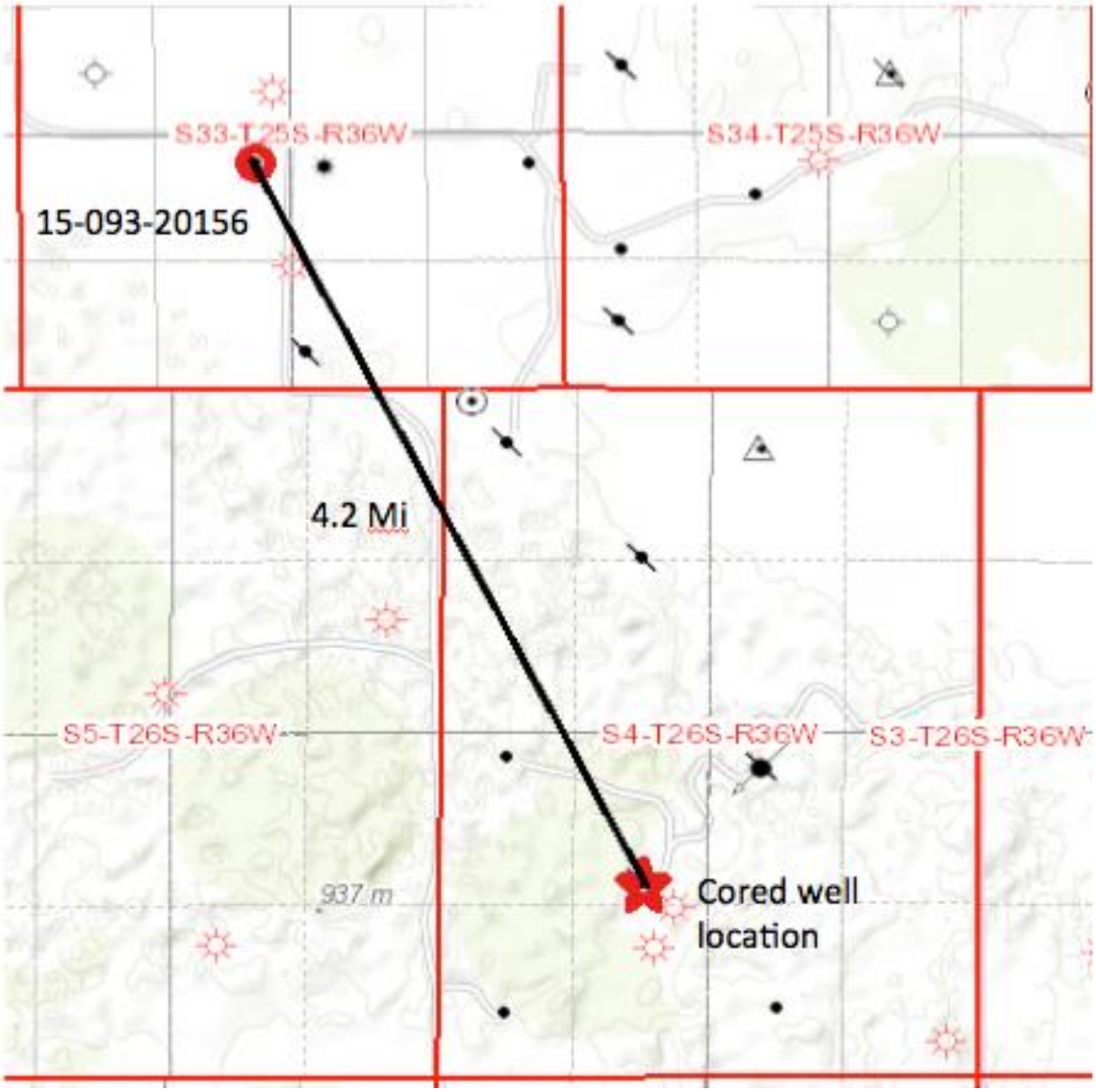

Figure 20. Cored neural network model well, and well 15-093-20156 used for cutting analysis.

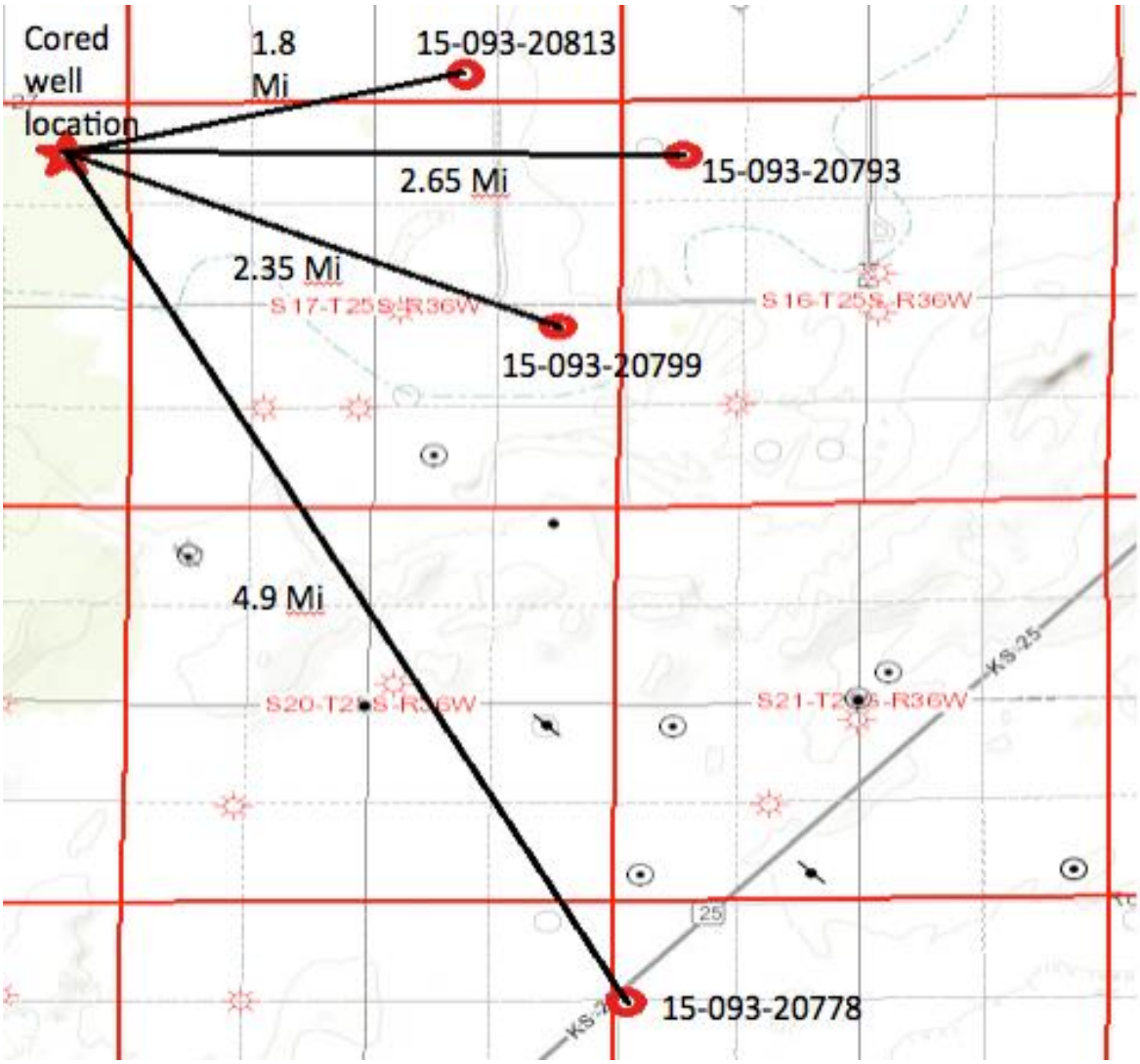

Figure 21. Cored neural network model well, and wells 15-093-20778, 20779, 20793, and 20813 used for cutting analysis.

It would have been ideal to look at wells within the cross sections that predicted facies one (the porous ooid grainstone). Cuttings from all of these wells were not available from the KGS library. In the wells with available cuttings, only one predicted the productive facies one. Even in this well, over the interval where the neural network predicted facies one, cuttings were missing. The dearth of samples over intervals predicted to have the important facies one is highly

suspicious, perhaps not included in the state repository for proprietary reasons. It's impossible to validate the prediction of facies one without a complete sample set available.

Of the five wells picked for cuttings analysis only two of them had complete cuttings throughout the entire drilling interval. In well 15-093-20156, 30 feet of cuttings were missing (in the most important interval). Also in wells 15-093-20793, and 20813 there were 20 feet of missing cuttings.

Thin-Sections

Thin-sections were made using blue dyed petropoxy resin. Resin and dye were mixed with previously hand-picked individual cuttings in a cup and placed inside a vacuum. The samples were evacuated multiple times to remove air from inside of open pore spaces. . As the vacuum is released the epoxy is drawn into the evacuated pore space. Cuttings were then picked out of the mixture and placed onto glass slides that were previously etched with the well API and depth interval. The glass slide was placed inside the vacuum again to remove any additional air in pore spaces, and further impregnate the cuttings with blue dyed epoxy. Slides were then placed on a hot plate for ten minutes to harden the epoxy and permanently attach the cuttings onto the glass slide. Slides were ground until they reached approximately 30 microns in thickness and polished.

Polished slides were observed using a petrographic microscope to determine the porosity types. Folk (1959) and Dunham (1962) classification schemes were used to describe the rock in better detail. Ultimately the petrographic analyses were used to determine the facies present after Martin, 2015.

Limitations

The neural network predicted facies distribution primarily upon well logs calibrated from the cored interval. Well log data are continuous measurements taken over the interval the log was run. Therefore the network computes predicted facies at every one-foot interval (as seen in Tables 5, and 6 in Appendix C).

When using cuttings to identify facies, however, you are limited by the interval in which the driller collected samples. In the wells studied, this was generally by ten-foot intervals. This makes it impossible to pinpoint a facies at a single foot of measured depth. In some cases, the neural network may have predicted four separate facies within a ten-foot interval. These would be collected together within any ten-foot interval, along with potential contamination from up hole caving during drilling. This not only limits the ability to pinpoint a facies per foot, but also effects the ability to accurately detect the accuracy of the neural network predictions. One major limitation is that the only well that had predicted the porous ooid grainstone was missing cuttings at that specific interval.

Different well log tools were combined to calibrate the model, all of which have varying resolutions in the well bore with respect to formation penetration, and bed thickness. The facies distribution in the cores used to calibrate the model were fairly thick, hence there is a probable limit of bed thickness which falls below the prediction limits of the model. This could result in the presence of very thin facies in wells where the model did not predict them.

Chapter 4 - Results

Well Cuttings

Table 1 lists the results of drill cutting examination with a binocular microscope. The Table includes the well API#, well location, sample depth in feet, porosity type, extra comments, facies predicted, and images taken at that specific depth. The depositional facies are as follows, along with photomicrographs of examples from each facies;

1) porous ooid grainstone (Figure 22)

Figure 22. Well cutting from well 15-093-20793.

2) highly-cemented ooid grainstone (Figure 23)

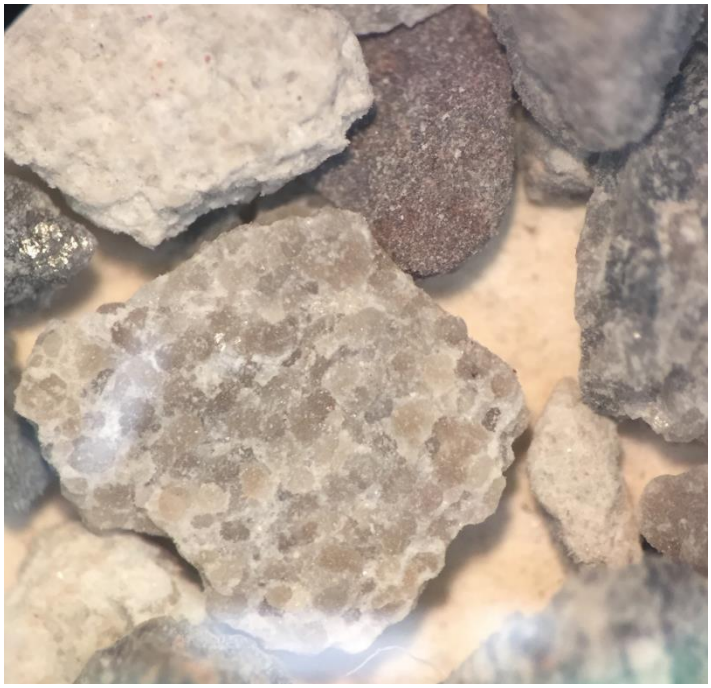

Figure 23. Well cutting from well 15-093-20813.

3) quartz-carbonate grainstone (Figure 24)

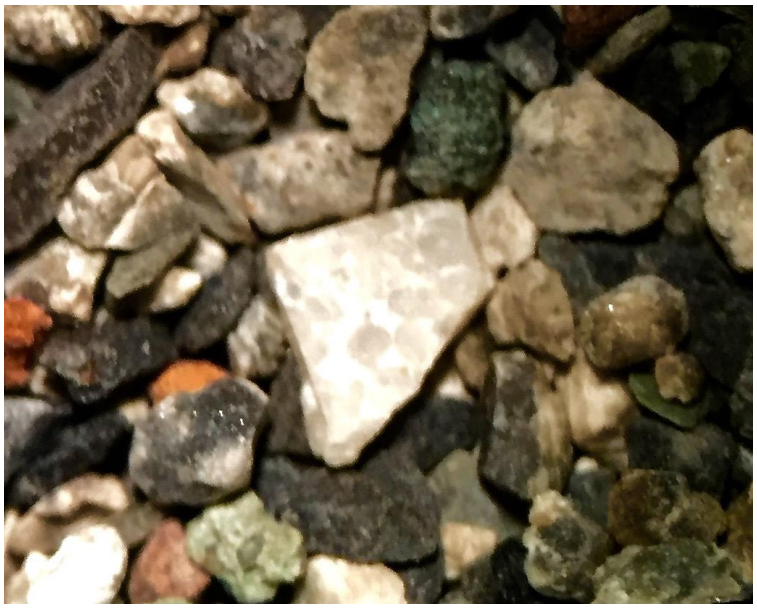

Figure 24. Well cutting from well 15-093-20793.

4) peloidal grainstone (Figure 25)

Figure 25. Well cutting from well 15-093-20778.

5) micritic mudstone (Figure 26,27)

Figure 26. Well cutting from well 15-093-20813.

Figure 27. Well cutting from well 15-093-20156.

6) Skeletal wackestone/packstone (Figure 28)

Figure 28. Well cutting from well 15-093-20799.

Table 1 Descriptions of Well Cuttings

API #	LOCATION	DEPTH FEET	POROSITY TYPE	COMMENTS	FACIES PREDICTED	IMAGE FIG #
15-093-20799	17-25S-36W	4810-4820	Intercrystaline	Pyrite, chalcopyrite, and some bryozoan	3	46
		4830-4840	Vuggy	Limestone is very vuggy with some pyrite present	3,5	
		4940-4950	Intercrystaline/ Vuggy	Limestone with ooids and small amounts of pyrite	5	
		4950-4960	Vuggy	Limestone very porous with chalcopyrite and bryozoan	3	
		4820-4830	Intercrystaline	Majority shale with bryozoan and pyrite	3	49
		4900-4910	Vuggy	Large open pore space between ooids with significant amount of chalcopyrite	3	55
15-093-20813	08-25S-36W	4870-4880	Intercrystaline	Crystalline limestone with minor amounts of shale	3,5	50
		4880-4890	Intercrystaline	Ooid rich limestone, majority cemented some porous	3	

		4900-4910	Intercrystaline	Ooid rich limestone highly cemented	5,3	56
		4930-4940	Vuggy	Limestone with large grains including some pyrite	3	
		4950-circ 45	Intercrystaline	Highly cemented oolitic limestone with some pyrite	5,3	
		5020-5030	Intercrystaline	Black to red shale	6	
15-093-20156	33-25S-36W	4840-4850	Intercrystaline	Sample is majority black to red shale, little to no limestone	4,2,5	48
		4850-4860	Intercrystaline	Majority shale with glauconite	4	47
		4890-4900	Intercrystaline	Limestone with apparent highly cemented ooids	4	
15-093-20778	28-25S-36W	4880-4890	Vuggy	Limestone has possible ooids and peloids along with some bryozoan	2,4,3	
		4940-4950	Vuggy	Very porous with possible peloids and ooids	2,3,4	
		4950-4960	Vuggy	Limestone has large grains much like above interval	2,3,4	

		4970-4980	Vuggy	Large grains with good porosity	2,3	54
		4979-circ 30	Vuggy	Same as above	3	
		4980-4990	Vuggy	Limestone has large grains and open pore space	2,3	
15-093-20793	16-25S-36W	4790-4800	Vuggy	Highly cemented oolitic limestone along with pyrite, bryozoan, and crinoids	3,5	
		4800-4810	Vuggy	A lot of crinoids along with limestone with open pores	5	51
		4810-4820	Intercrystaline	Highly cemented oolites and peloids in limestone with some chalcopyrite	3	57
		4820-4830	Vuggy/ Intercrystaline	Porous limestone with large amount of bryozoan	3,5	
		4870-4880	Vuggy	Vuggy ooilitic limestone	2,4	
		4895-4900	Vuggy	Majority shale with pyrite and chalcopyrite	3,5	

		4915-4920	Intercrystaline	Large amount of chalcopyrite with shale	3	52
		4960-4965	Vuggy	Abundant amount of ooids and peloids with little to no cementation	4,5	53

Thin-Sections

Table 2 lists the thin-section descriptions using a petrographical microscope. The Table includes the well API#, well location, sample depth in feet, porosity type, Folk and Dunham classifications, facies observed, extra comments, and images taken at that specific depth. The facies observed numbers are as follows, again with representative photomicrographs;

1) porous ooid grainstone (Figure 29)

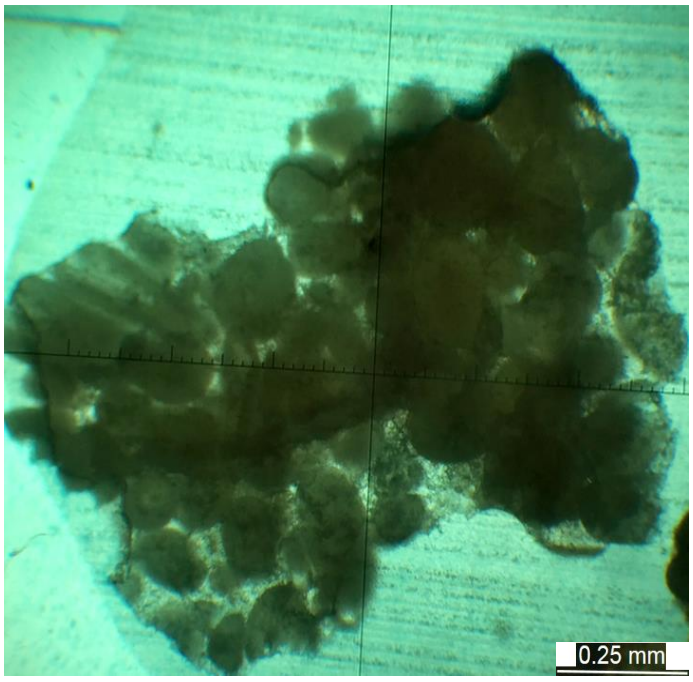

Figure 29. Thin section from well 15-093-20813.

2) highly-cemented ooid grainstone (Figure 30)

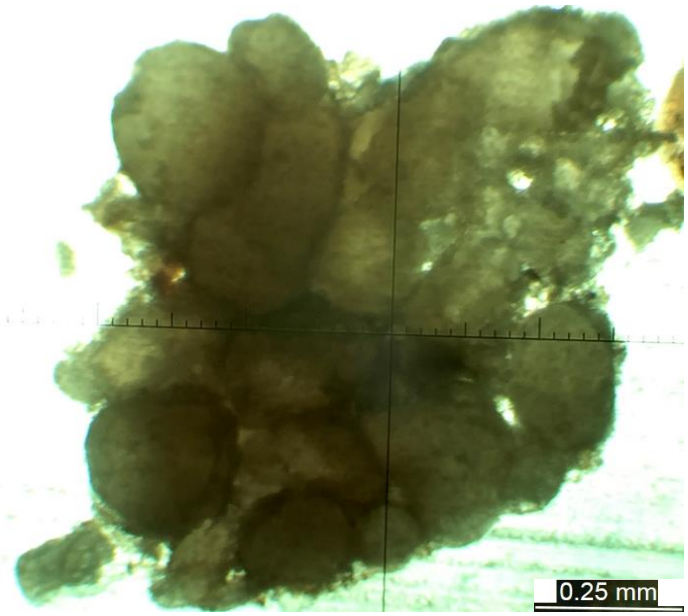

Figure 30. Thin-section from well 15-093-20778.

3) quartz-carbonate grainstone (Figure 32)

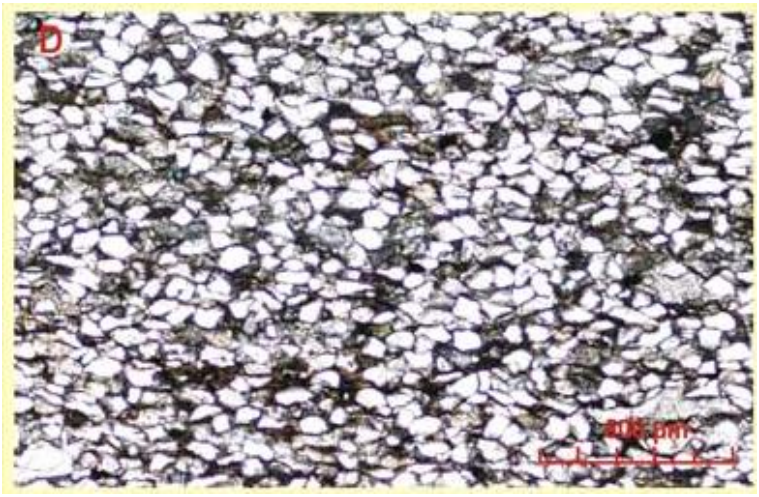

Figure 31. Example of the quartz-rich carbonate grainstone (Lianshuang and Carr, 2005).

4) peloidal grainstone (Figure 32)

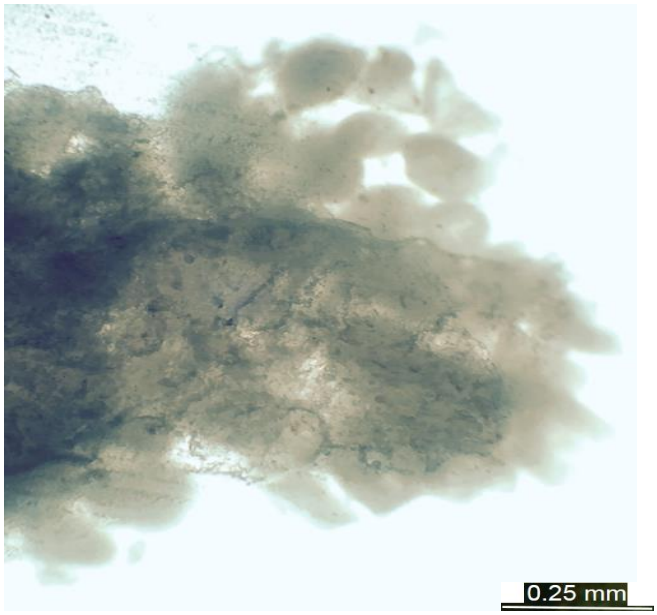

Figure 32. Thin-section from well 15-093-20778.

5) micritic mudstone (Figures 33,34)

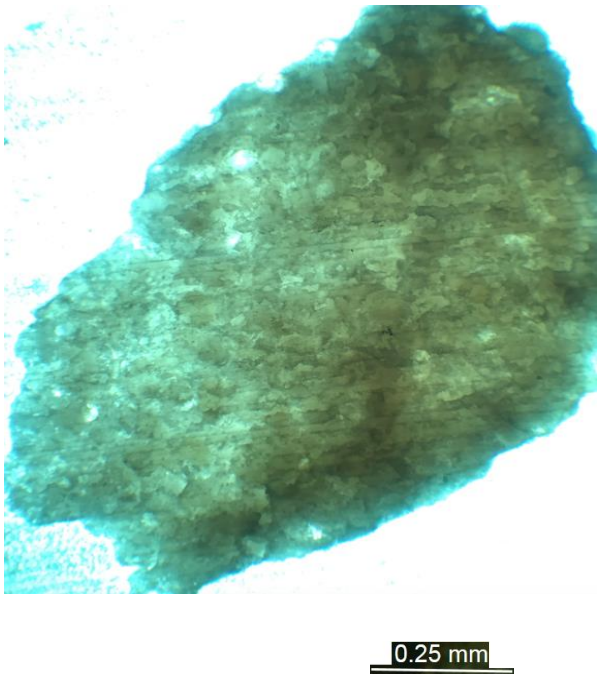

Figure 33. Thin-section from well 15-093-20813.

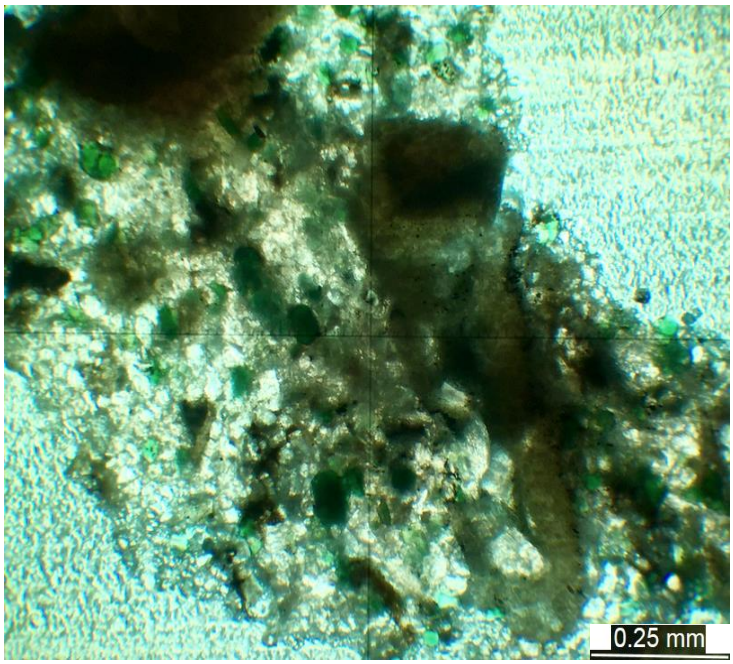

Figure 34. Thin-section from well 15-093-20156.

6) skeletal wackestone/packstone (Figures 35,36)

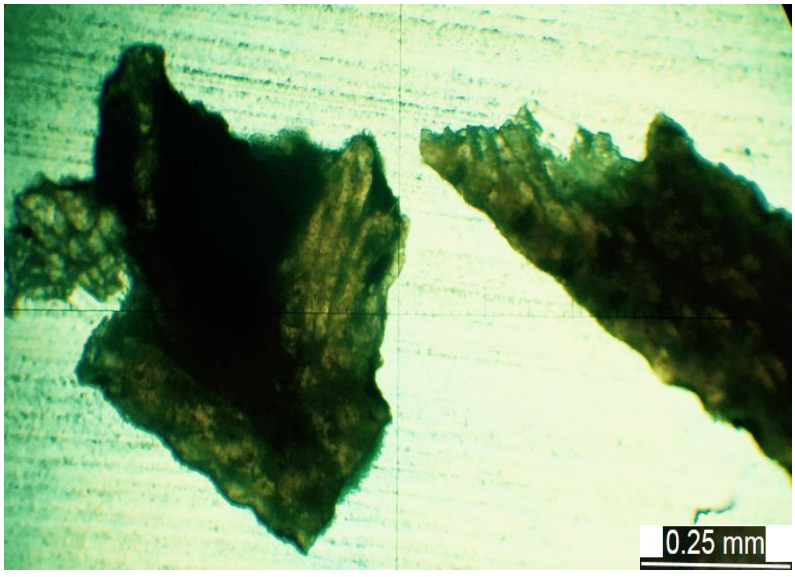

Figure 35. Thin-section from well 15-093-20793.

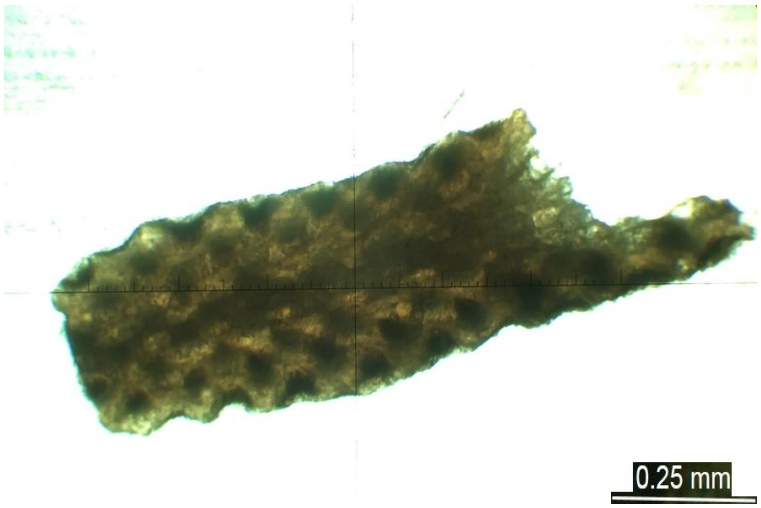

Figure 36**. Thin-section from well 15-093-20793**

Table 2 Descriptions of Thin-Sections

API#	LOCA-TION	DEPTH FEET	POROSITY TYPE	FOLK	DUNHAM	OBSERVED FACIES	COMMENTS	IMAGE FIG#
15-093-20156	33-25S-36W	4840-4850	Intercrystaline	Micrite	Mudstone	5		
		4850-4860	Intercrystaline	Micrite	Mudstone	5	Glauconite visible	57, 58
15-093-20778	28-25S-36W	4880-4890	Interooid	Oomicrite	Grainstone	1,2	Ooids and peloids	59
		4940-4950	Interooid	Oomicrite	Grainstone	1,2	Ooids and peloids	

		4950-4960	Interooid	Oosparite	Grainstone	1,4	Large ooid with majority peloid grains, good porosity	60, 61
		4970-4980	Interooid	Oomicrite	Grainstone	2,4	Large ooid and peloid grains with no porosity present	62
		4980-4990	Interooid	Oomicrite	Grainstone	1,2	Some cementation and porosity with ooid and peloid grains	63
15-093-20799	28-25S-36W	4810-4820	Intercrystaline	Micrite	Mudstone	5	Micritic mud with shale	
		4830-4840	Interooid	Oomicrite	Grainstone	2	Some ooids visible with majority micritic mud	

		4930-4940	Interooid	Oomicrite	Grainstone	1,2	Abundance of small ooids with micrite	64
		4940-4950	Interooid/Intra ooid	Oomicrite	Grainstone	1,2	Large ooids with micritic mud	
		4950-4960	Intercrystaline /Moldic	Micrite/ Oomicrite	Wackstone	5,2	Ooids present held together by micritic mud	65
15-093-20793	16-25S-36W	4790-4800	Intercrystaline	Micrite	Mudstone	5	Micrite with crinoids	66
		4800-4810	Interooid	Oomicrite	Grainstone	1,2	Porous ooids with crinoids	
		4810-4820					Chalcopyrite	67
		4820-4830					Abundance bryozoans	68, 69
		4870-4880	Intraooid	Oosparite	Grainstone	2,4	Highly crystalized with ooids and peloids	70

		4895-4900					Chalcopyrite with bryozoans	
		4960-4965	Interooid	Oosparite	Grainstone	1,4	Ooid and peloids with open pore spaces and little to no cement	71
15-093-20813	08-25S-36W	4870-4880	Intercrystaline	Micrite	Mudstone	5	Some ooids but majority cement	72
		4880-4890	Intercrystaline	Oomicrite	Packstone	2	Ooids present but highly crystalized	
		4900-4910	Growth or Framework				Bryozoan	72
		4930-4940	Intercrystaline	Micrite	Mudstone	5	Micritic mud with no distinct features	

		4950-Circ 45	Interooid	Oolite	Grainstone	1	Grain supported ooids and peloids	73
		5020-5030	Intercrystaline		Mudstone		Majority shale	

Chapter 5 - Discussion

Cuttings and Thin-Sections

A problem encountered in testing the reliability of the neural network model was the difficulty of procuring available cuttings. Of the 16 wells that were included in the model, only five had cuttings available at the KGS Library. Most problematic was the lack of cuttings from wells with predicted facies one (the porous ooid grainstone). One well with cuttings has 30 feet missing precisely over the predicted area, which suggests that evidence of this facies has been influenced by controlling which samples were released. Hence a direct test of the model is limited to these 5 wells. In well 15-093-20156 where the neural network predicted the presence of facies one, the cuttings were missing from the box. Well cuttings were used to determine the depositional facies within the St. Louis Limestone. I identified four different porosity types within the St. Louis; interparticle, intraparticle, vuggy, and intercrystaline. The reservoir quality facies (porous ooid grainstone) generally exhibited vuggy to interparticle porosity, while the other facies tended to be more intercrystaline.

Thin-sections made it possible to more accurately determine the facies by including the Folk and Dunham carbonate classification schemes. This is important when finding the porous

ooids grainstone facies because of its great reservoir potential compared to the other facies within the St. Louis.

Table one and Table two both agree on the descriptions of the cuttings, and what was observed in thin-section. Although I was not able to determine a facies solely based on cuttings, I was able to validate what I saw in cuttings with the thin-sections analyses.

Cross Section Comparisons

The original study by Martin included cross sections to show the distribution of facies in the stratigraphy that had been predicted by the neural network. I generated stratigraphic columns in the five wells of my observed facies to compare the predicted facies generated by the model with what is actually present.

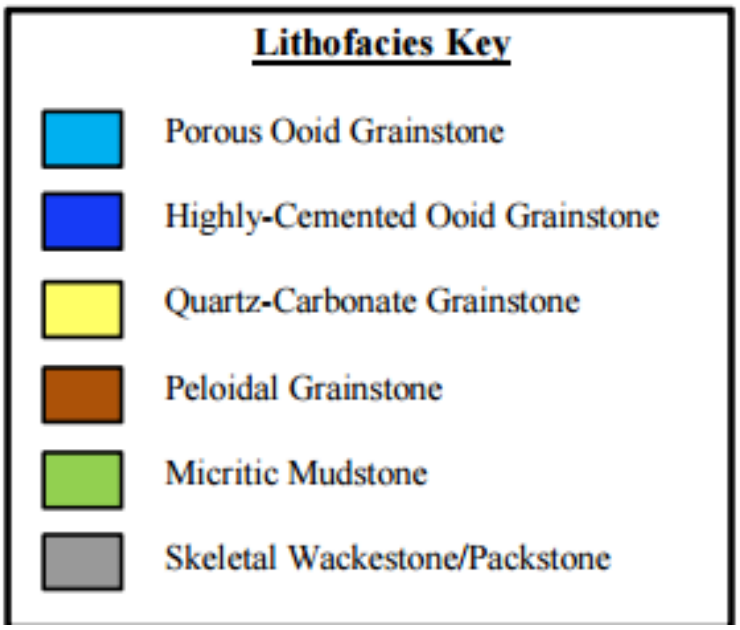

Figure 37. Predicted and observed lithofacies key.

In well 15-093-20813 cuttings were missing from the 4850-4870 foot interval (Figure 39). The neural network didn't predict producing facies one, even though I observed it in

cuttings analysis. It did appear relatively thin, based upon the number of cuttings, hence this could be below the resolution of the model.

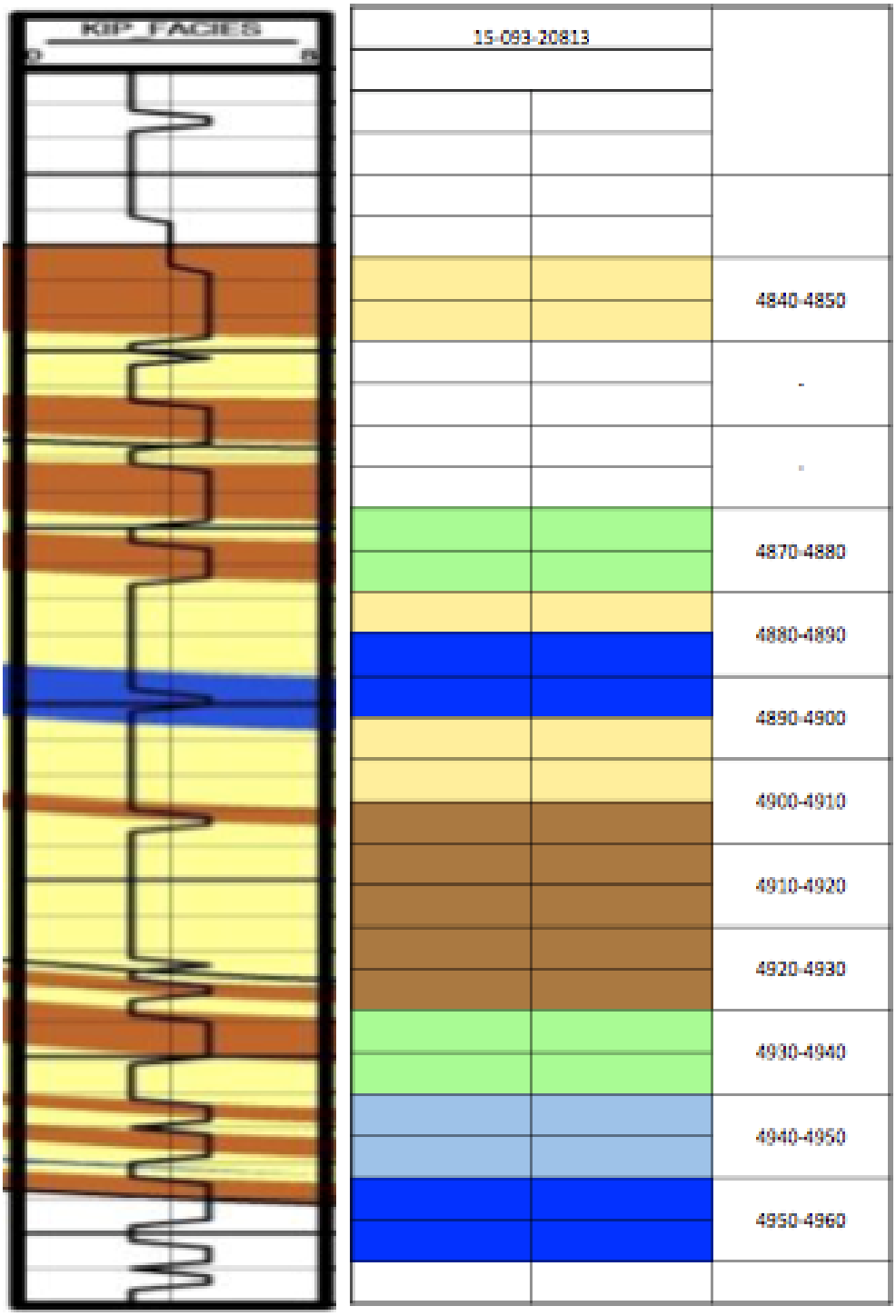

Figure 38. Well 15-093-20813 predicted facies cross section and observed facies cross section.

In well 15-093-20156 (Figure 40) the neural network predicted facies one, which was not observed in cuttings. The reason for this was missing cuttings after a depth of 4960, which is where the facies was predicted. Even though cuttings weren't available the presence of the facies is validated based on the production of this well, as discussed below.

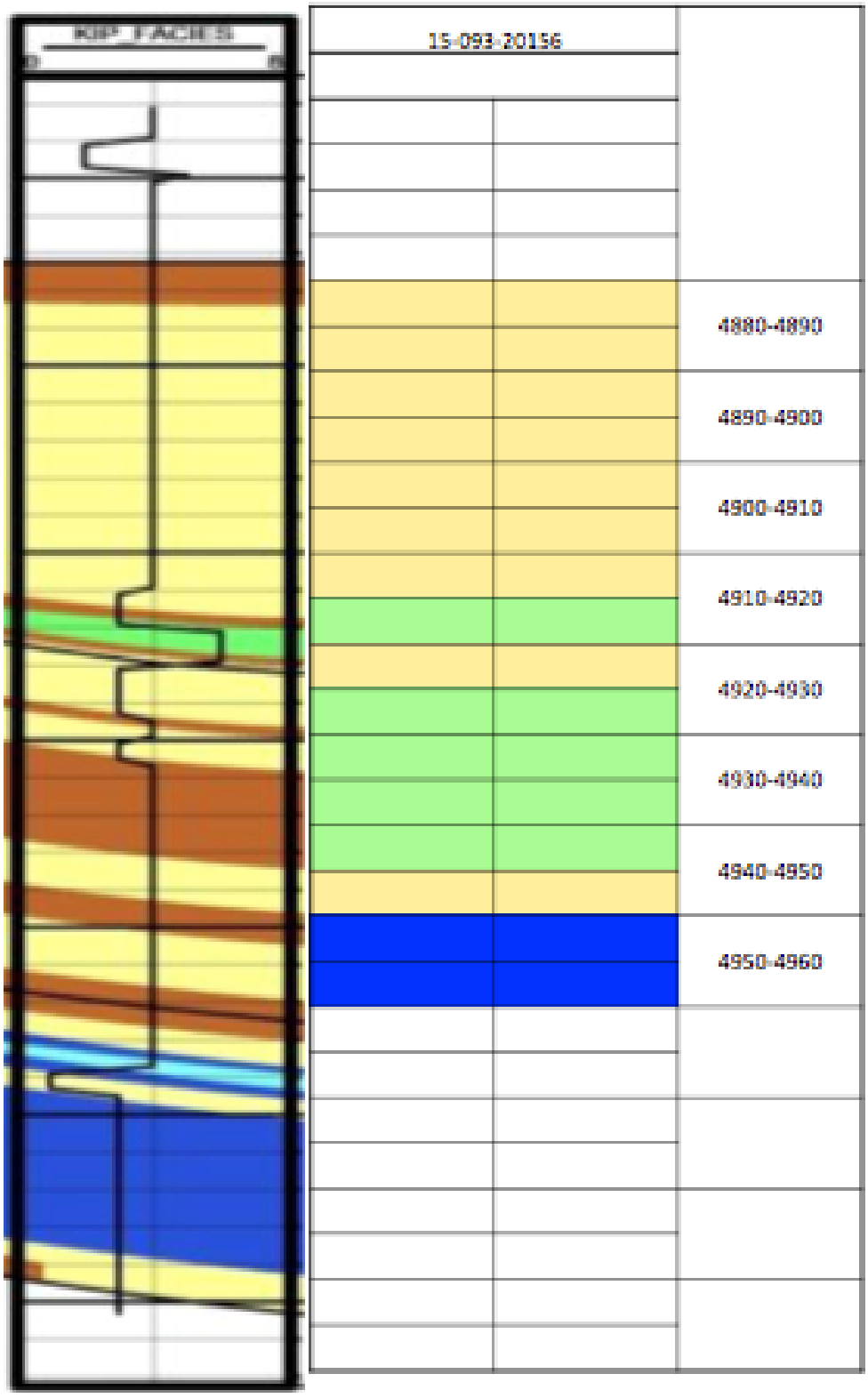

Figure 39. Well 15-093-20156 predicted facies cross section and observed facies cross section.

In well 15-093-20799 (Figure 41) the neural network never predicted facies one, but was seen in cuttings.

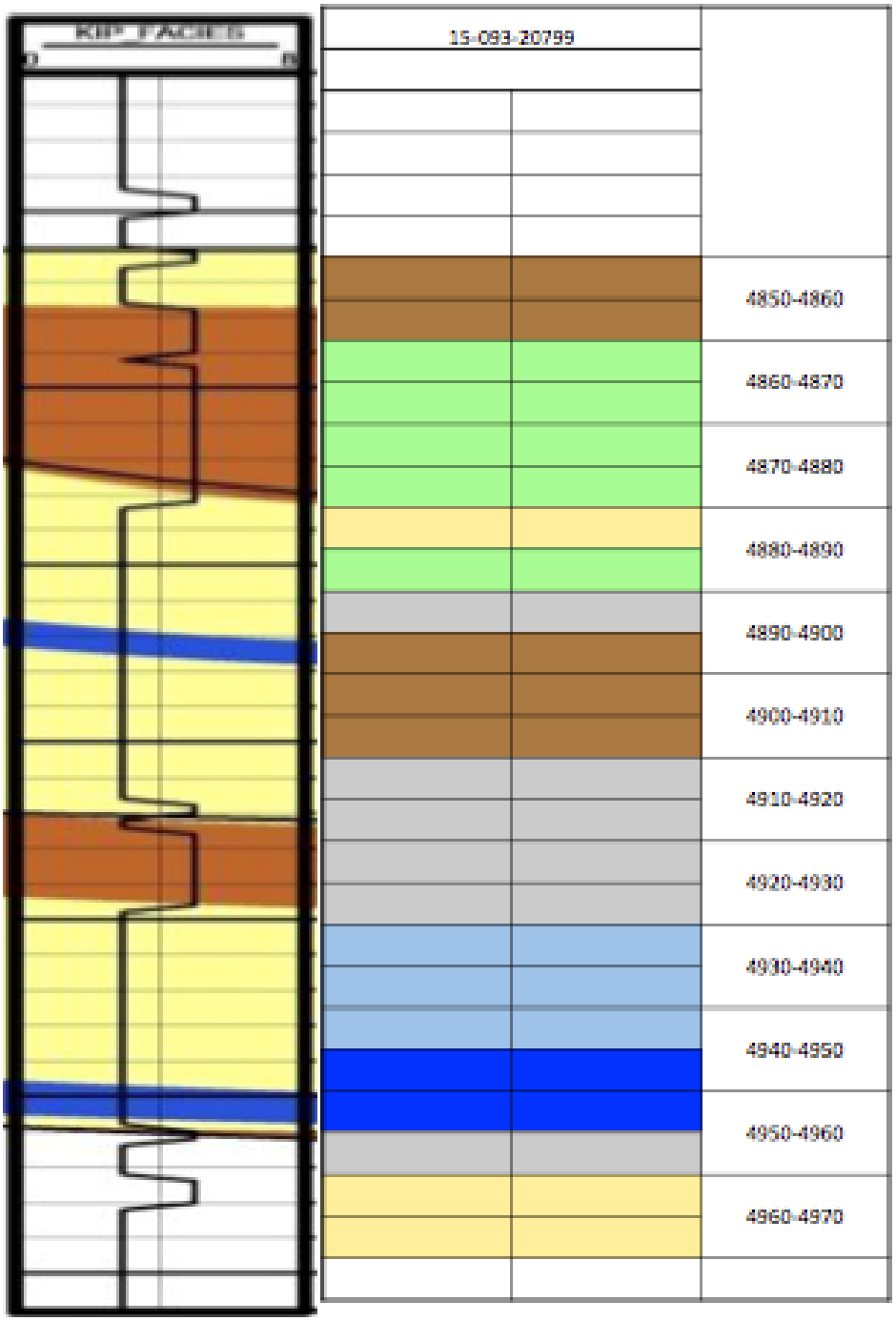

Figure 40. Well 15-093-20799 predicted facies cross section and observed facies cross section.

Well 15-093-20778 (Figure 42) was a dry hole giving the assumption that facies one wasn't present. In cuttings a large amount of facies four was observed, but was minimally predicted by the neural network.

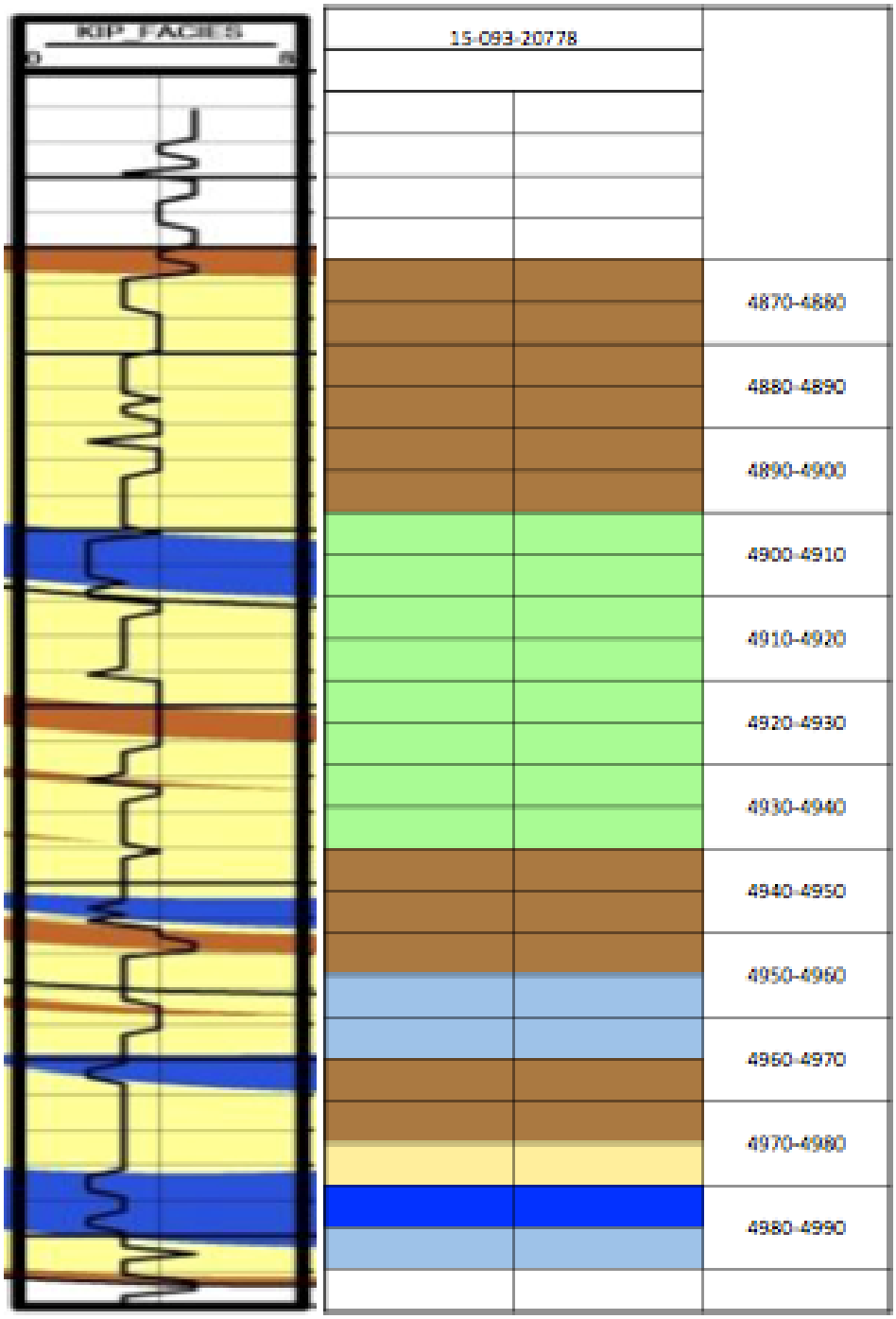

Figure 41. Well 15-093-20778 predicted facies cross section and observed facies cross section.

Well 15-093-20793 (Figure 43) was plugged and abandoned and was never predicted to have facies one, but was observed in small amounts. The well was also missing cuttings from 4935-4955 feet which made it difficult to validate the presence of facies one.

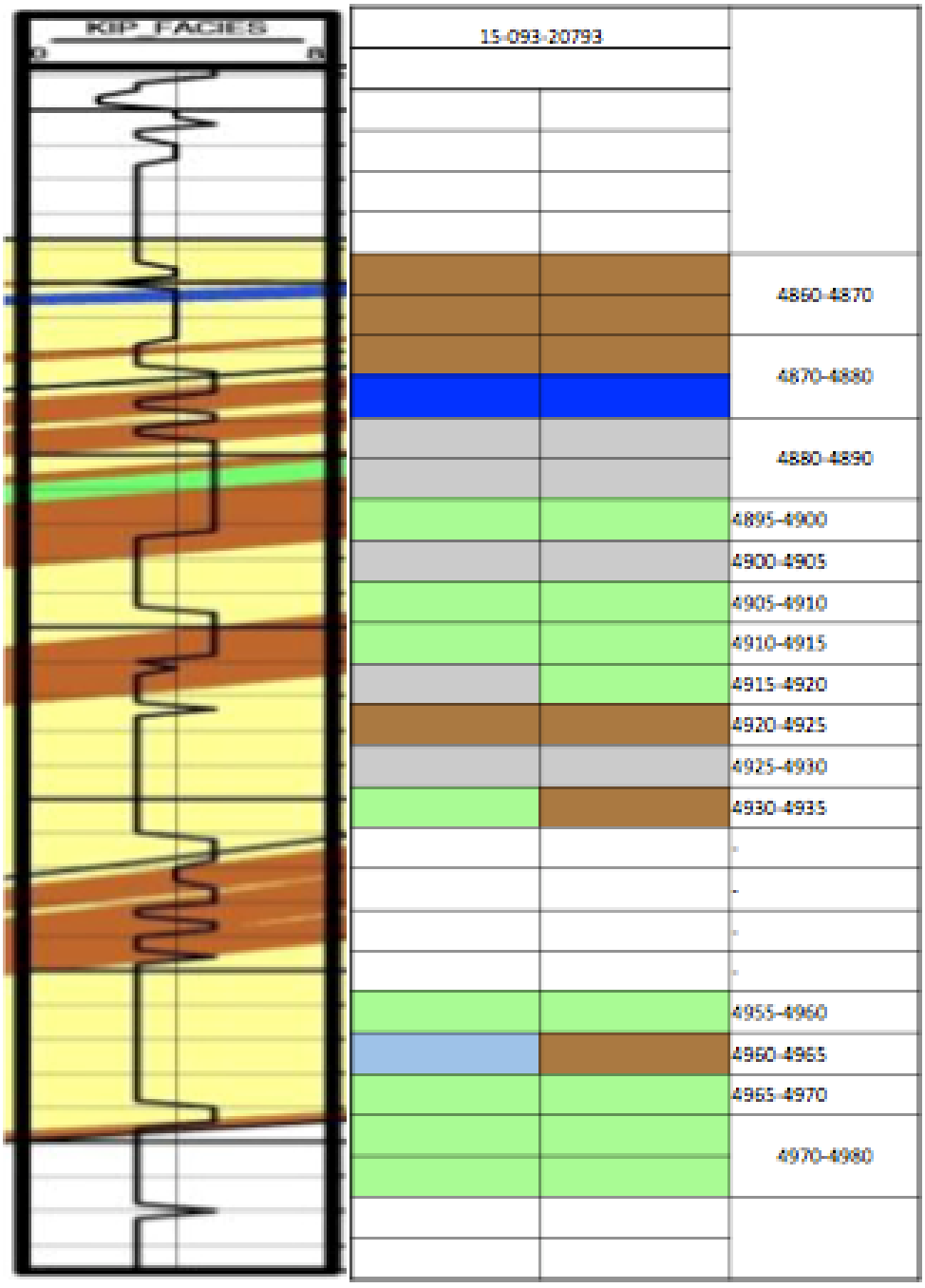

Figure 42. Well 15-093-20793 predicted facies cross section and facies observed cross section.

The poor correlation between the predicted cross sections by Martin (2015) and the observed facies can be attributed to many different factors. The dominant factor was the number of wells without cuttings, as well as the fact that three of the remaining wells had missing cuttings over the most important intervals.

Predicted and Observed Facies

The prediction of the six facies was made using the neural network model in the previous study by Martin (2015). Utilizing both cuttings and thin-sections a determination of the actual facies present at the given depth intervals was made. Scorecards were made for each individual well, as well as a master scorecard for all five of the wells used in the study. Overall the scorecard gives a percentage of absolute accuracy of the neural network at predicting each facies, and a combined accuracy predicting all the facies (Table 3). On the far right column of the scorecard the absolute accuracy at predicting each of the six facies is listed. The absolute accuracy of facies one (the target porous ooid grainstone) the accuracy is unknown. The reasoning for this is that of the five wells observed only one of them predicted facies one, and in that one well the cuttings were missing within the predicted interval. A determination of the predictive ability of the model for the productive facies was not testable using cuttings

The highest percent of accuracy (42%) came from facies three (the quartz carbonate packstone). This makes sense because this facies comprises approximately 60% of the St. Louis Limestone (Martin, 2015), which is also why the predicted percentage of facies three is significantly higher than that of the other facies. For these reasons the scorecard is giving either a low percentage of accuracy because the facies wasn't present, or giving a high percentage of accuracy because the facies makes up a majority of the stratigraphy. The overall absolute accuracy (located in the bottom right of the scorecard) gives a very low percentage of accuracy

for the neural network. This is not realistic because the accuracy is artificially lowered by missing cuttings, but also potentially boosted by facies that make up a majority of the limestone unit. The interval by which the neural network predicted (one-foot intervals) and the interval that cuttings were observed (ten-foot intervals) also makes it impossible to pinpoint an observed facies at every foot, significantly lowering the overall accuracy.

Table 3 Scorecard for 5 Predicted Wells and Their Accuracies

Observed Facies		Predicted Facies							Absolute Accuracy
		1	2	3	4	5	6	Grand Total	
	1		3	7	3	6		19	Unknown
	2		6	13	5	6		30	20%
	3			11	8	5	1	24	42%
	4		5	21	11	7		44	25%
	5		4	23	11	14	3	55	25%
	6			11	1	7	1	20	5%
	Grand Total	0	18	85	39	45	5	192	Facies Prediction Model Accuracy
	Proportion Percentage	0%	60%	354%	89%	82%	25%		Absolute Accuracy
	Difference	19	11	61	6	10	15	122	23%

Table Formulas

Body of the Table: Count of Predicted Facies

Proportion Percentage: (Grand Total (x-axis)/ Grand Total (y-axis))*100

Difference: Absolute value of Grand Total (x-axis)–Grand Total (y-axis)

Absolute Accuracy: (Count of Predicted Facies/ Grand Total (y-axis))*100

Facies Predicted Absolute Accuracy: Average of Facies Absolute Accuracy

Neural Network Accuracy

The agreement between observed facies using cuttings and the predictions made by the neural network appeared to be extremely hit and miss. The assumption by Martin that the distance from the network model effected accuracy was also not observed. In well 15-093-20156, where the distance from the model was approximately 4.2 miles, the overall accuracy of the predictions was at 60% (Figure 20). In contrast the accuracy observed in the well closest (1.8 miles) to the model (well 15-093-20813), was at a lower 33% accuracy (Figure 21). There are many factors that could have affected the accuracies of the predictions, such as the quality of cuttings, missing cuttings, and the subsurface geometry of the depositional environment. Perhaps the most important factor affecting the accuracy of the model was the different resolutions of data. Predictions were made every one-foot, while the cuttings were collected every ten feet. This lowered the accuracy because within ten feet there could have been four of the six facies predicted, when I only observed one of the facies. If the network predicted facies 2, 3, 4, and 6 when I only observed facies 2, the accuracy drops to 25%. The change in facies from foot to foot can be seen in the predictions in Appendix C. This illustrates that the network is perhaps unreliable because of the improbability that facies will change four times within 10 feet. The problem of missing cuttings also hindered the ability to test the accuracy of predicted facies one (the porous ooid grainstone). In the one well that the neural network predicted this facies, cuttings were missing from the box.

The fact that this well produces indicates that the producing facies must be present, even though it couldn't be validated by an analysis of the cuttings. In this manner, a test of the model's robustness in predicting the producing facies is possible, assuming that facies one must

be present in producing wells, because it is the only productive facies in this formation (Martin, 2015).

Production data of the five wells studied can give insight to the accuracy of the neural network. Well 15-093-20156, the only well that had a prediction of facies one (the porous ooid grainstone), produced 297,634 bbls since its completion in 1997. Facies one must be present because of the well's production. Well 15-093-20786 (Figure 19) also produced where facies one was predicted. Well 15-093-20289 (Figure 19) has produced 1,874,584 mcf, validating the prediction of facies one. Well 15-093-20799 has produced 80,030 bbls, which indicates that the producing facies must be present, as indicated by the cuttings analysis.

The accuracy of the model may be tested across all of the wells included by Martin (2015) using the same assumption that production must indicate the presence of the productive facies one. In Figure 43 the 16 wells included in the previous study are placed on an isopach map showing the thickness of the St. Louis C zone, which includes the producing facies (the porous ooid grainstone). These wells are indicated by colored open circles, and the cored wells used to calibrate the neural network predictions are identified by black stars. The green circles indicate agreement between the predicted facies one and a producing well. The orange circles indicate wells where the facies wasn't predicted but the well produced oil. The red circles indicate wells where facies one was not predicted and the wells were not productive (dry holes).

As can be seen on the map (green circles) all of the wells predicted to have facies one are producers. There is complete agreement between the network model in its prediction of the presence of the productive facies. The model is not as robust when facies one is not predicted. Slightly over half (55%) of the wells that did not predict the facies were indeed dry, and presumably did not have facies one present (red circles) and were in agreement with the model.

The remaining wells produced, even the model did not predict a productive facies (orange circles). These were clearly not in agreement with the model, which occurred 45% of the time.

The presence of productive facies in wells not predicted by the model might be due to thickness variations between wells used to calibrate the model and the wells that produce without the prediction. The cored well used to make the neural network predictions located in T26S R36W penetrates the thickest portion of the St. Louis C zone at about 22 feet thick. All of the predicted wells near this were productive. On the other hand, the cored well used to calibrate the neural network located in T25S R36W penetrates the St. Louis C zone at a thickness of approximately 8 feet. None of the wells predicted within that township and range had a prediction of facies one, although three of them were producers. Based on these observations, the ability of the neural network to predict facies one might be a function of the thickness of the target facies in the cored well rather than the distance from the cored well as previously believed. This is related to the process used by neural network model to predict these facies. When facies in the cored wells are correlated to signatures on the continuous well logs, there is a more prominent well log signature on facies 20 or more feet thick. A cored well that has 6-8 feet thickness of facies one does not have as prominent well log signature, making it difficult for the network to predicted that facies. This can also be seen in the cored well located in T24S R36W, where none of the five wells had facies one predicted, but two of the wells were producers, indicating the presence of the facies. Had more cuttings been available related better test of the predicted facies to actual production as a function of facies thickness could be made.

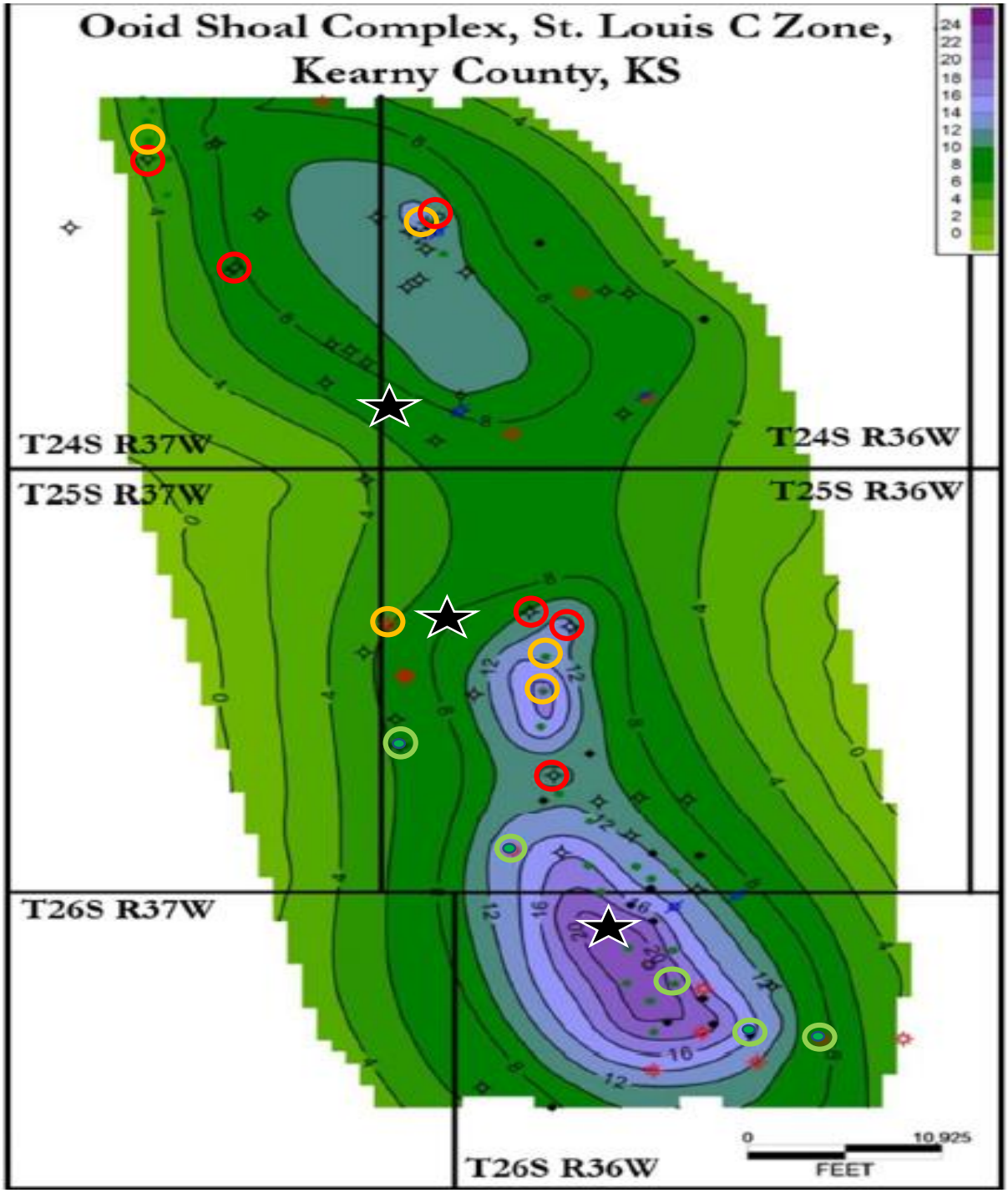

Figure 43. Map of neural network predicted wells. Green dots represent well with predicted facies one and are producing (agreement). Red dots represent facies one not predicted of and no production (agreement). Orange dots represent facies one not predicted but are producing (no agreement).

Chapter 6 - Conclusion

The St. Louis Limestone of south-central Kansas has experienced a great deal of oil and gas production over the years. The St. Louis can be broken into six different depositional facies including 1) porous ooid grainstone, 2) highly-cemented ooid grainstone, 3) quartz-carbonate grainstone, 4) peloidal grainstone, 5) micritic mudstone, 6) skeletal wackestone/packstone. The majority of this great production has been from the porous ooid grainstone depositional facies. This facies is relatively thin, ranging up to approximately 24 feet at its thickest, with excellent porosity. Identifying these facies is important when trying to predict where this productive reservoir quality facies is located.

A neural network was constructed to predict the facies within the St. Louis laterally from multiple cored wells in Kearny County, Kansas in a previous study by Martin (2015). This model predicted the lateral distribution of all six facies in wells in the area. This study attempted to validate the accuracy of these predictions by looking at cuttings in five of the predicted wells.

The predictions made by the neural network and the facies observed through cutting and thin-section analyses were compared to determine accuracy. The overall accuracy of the predictions was at 23%. This is not considered a good test of the model because of the lack of wells with cuttings available, and missing cuttings across key intervals in those wells that had cuttings.

A test of the model's ability to predict the productive facies was made using the production of the wells included in the previous study. There was 100% agreement between wells with predicted facies one and actual production. Every time the neural network predicted facies one the well was a producer. In wells where facies one was not predicted, however, 45%

of these were producing wells. These wells might represent a thickness of the productive facies below a critical value compared to the well used to calibrate the model.

The correlation of producing wells and missing cuttings strongly suggests that the productive facies was indeed present where the neural network predicted. The thickness of the porous ooid facies in the cored wells used to make predictions may also have been a major factor in the networks ability to predict the presence of this facies. The only alternate conclusion would be an additional productive facies, not recognized by previous studies in the area.

There was no correlation observed in the accuracy of the prediction and the distance away from the cored well used in the neural network model. The neural network model is very accurate in predicting the production potential of a well. Further tuning to increase the sensitivity of the model could reduce the number of wells without the prediction that actually contain the producing facies.

References

Baars, D.L., W. Lynn Watney, Don W. Steeples, and Erling A. Brostuen. "Petroleum: A Primer for Kansas." *www.kgs.ku.edu*. Kansas Geologic Survey, 1989. Web. 29 Dec. 2015.

Dikkers, A. J., 1985, Geology in petroleum production: New York, Elsevier, 239p.

Dunham, R. J., 1962, Classification of carbonate rocks according to depositional texture. In: Ham, W. E. (ed.), Classification of carbonate rocks: American Association of Petroleum Geologists Memoir, p. 108-121.

Embry, AF, and Klovan, JE, 1971, A Late Devonian reef tract on Northeastern Banks Island, NWT: Canadian Petroleum Geology Bulletin, v. 19, p. 730-781.

Evans, P.S., and Newell, K.D., 2013, The Mississippian Limestone Play in Kansas: Oil and Gas in a Complex Geologic Setting, http://www.kgs.ku.edu/Publications/PIC/pic33.html

Flenthrope, Chris. 2007 "Developing an Exploration Model by Investigating the Geologic Controls on Reservoir Production within the Fort Scott Limestone, Ness County, Kansas." Thesis. Kansas State University. Print.

Folk, R.L., 1959, Spectral subdivision of limestone types, in Ham, W.E., ed., Classification of carbonate Rocks-A Symposium: American Association of Petroleum Geologists Memoir 1, p. 62-84.

Goebel, E.D., December 1968, Stratigraphic Succession in Kansas: Mississippian System, http://www.kgs.ku.edu/Publications/Bulletins/189/06_miss.html

Handford, C.R., 1988, Review of carbonate sand-belt deposition of ooid grainstones and application to Mississippian reservoir, Damme Field, southwestern Kansas: American Association of Petroleum Geologists Bulletin, v. 72, p. 1184-1199. http://www.kgs.ku.edu/PRS/County/klm/kearny.html

"Kansas Crude Oil Proved Reserves." *www.eia.gov*. U.S. Department of Energy, 19 Nov. 2015. Web. 29 Dec. 2015.

Kearny County, Oil and Gas Fields, Kansas Geologic Survey, 2016.

Lianshuang, and Carr. "Core Description of the St. Louis Limestone in the Big Bow West, Sand Arroyo Creek, and Sand Arroyo Creek Southwest Fields, Southwest Kansas." *KGS.KU.EDU*. Kansas Geologic Survey, 1 May 2005. Web. 4 Jan. 2016.

Martin, Keithan. 2015 "Integrating Depositional Facies and Sequence Stratigraphy in Characterizing Carbonate Reservoirs: Mississippian Limestone, Western Kansas." Thesis. Kansas State University, Print.

Montgomery, S., and Frans, E. 2000. Schaben Field, Kansas: Improving Performance in a Mississippian Shallow-Shelf Carbonate (E&P Notes). AAPG Bulletin, 84(8), 1069- 1086.

Moore, C.H., 1989, Carbonate diagenesis and porosity: New York, Elsevier, 338p.

"Reservoir Characterization of Mississippian St. Louis Carbonate Reservoir Systems in Kansas, Stratigraphic and Facies Architecture Modeling." *Www.kgs.ku.edu*. Kansas Geologic Survey, 2003. Web. 29 Dec. 2015.

Scoffin, T. P., 1987, An introduction to carbonate sediments and rocks: New York, Chapman and Hall, 274p.

Skelton, Lawrence H. "A Brief History of the Kansas Oil and Gas. Web. 29 Dec. 2015.

Wilson, J. L., 1975, Carbonate Facies in Geologic History: New York, Springer-Verlag, p. 94.

Appendix A – Images of Well Cuttings at Approximately 20X Power

Figure 44. Well cutting from well 15-093-20799.

Figure 45. Well cutting from well 15-093-20156.

Figure 46. Well cutting from well 15-093-20156.

Figure 47. Well cutting from well 15-093-20799.

Figure 48. Well cutting from well 15-093-20813.

Figure 49. Well cutting from well 15-093-20793.

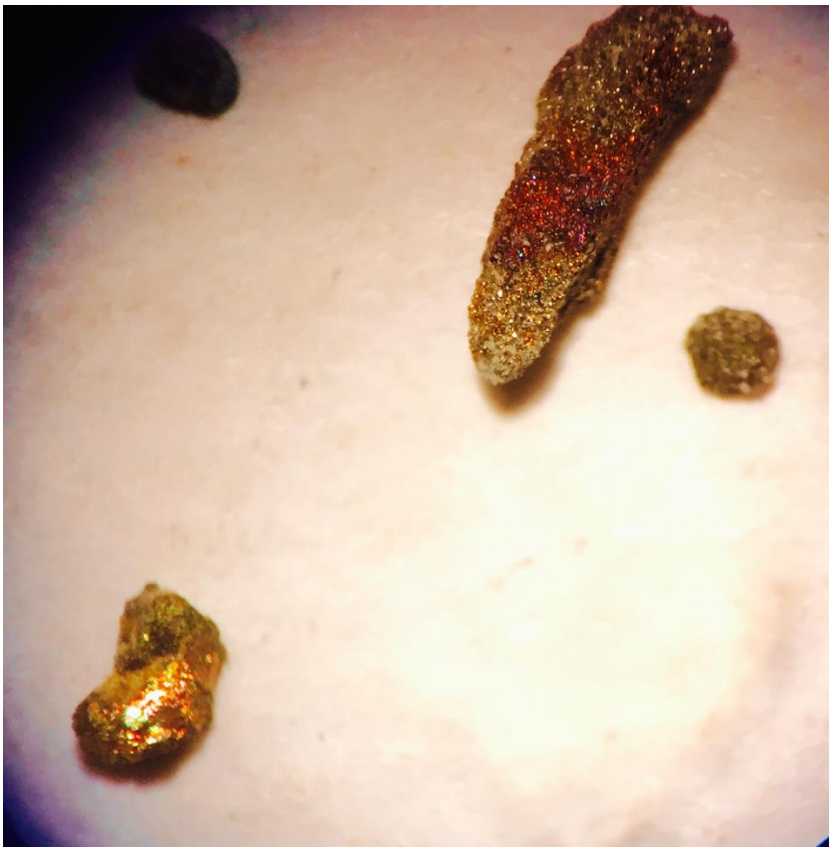

Figure 50. Well cutting from well 15-093-20793.

Figure 51. Well cutting from well 15-093-20793.

Figure 52. Well cutting from well 15-093-20778.

Figure 53. Well cutting from well 15-093-20799.

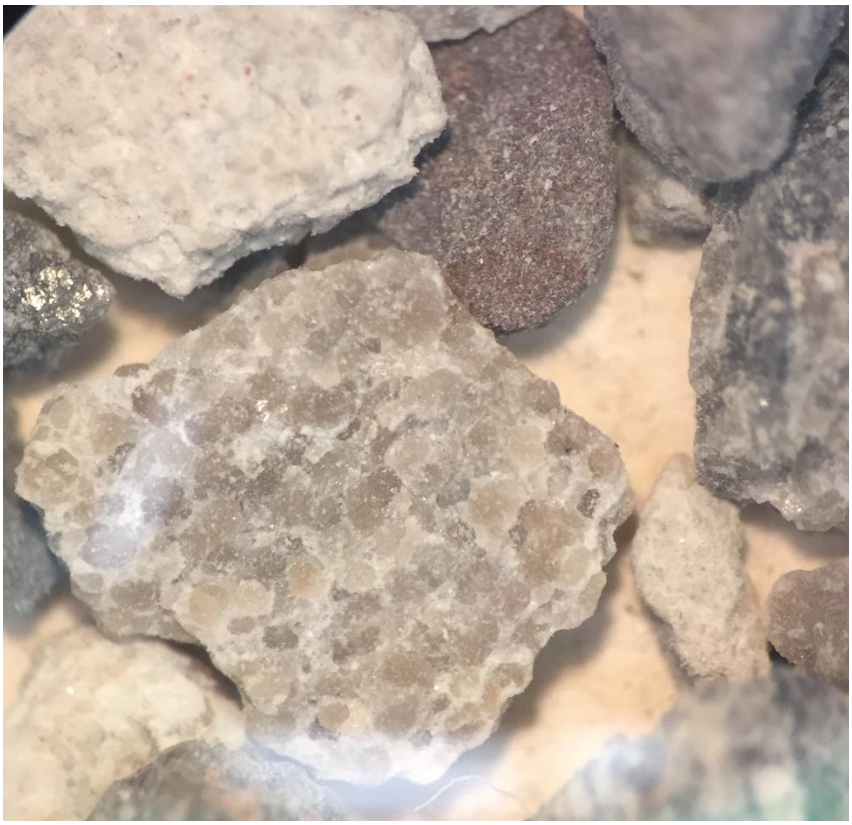

Figure 54. Well cutting from well 15-093-20813.

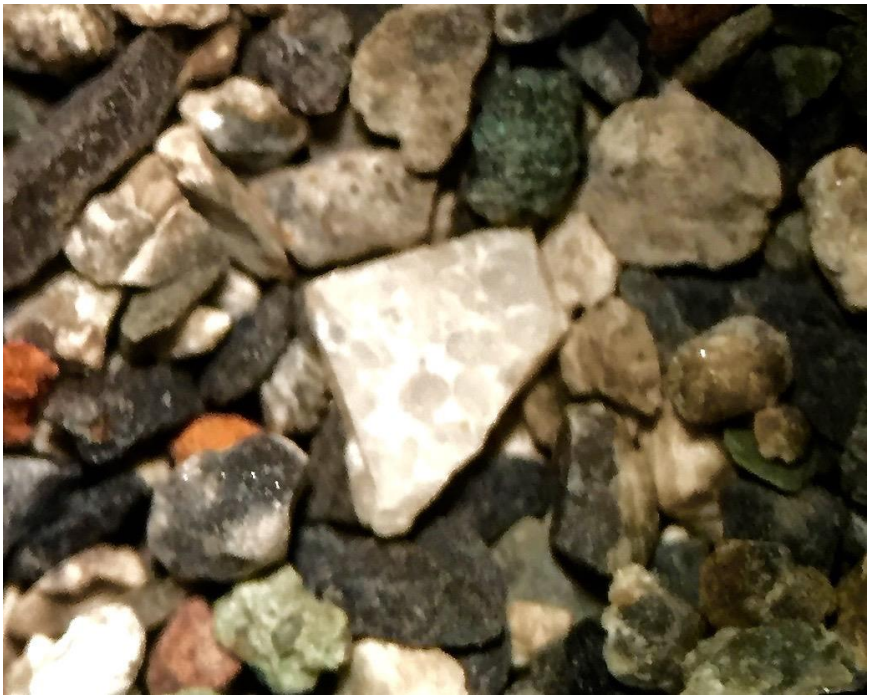

Figure 55. Well cutting from well 15-093-20793.

Appendix B – Pictures of Thin-Sections at 4X/.10 Power

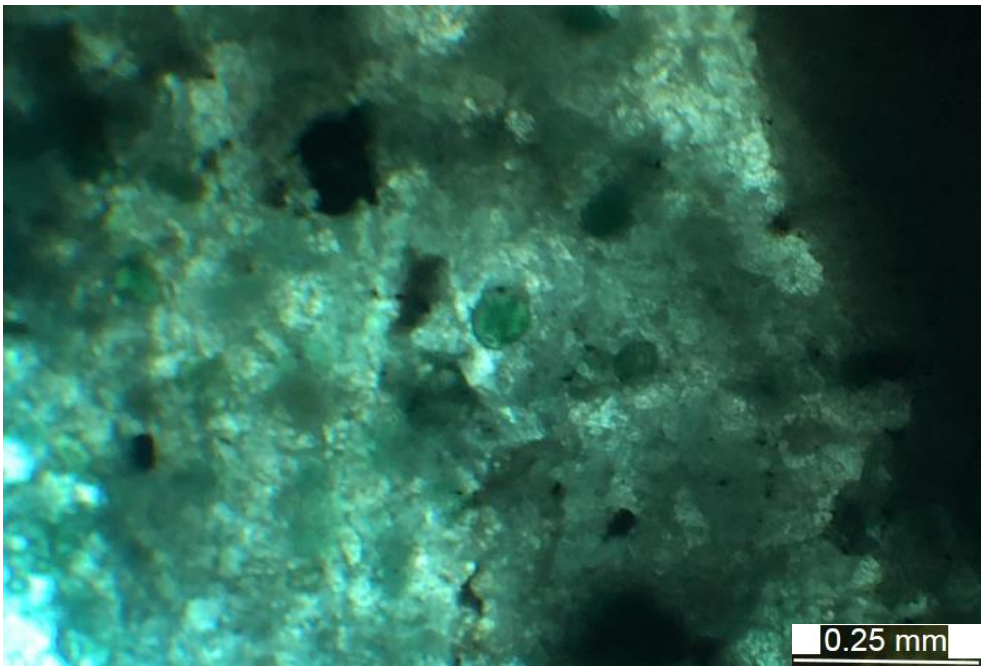

Figure 56. Thin-section from well 15-093-20156.

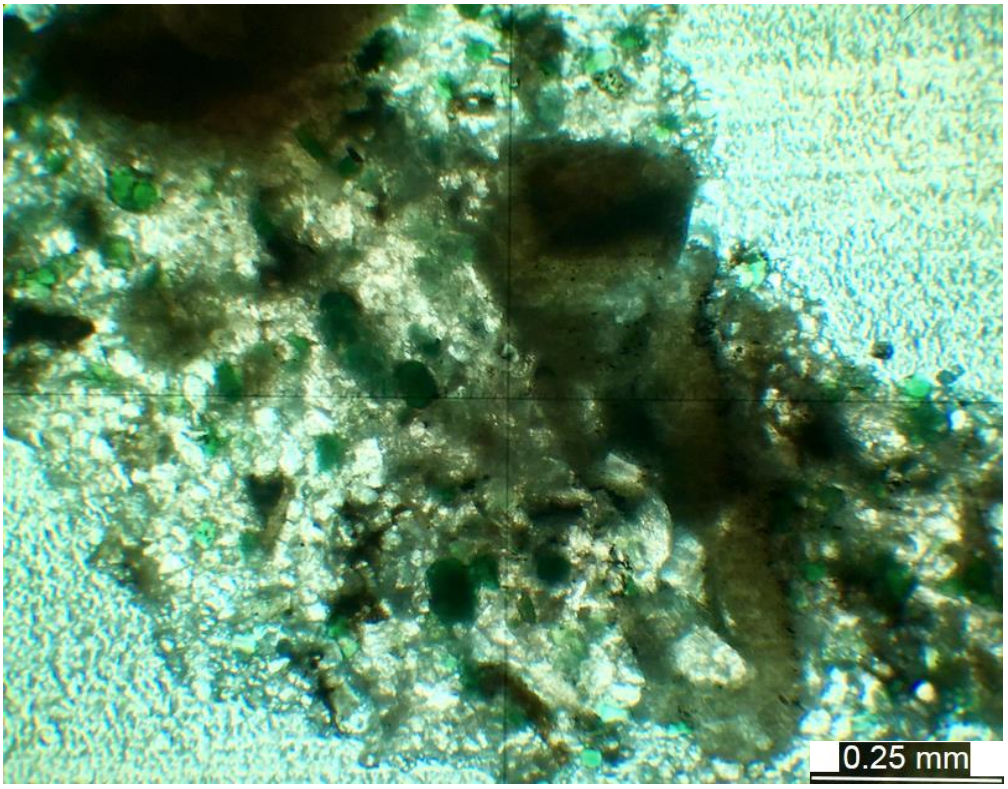

Figure 57. Thin-section from well 15-093-20156.

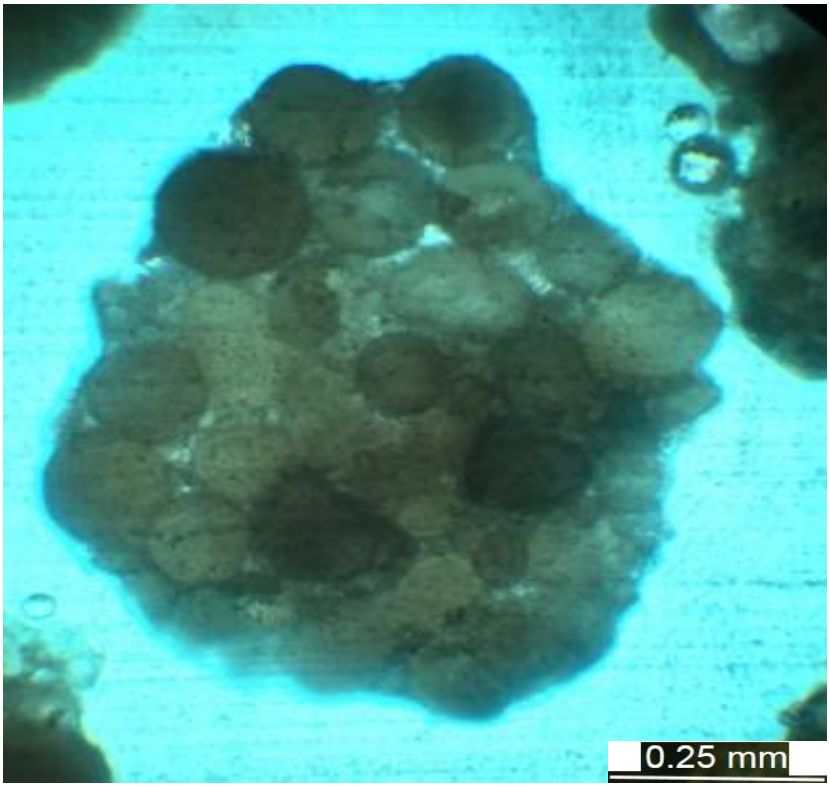

Figure 58. Thin section from well 15-093-20778.

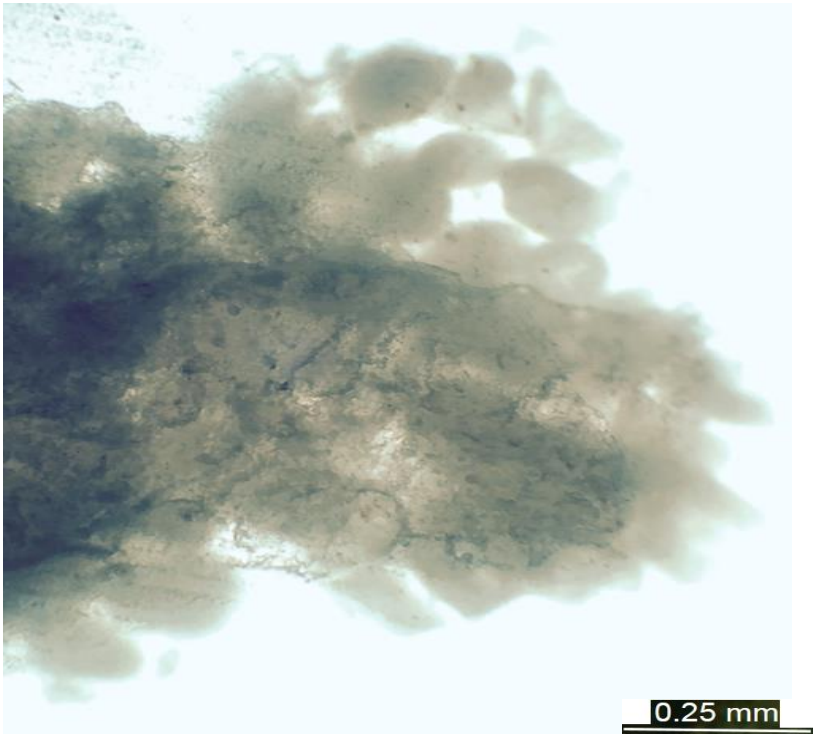

Figure 59. Thin-section from well 15-093-20778.

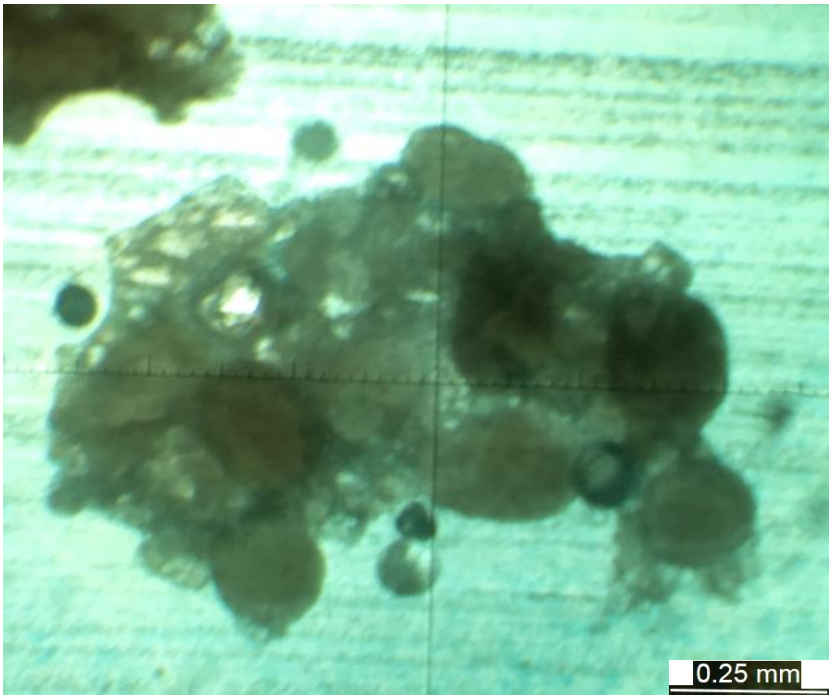

Figure 60. Thin-section from well 15-093-20778.

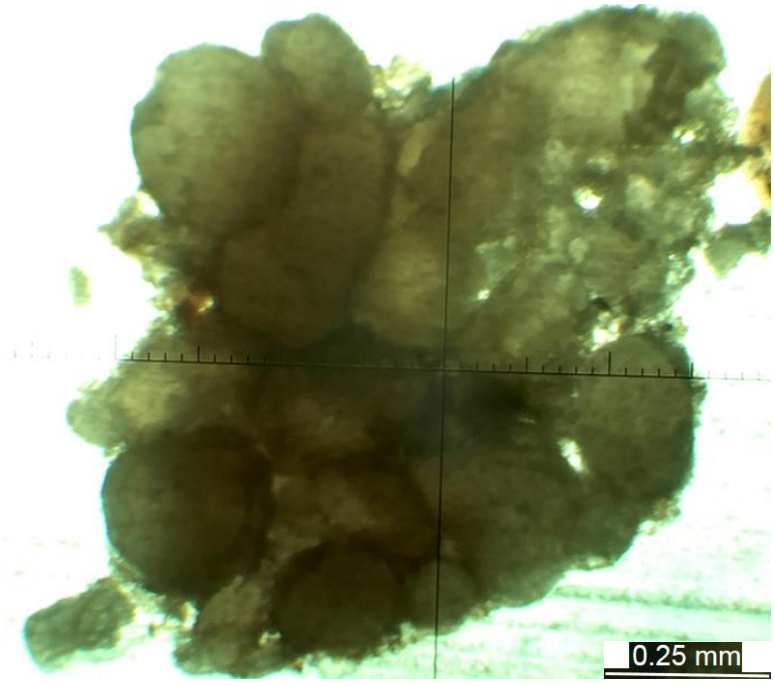

Figure 61. Thin-section from well 15-093-20778.

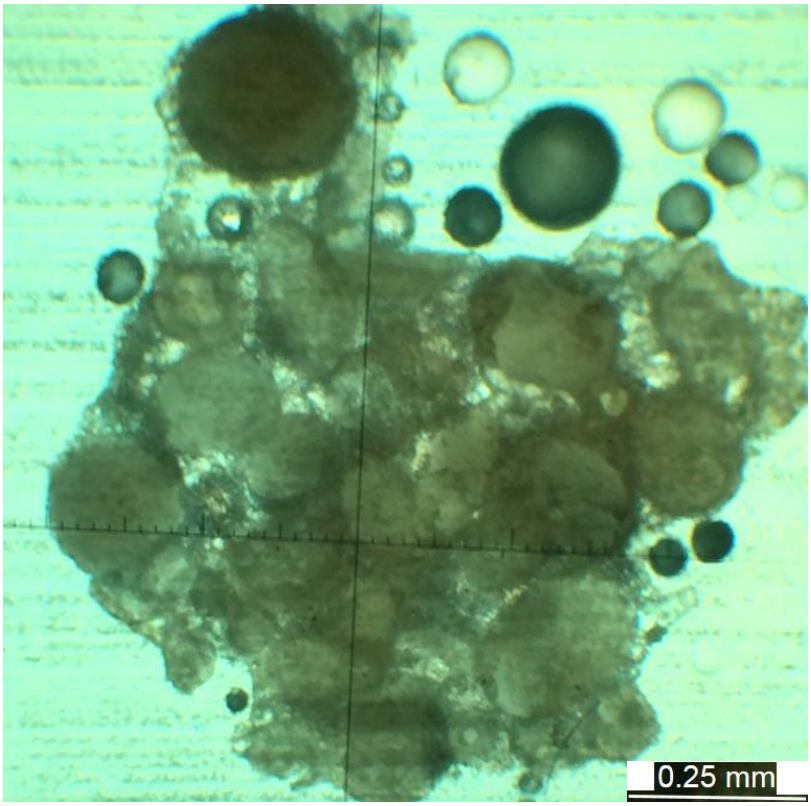

Figure 62. Thin-section from well 15-093-20778.

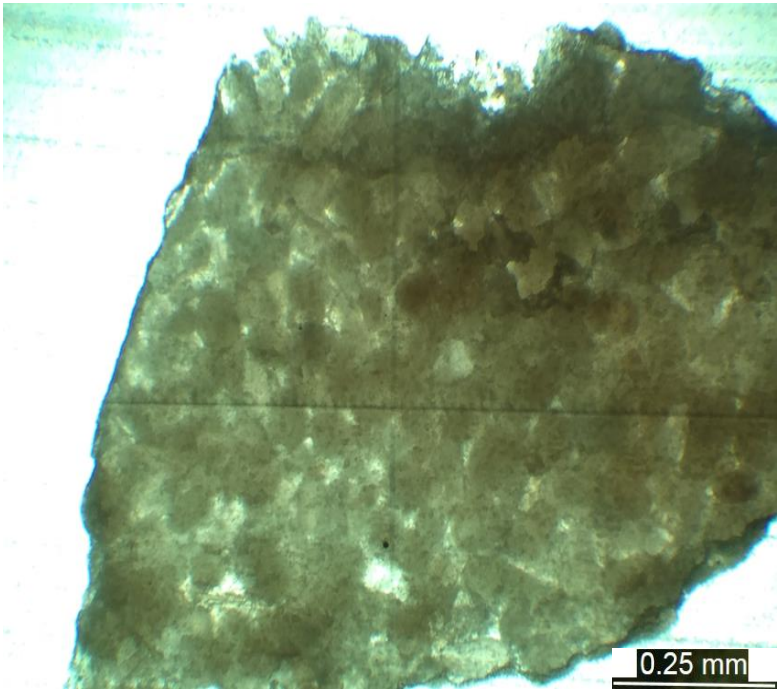

Figure 63. Thin-section from well 15-093-20779.

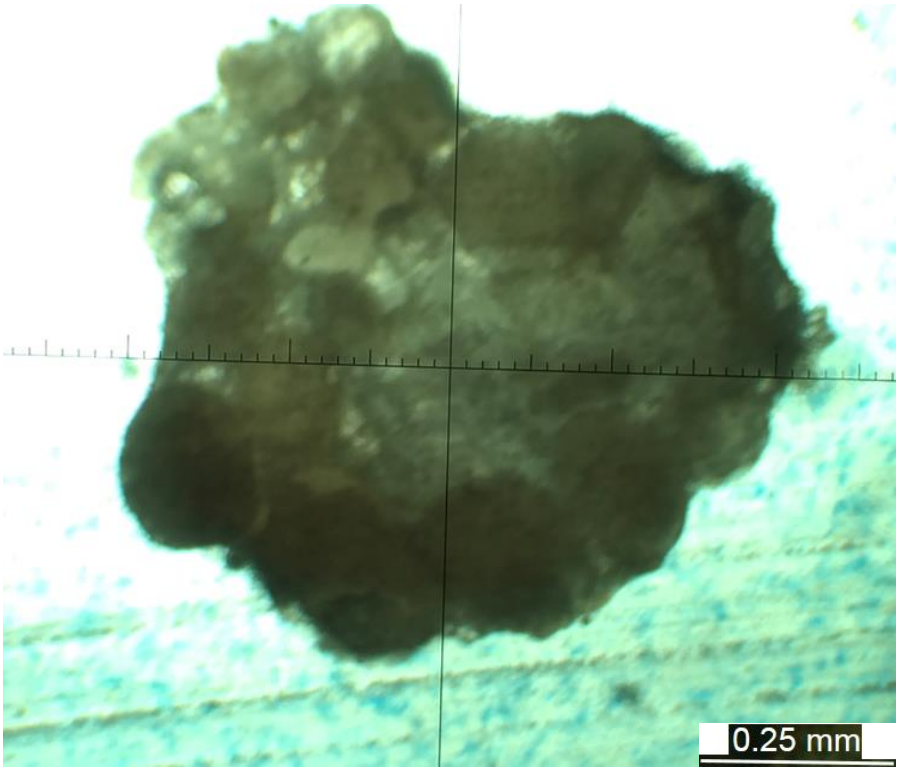

Figure 64. Thin-section from well 15-093-20799.

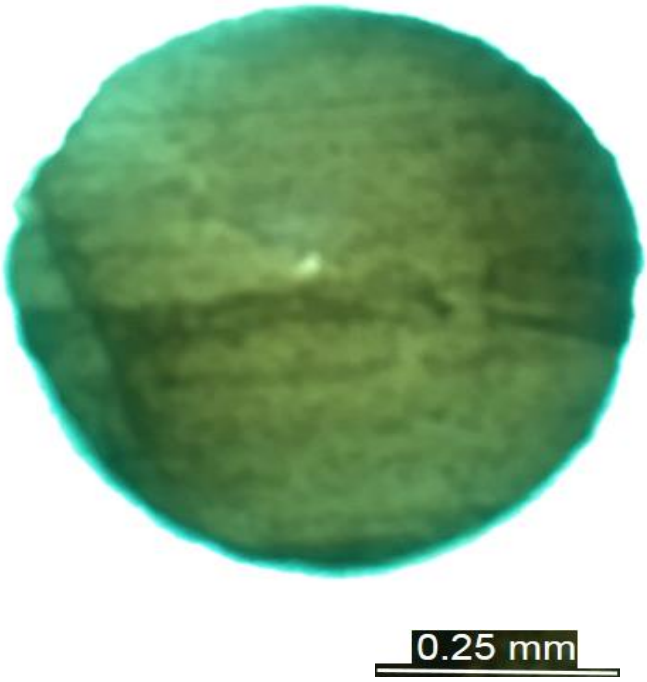

Figure 65. Thin-section from well 15-093-20793.

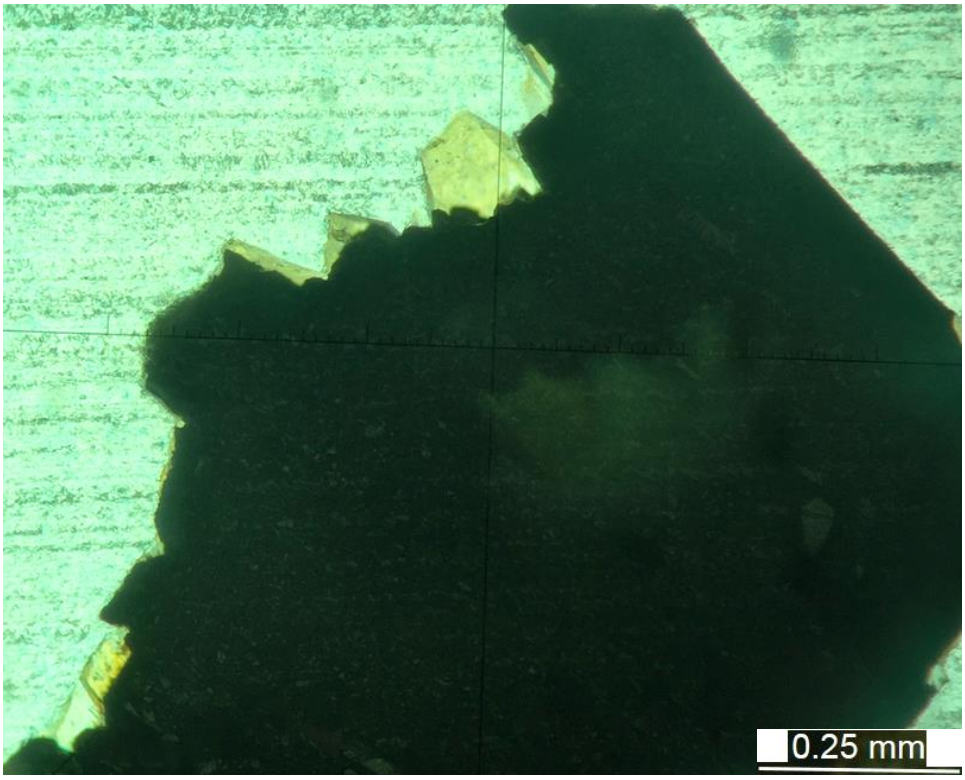

Figure 66. Thin-section from well 15-093-20793.

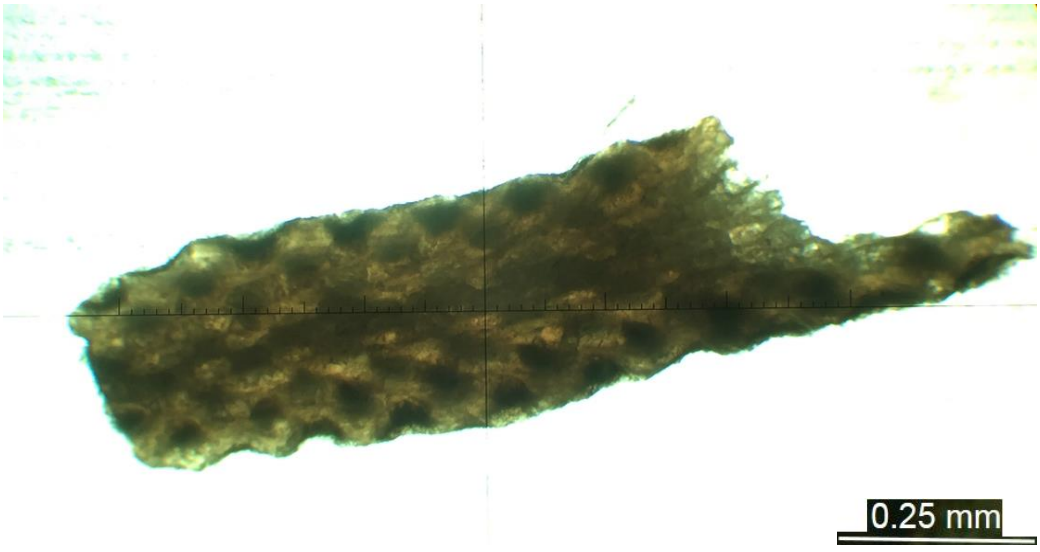

Figure 67. Thin-section from well 15-093-20793

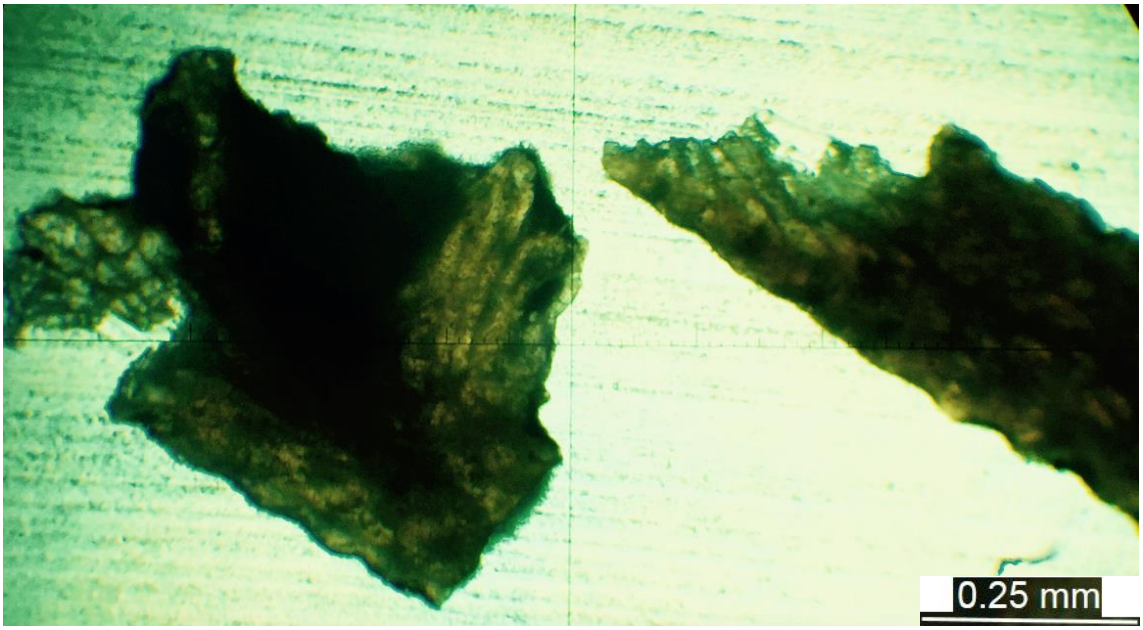

Figure 68. Thin-section from well 15-093-20793.

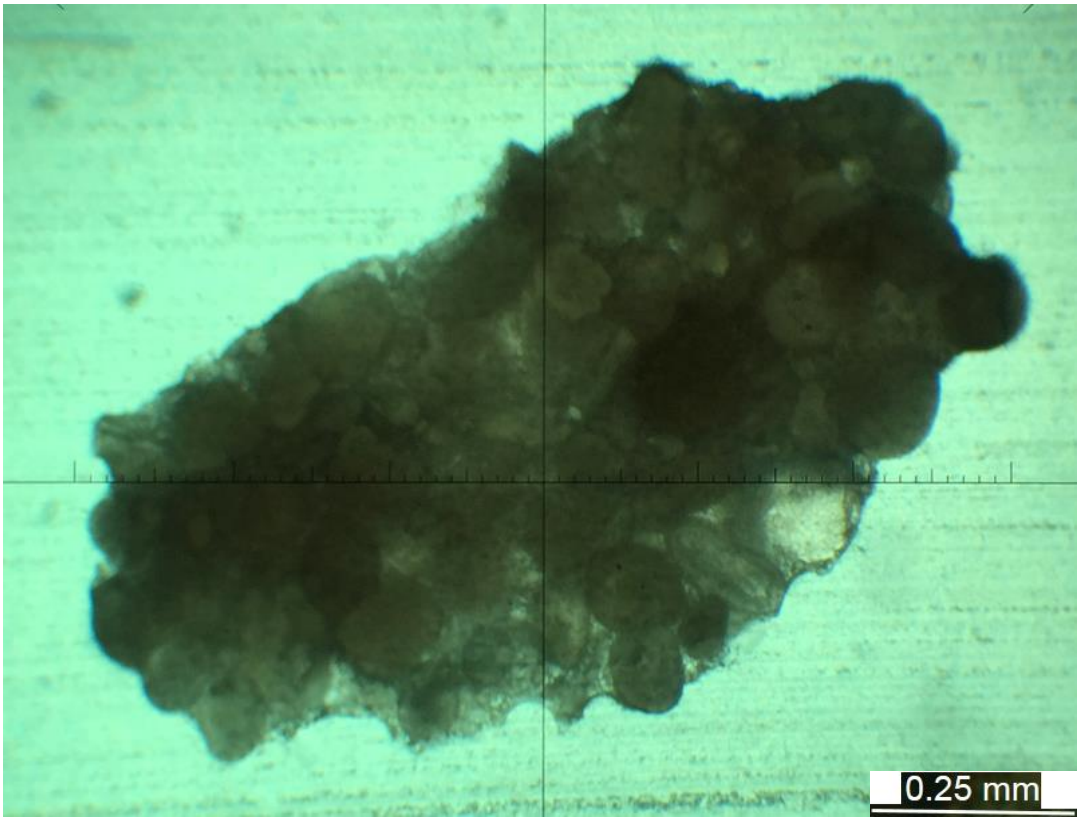

Figure 69. Thin-section from well 15-093-20793.

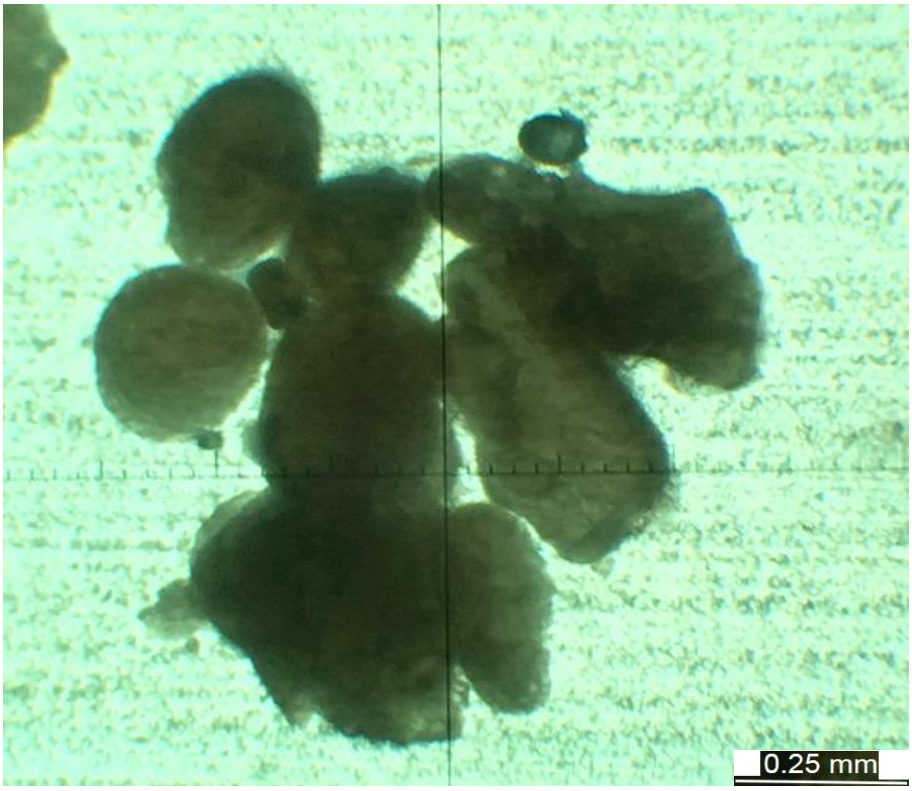

Figure 70. Thin-section from well 15-093-20793.

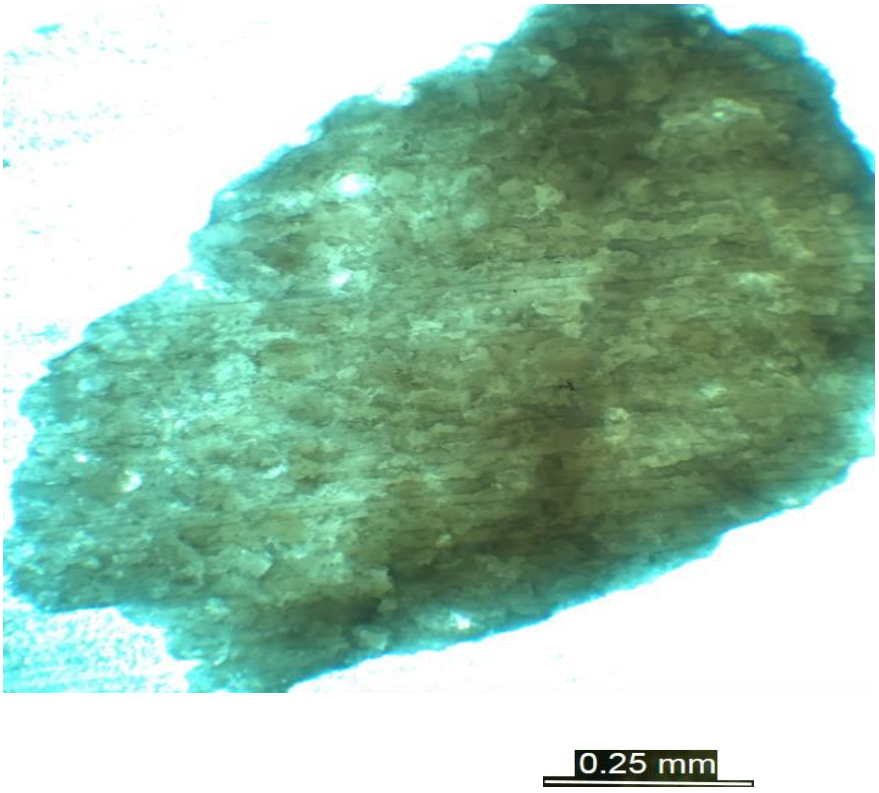

Figure 71. Thin-section from well 15-093-20813.

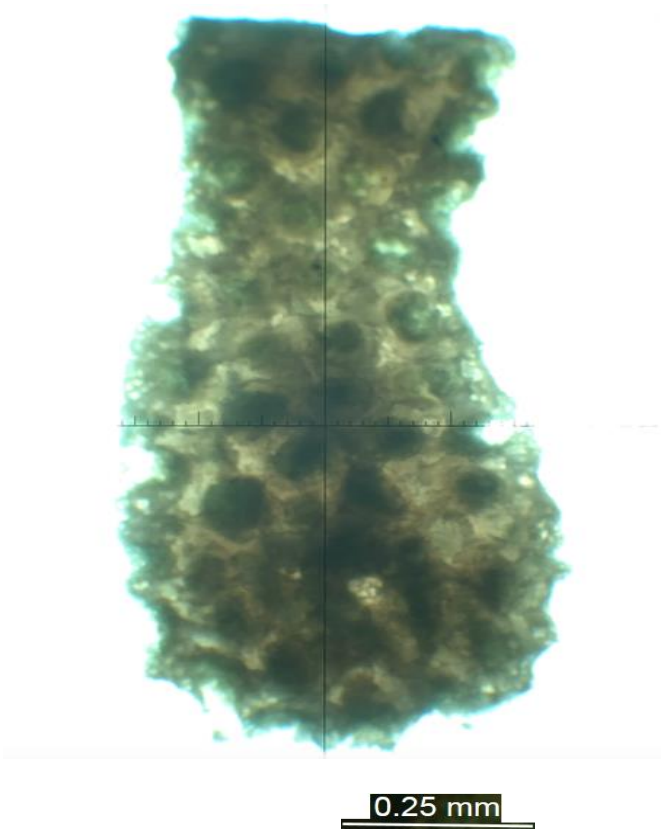

Figure 72. Thin-section from well 15-093-20813.

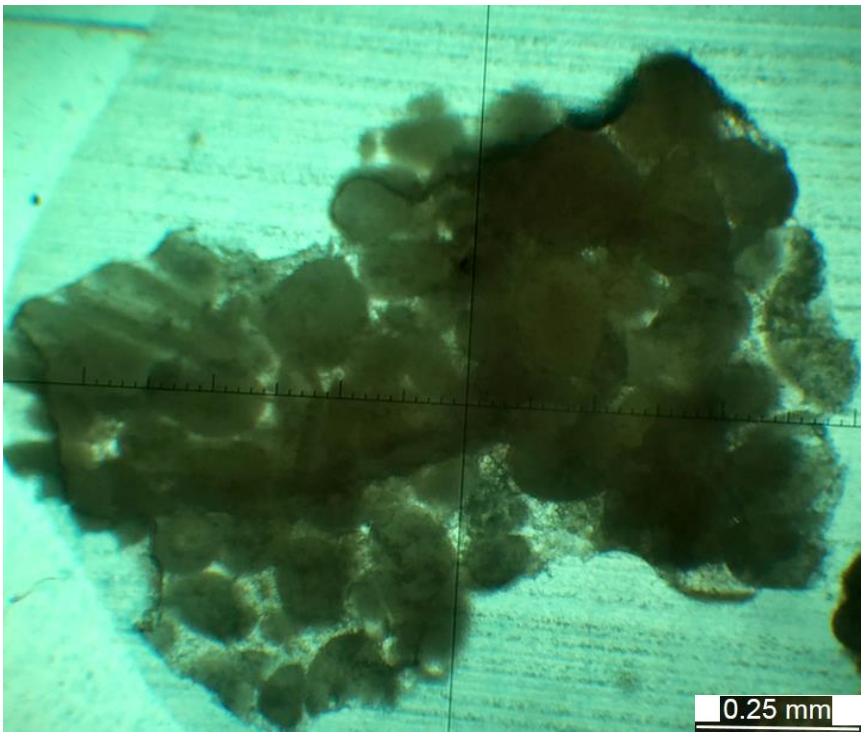

Figure 73. Thin section from well 15-093-20813.

Appendix C – Neural Network Predictions

Table 4 Neural network predictions for wells 15-093-20813, 20799, and 20793.

15-093-20813		15-093-20799		15-093-20793	
DEPTH	Pred.Facies	DEPTH	Pred.Facies	DEPTH	Pred.Facies
4790	3	4790	3	4787	3
4790.5	3	4790.5	3	4787.5	3
4791	3	4791	3	4788	3
4791.5	3	4791.5	3	4788.5	5
4792	3	4792	3	4789	5
4792.5	3	4792.5	3	4789.5	5
4793	3	4793	3	4790	5
4793.5	3	4793.5	3	4790.5	3
4794	3	4794	3	4791	3
4794.5	3	4794.5	5	4791.5	5
4795	3	4795	5	4792	5
4795.5	5	4795.5	5	4792.5	5
4796	5	4796	5	4793	5
4796.5	5	4796.5	5	4793.5	5
4797	3	4797	5	4794	5
4797.5	3	4797.5	5	4794.5	5
4798	3	4798	3	4795	5
4798.5	3	4798.5	3	4795.5	5
4799	3	4799	3	4796	5
4799.5	3	4799.5	3	4796.5	5
4800	3	4800	3	4797	5
4800.5	3	4800.5	5	4797.5	5
4801	3	4801	5	4798	5
4801.5	3	4801.5	5	4798.5	5
4802	3	4802	3	4799	5
4802.5	3	4802.5	5	4799.5	5
4803	3	4803	5	4800	5
4803.5	3	4803.5	5	4800.5	5
4804	3	4804	5	4801	5
4804.5	3	4804.5	5	4801.5	5
4805	3	4805	5	4802	5
4805.5	3	4805.5	5	4802.5	5
4806	3	4806	5	4803	5
4806.5	3	4806.5	5	4803.5	5

4807	3	4807	5	4804	5
4807.5	3	4807.5	5	4804.5	5
4808	3	4808	5	4805	5
4808.5	3	4808.5	3	4805.5	5
4809	3	4809	3	4806	5
4809.5	3	4809.5	3	4806.5	5
4810	3	4810	3	4807	5
4810.5	3	4810.5	3	4807.5	5
4811	3	4811	3	4808	5
4811.5	3	4811.5	3	4808.5	5
4812	3	4812	3	4809	5
4812.5	3	4812.5	3	4809.5	3
4813	3	4813	3	4810	3
4813.5	3	4813.5	3	4810.5	3
4814	3	4814	3	4811	3
4814.5	3	4814.5	3	4811.5	3
4815	3	4815	3	4812	3
4815.5	3	4815.5	3	4812.5	3
4816	3	4816	3	4813	3
4816.5	3	4816.5	3	4813.5	3
4817	5	4817	3	4814	3
4817.5	5	4817.5	3	4814.5	3
4818	5	4818	3	4815	3
4818.5	3	4818.5	3	4815.5	3
4819	3	4819	3	4816	3
4819.5	3	4819.5	3	4816.5	3
4820	3	4820	3	4817	3
4820.5	3	4820.5	3	4817.5	3
4821	3	4821	3	4818	3
4821.5	3	4821.5	3	4818.5	3
4822	3	4822	3	4819	5
4822.5	3	4822.5	3	4819.5	5
4823	3	4823	3	4820	3
4823.5	3	4823.5	3	4820.5	3
4824	3	4824	3	4821	3
4824.5	3	4824.5	3	4821.5	3
4825	3	4825	3	4822	3
4825.5	3	4825.5	3	4822.5	3
4826	3	4826	3	4823	3

4826.5	3	4826.5	3	4823.5	5
4827	3	4827	3	4824	5
4827.5	3	4827.5	3	4824.5	5
4828	3	4828	3	4825	5
4828.5	3	4828.5	3	4825.5	5
4829	3	4829	3	4826	3
4829.5	3	4829.5	5	4826.5	3
4830	3	4830	5	4827	3
4830.5	3	4830.5	3	4827.5	3
4831	3	4831	3	4828	3
4831.5	3	4831.5	3	4828.5	3
4832	4	4832	3	4829	3
4832.5	4	4832.5	3	4829.5	3
4833	4	4833	3	4830	3
4833.5	4	4833.5	3	4830.5	3
4834	4	4834	3	4831	3
4834.5	4	4834.5	3	4831.5	3
4835	4	4835	3	4832	3
4835.5	4	4835.5	3	4832.5	3
4836	4	4836	3	4833	3
4836.5	4	4836.5	3	4833.5	3
4837	4	4837	3	4834	3
4837.5	4	4837.5	3	4834.5	5
4838	4	4838	3	4835	5
4838.5	4	4838.5	3	4835.5	5
4839	5	4839	3	4836	5
4839.5	5	4839.5	3	4836.5	5
4840	5	4840	3	4837	5
4840.5	5	4840.5	3	4837.5	5
4841	5	4841	3	4838	5
4841.5	5	4841.5	3	4838.5	5
4842	5	4842	3	4839	5
4842.5	5	4842.5	3	4839.5	5
4843	5	4843	3	4840	5
4843.5	5	4843.5	3	4840.5	5
4844	5	4844	3	4841	5
4844.5	5	4844.5	3	4841.5	5
4845	5	4845	3	4842	4
4845.5	5	4845.5	3	4842.5	4

4846	5	4846	3	4843	5
4846.5	5	4846.5	3	4843.5	5
4847	5	4847	3	4844	5
4847.5	5	4847.5	5	4844.5	5
4848	5	4848	5	4845	5
4848.5	3	4848.5	5	4845.5	5
4849	3	4849	5	4846	3
4849.5	3	4849.5	5	4846.5	3
4850	3	4850	5	4847	3
4850.5	3	4850.5	3	4847.5	2
4851	5	4851	3	4848	2
4851.5	5	4851.5	3	4848.5	2
4852	3	4852	3	4849	2
4852.5	3	4852.5	3	4849.5	4
4853	3	4853	3	4850	4
4853.5	3	4853.5	3	4850.5	4
4854	3	4854	3	4851	4
4854.5	3	4854.5	3	4851.5	5
4855	3	4855	3	4852	5
4855.5	3	4855.5	5	4852.5	3
4856	3	4856	5	4853	3
4856.5	3	4856.5	5	4853.5	3
4857	3	4857	5	4854	3
4857.5	3	4857.5	5	4854.5	4
4858	5	4858	3	4855	4
4858.5	5	4858.5	3	4855.5	4
4859	5	4859	3	4856	4
4859.5	5	4859.5	3	4856.5	4
4860	5	4860	3	4857	4
4860.5	5	4860.5	3	4857.5	4
4861	5	4861	3	4858	3
4861.5	5	4861.5	3	4858.5	3
4862	5	4862	3	4859	3
4862.5	5	4862.5	3	4859.5	3
4863	5	4863	3	4860	3
4863.5	3	4863.5	3	4860.5	3
4864	3	4864	5	4861	3
4864.5	3	4864.5	5	4861.5	3
4865	3	4865	5	4862	3

4865.5	3	4865.5	5	4862.5	3
4866	3	4866	5	4863	3
4866.5	5	4866.5	5	4863.5	3
4867	5	4867	5	4864	3
4867.5	5	4867.5	5	4864.5	3
4868	5	4868	5	4865	3
4868.5	5	4868.5	5	4865.5	3
4869	5	4869	5	4866	3
4869.5	5	4869.5	5	4866.5	3
4870	5	4870	5	4867	3
4870.5	5	4870.5	5	4867.5	3
4871	5	4871	3	4868	3
4871.5	5	4871.5	3	4868.5	3
4872	5	4872	5	4869	3
4872.5	5	4872.5	5	4869.5	3
4873	5	4873	5	4870	3
4873.5	5	4873.5	5	4870.5	3
4874	5	4874	5	4871	3
4874.5	3	4874.5	5	4871.5	3
4875	3	4875	5	4872	3
4875.5	3	4875.5	5	4872.5	4
4876	3	4876	5	4873	4
4876.5	3	4876.5	5	4873.5	4
4877	3	4877	5	4874	4
4877.5	5	4877.5	5	4874.5	4
4878	5	4878	5	4875	2
4878.5	5	4878.5	5	4875.5	2
4879	5	4879	5	4876	4
4879.5	5	4879.5	5	4876.5	4
4880	5	4880	5	4877	4
4880.5	5	4880.5	5	4877.5	4
4881	5	4881	5	4878	4
4881.5	5	4881.5	5	4878.5	4
4882	5	4882	5	4879	4
4882.5	3	4882.5	5	4879.5	4
4883	3	4883	5	4880	4
4883.5	3	4883.5	5	4880.5	4
4884	3	4884	5	4881	4
4884.5	3	4884.5	5	4881.5	4

4885	3	4885	5	4882	4
4885.5	3	4885.5	5	4882.5	4
4886	3	4886	5	4883	4
4886.5	3	4886.5	5	4883.5	3
4887	3	4887	5	4884	3
4887.5	3	4887.5	5	4884.5	3
4888	3	4888	5	4885	3
4888.5	3	4888.5	5	4885.5	3
4889	3	4889	5	4886	3
4889.5	3	4889.5	5	4886.5	3
4890	3	4890	5	4887	3
4890.5	3	4890.5	5	4887.5	5
4891	3	4891	5	4888	5
4891.5	3	4891.5	3	4888.5	5
4892	3	4892	3	4889	5
4892.5	3	4892.5	3	4889.5	5
4893	3	4893	3	4890	5
4893.5	3	4893.5	3	4890.5	5
4894	3	4894	3	4891	5
4894.5	3	4894.5	3	4891.5	3
4895	3	4895	3	4892	3
4895.5	3	4895.5	3	4892.5	3
4896	3	4896	3	4893	3
4896.5	3	4896.5	3	4893.5	3
4897	3	4897	3	4894	5
4897.5	3	4897.5	3	4894.5	5
4898	3	4898	3	4895	5
4898.5	5	4898.5	3	4895.5	3
4899	5	4899	3	4896	3
4899.5	5	4899.5	3	4896.5	3
4900	5	4900	3	4897	3
4900.5	3	4900.5	3	4897.5	3
4901	3	4901	3	4898	5
4901.5	3	4901.5	3	4898.5	5
4902	3	4902	3	4899	5
4902.5	3	4902.5	3	4899.5	5
4903	3	4903	3	4900	5
4903.5	3	4903.5	3	4900.5	5
4904	3	4904	3	4901	5

4904.5	3	4904.5	3	4901.5	5
4905	3	4905	3	4902	5
4905.5	3	4905.5	3	4902.5	5
4906	3	4906	3	4903	5
4906.5	3	4906.5	3	4903.5	5
4907	3	4907	3	4904	5
4907.5	3	4907.5	3	4904.5	5
4908	3	4908	3	4905	5
4908.5	3	4908.5	3	4905.5	5
4909	3	4909	3	4906	5
4909.5	3	4909.5	3	4906.5	5
4910	3	4910	3	4907	5
4910.5	3	4910.5	3	4907.5	5
4911	3	4911	3	4908	5
4911.5	3	4911.5	3	4908.5	5
4912	3	4912	3	4909	5
4912.5	3	4912.5	3	4909.5	5
4913	3	4913	3	4910	5
4913.5	3	4913.5	3	4910.5	5
4914	3	4914	3	4911	5
4914.5	3	4914.5	3	4911.5	5
4915	3	4915	3	4912	3
4915.5	3	4915.5	3	4912.5	3
4916	5	4916	3	4913	3
4916.5	5	4916.5	3	4913.5	3
4917	5	4917	3	4914	3
4917.5	3	4917.5	3	4914.5	3
4918	3	4918	3	4915	3
4918.5	3	4918.5	3	4915.5	3
4919	3	4919	3	4916	3
4919.5	3	4919.5	3	4916.5	3
4920	3	4920	3	4917	3
4920.5	3	4920.5	3	4917.5	3
4921	3	4921	3	4918	3
4921.5	3	4921.5	3	4918.5	3
4922	3	4922	3	4919	3
4922.5	3	4922.5	3	4919.5	3
4923	3	4923	3	4920	3
4923.5	3	4923.5	3	4920.5	3

4924	3	4924	3	4921	3
4924.5	3	4924.5	3	4921.5	3
4925	3	4925	3	4922	3
4925.5	3	4925.5	3	4922.5	3
4926	3	4926	3	4923	5
4926.5	3	4926.5	3	4923.5	5
4927	3	4927	3	4924	5
4927.5	3	4927.5	3	4924.5	5
4928	3	4928	3	4925	5
4928.5	3	4928.5	3	4925.5	5
4929	3	4929	3	4926	5
4929.5	3	4929.5	3	4926.5	5
4930	3	4930	3	4927	5
4930.5	3	4930.5	3	4927.5	5
4931	3	4931	3	4928	5
4931.5	3	4931.5	3	4928.5	5
4932	3	4932	3	4929	5
4932.5	3	4932.5	3	4929.5	4
4933	3	4933	3	4930	3
4933.5	3	4933.5	5	4930.5	3
4934	3	4934	5	4931	4
4934.5	3	4934.5	5	4931.5	3
4935	3	4935	5	4932	3
4935.5	3	4935.5	3	4932.5	3
4936	3	4936	3	4933	3
4936.5	3	4936.5	3	4933.5	3
4937	5	4937	3	4934	3
4937.5	3	4937.5	3	4934.5	3
4938	3	4938	5	4935	3
4938.5	3	4938.5	5	4935.5	3
4939	3	4939	5	4936	3
4939.5	5	4939.5	5	4936.5	3
4940	5	4940	5	4937	5
4940.5	5	4940.5	5	4937.5	5
4941	5	4941	5	4938	3
4941.5	5	4941.5	5	4938.5	3
4942	3	4942	5	4939	3
4942.5	3	4942.5	5	4939.5	3
4943	3	4943	5	4940	3

4943.5	3	4943.5	5	4940.5	3
4944	3	4944	5	4941	3
4944.5	5	4944.5	5	4941.5	3
4945	5	4945	5	4942	3
4945.5	5	4945.5	5	4942.5	3
4946	5	4946	5	4943	3
4946.5	5	4946.5	5	4943.5	3
4947	5	4947	5	4944	3
4947.5	5	4947.5	5	4944.5	3
4948	5	4948	5	4945	3
4948.5	5	4948.5	3	4945.5	3
4949	5	4949	3	4946	3
4949.5	5	4949.5	3	4946.5	3
4950	5	4950	3	4947	3
4950.5	5	4950.5	3	4947.5	3
4951	3	4951	3	4948	3
4951.5	3	4951.5	3	4948.5	3
4952	3	4952	3	4949	3
4952.5	3	4952.5	3	4949.5	3
4953	3	4953	3	4950	3
4953.5	3	4953.5	3	4950.5	3
4954	3	4954	3	4951	3
4954.5	3	4954.5	3	4951.5	3
4955	3	4955	3	4952	3
4955.5	3	4955.5	3	4952.5	3
4956	3	4956	3	4953	3
4956.5	3	4956.5	3	4953.5	3
4957	5	4957	3	4954	3
4957.5	5	4957.5	3	4954.5	3
4958	5	4958	3	4955	3
4958.5	5	4958.5	3	4955.5	3
4959	5	4959	3	4956	5
4959.5	5	4959.5	3	4956.5	5
4960	3	4960	3	4957	5
4960.5	3	4960.5	3	4957.5	5
4961	5	4961	3	4958	5
4961.5	5	4961.5	3	4958.5	5
4962	5	4962	3	4959	5
4962.5	5	4962.5	3	4959.5	5

4963	5	4963	3	4960	4
4963.5	5	4963.5	3	4960.5	4
4964	5	4964	3	4961	4
4964.5	5	4964.5	3	4961.5	4
4965	3	4965	3	4962	4
4965.5	3	4965.5	3	4962.5	4
4966	3	4966	3	4963	5
4966.5	3	4966.5	3	4963.5	5
4967	3	4967	3	4964	5
4967.5	5	4967.5	3	4964.5	5
4968	5	4968	3	4965	5
4968.5	5	4968.5	3	4965.5	5
4969	5	4969	3	4966	3
4969.5	5	4969.5	3	4966.5	3
4970	5	4970	3	4967	3
4970.5	5	4970.5	3	4967.5	3
4971	5	4971	3	4968	5
4971.5	5	4971.5	3	4968.5	5
4972	5	4972	3	4969	5
4972.5	5	4972.5	3	4969.5	3
4973	5	4973	3	4970	3
4973.5	5	4973.5	3	4970.5	3
4974	3	4974	3	4971	3
4974.5	3	4974.5	3	4971.5	3
4975	3	4975	3	4972	3
4975.5	3	4975.5	3	4972.5	5
4976	3	4976	3	4973	5
4976.5	3	4976.5	3	4973.5	3
4977	5	4977	3	4974	3
4977.5	5	4977.5	3	4974.5	3
4978	5	4978	3	4975	3
4978.5	5	4978.5	3	4975.5	3
4979	5	4979	3	4976	3
4979.5	5	4979.5	5	4976.5	3
4980	3	4980	5	4977	3
4980.5	5	4980.5	5	4977.5	3
4981	5	4981	5	4978	3
4981.5	5	4981.5	3	4978.5	3
4982	5	4982	3	4979	3

4982.5	3	4982.5	3	4979.5	3
4983	3	4983	3	4980	3
4983.5	3	4983.5	3	4980.5	3
4984	3	4984	3	4981	3
4984.5	3	4984.5	3	4981.5	3
4985	3	4985	3	4982	3
4985.5	3	4985.5	3	4982.5	3
4986	3	4986	3	4983	3
4986.5	3	4986.5	5	4983.5	3
4987	3	4987	5	4984	3
4987.5	3	4987.5	5	4984.5	3
4988	3	4988	5	4985	3
4988.5	3	4988.5	5	4985.5	3
4989	3	4989	5	4986	3
4989.5	3	4989.5	5	4986.5	3
4990	3	4990	5	4987	3
4990.5	3	4990.5	5	4987.5	3
4991	3	4991	3	4988	3
4991.5	3	4991.5	3	4988.5	3
4992	3	4992	3	4989	3
4992.5	3	4992.5	3	4989.5	3
4993	3	4993	3	4990	3
4993.5	3	4993.5	3	4990.5	3
4994	3	4994	3	4991	3
4994.5	3	4994.5	3	4991.5	3
4995	3	4995	3	4992	3
4995.5	3	4995.5	3	4992.5	3
4996	3	4996	3	4993	3
4996.5	3	4996.5	3	4993.5	3
4997	3	4997	3	4994	3
4997.5	3	4997.5	3	4994.5	3
4998	3	4998	3	4995	5
4998.5	3	4998.5	3	4995.5	5
4999	5	4999	3	4996	5
4999.5	5	4999.5	3	4996.5	5
5000	5	5000	3	4997	5
5000.5	5	5000.5	3	4997.5	5
5001	5	5001	3	4998	3
5001.5	5	5001.5	3	4998.5	3

5002	5	5002	3	4999	3
5002.5	3	5002.5	3	4999.5	3
5003	3	5003	3	5000	3
5003.5	3	5003.5	3	5000.5	3
5004	3	5004	3	5001	3
5004.5	3	5004.5	3	5001.5	3
5005	5	5005	3	5002	3
5005.5	5	5005.5	6	5002.5	3
5006	5	5016	5	5003	3
5006.5	5	5016.5	5	5003.5	3
5007	5	5017	5	5004	3
5007.5	6	5017.5	5	5004.5	3
5008	6	5018	5	5005	3
5008.5	6	5018.5	5	5005.5	3
5009	6	5019	5	5006	3
5009.5	6	5019.5	5	5006.5	3
5010	6	5020	5	5007	3
5010.5	6	5020.5	5	5007.5	3
5011	6	5021	5	5008	3
5011.5	6	5021.5	5	5008.5	3
5012	6	5022	5	5009	3
5012.5	6	5022.5	5	5009.5	3
5013	6	5023	3	5010	5
5013.5	6	5023.5	3	5010.5	5
5014	6	5024	3	5011	3
5014.5	6	5024.5	3	5011.5	3
5015	6	5025	3	5012	3
5015.5	6	5025.5	3	5012.5	3
5016	6	5026	3	5013	3
5016.5	6	5026.5	3	5013.5	3
5017	6	5027	3	5014	3
5017.5	6	5027.5	3	5014.5	3
5018	6	5028	3	5015	3
5018.5	6	5028.5	3	5015.5	3
5019	6	5029	3	5016	3
5019.5	6	5029.5	3	5016.5	3
5020	6	5030	3	5017	3
5020.5	6	5030.5	3	5017.5	5
5021	6	5031	3	5018	3

5021.5	6	5031.5	3	5018.5	3
5022	6	5032	3	5019	3
5022.5	6	5032.5	3	5019.5	3
5023	6	5033	3	5020	3
5023.5	6	5033.5	3	5020.5	3
5024	6	5034	5	5021	3
5024.5	6	5034.5	5	5021.5	3
5025	6	5035	3	5022	3
5025.5	6	5035.5	3	5022.5	3
5026	6	5036	3	5023	3
5026.5	6	5036.5	3	5023.5	3
5027	6	5037	3	5024	5
5027.5	6	5037.5	3	5024.5	5
5028	6	5038	3	5025	5
5028.5	6	5038.5	3	5025.5	5
5029	6	5039	3	5026	5
5026.5	5	5039.5	3	5026.5	5
5027	3	5040	5	5027	3
5027.5	3	5040.5	5	5027.5	3
5028	3	5041	3	5028	3
5028.5	3	5041.5	3	5028.5	3
5029	3	5042	3	5029	3
5029.5	3	5042.5	3	5029.5	3
5030	3	5043	3	5030	3
5030.5	3	5043.5	3	5030.5	3
5031	3	5044	3	5031	3
5031.5	3	5044.5	5	5031.5	3
5032	2	5045	5	5032	2
5032.5	4	5045.5	5	5032.5	4
5033	4	5046	5	5033	4
5033.5	4	5046.5	5	5033.5	4
5034	3	5047	3	5034	3
5034.5	3	5047.5	3	5034.5	3
5035	3	5048	3	5035	3
5035.5	3	5048.5	3	5035.5	3
5036	3	5049	3	5036	3
5036.5	3	5049.5	3	5036.5	3
5037	3	5050	3	5037	3
5037.5	3	5050.5	3	5037.5	3

5038	3	5051	3	5038	3
5038.5	3	5051.5	3	5038.5	3
5039	3	5052	5	5039	3
5039.5	3	5052.5	5	5039.5	3
5040	3	5053	5	5040	3
5040.5	3	5053.5	5	5040.5	3
5041	2	5054	5	5041	2
5041.5	4	5054.5	5	5041.5	4
5042	4	5055	5	5042	4
5055.5	5	5055.5	5	5055.5	5
5056	3	5056	3	5056	3
5056.5	3	5056.5	3	5056.5	3
5057	5	5057	5	5057	5
5057.5	5	5057.5	5	5057.5	5
5058	3	5058	3	5058	3
5058.5	3	5058.5	3	5058.5	3
5059	3	5059	3	5059	3
5059.5	3	5059.5	3	5059.5	3
5060	3	5060	3	5060	3
5060.5	3	5060.5	3	5060.5	3
5061	3	5061	3	5061	3
5061.5	3	5061.5	3	5061.5	3
5062	3	5062	3	5062	3
5062.5	3	5062.5	3	5062.5	3
5063	5	5063	5	5063	5
5063.5	5	5063.5	5	5063.5	5
5064	5	5064	5	5064	5
5064.5	5	5064.5	5	5064.5	5
5065	5	5065	5	5065	5
5065.5	5	5065.5	5	5065.5	5
5066	5	5066	5	5066	5
5066.5	3	5066.5	3	5066.5	3
5067	3	5067	3	5067	3
5067.5	3	5067.5	3	5067.5	3
5068	5	5068	5	5068	5
5068.5	5	5068.5	5	5068.5	5
5069	5	5069	5	5069	5
5069.5	5	5069.5	5	5069.5	5
5070	5	5070	5	5070	5

5070.5	5	5070.5	5	5070.5	5
5071	5	5071	5	5071	5
5071.5	5	5071.5	5	5071.5	5
5072	5	5072	5	5072	5
5072.5	5	5072.5	5	5072.5	5
5073	5	5073	5	5073	5
5073.5	5	5073.5	5	5073.5	5
5074	5	5074	5	5074	5
5074.5	5	5074.5	5	5074.5	5
5075	5	5075	5	5075	5
5075.5	5	5075.5	5	5075.5	5
5076	5	5076	5	5076	5
5076.5	5	5076.5	5	5076.5	5
5077	5	5077	5	5077	5
5077.5	5	5077.5	5	5077.5	5
5078	5	5078	5	5078	5
5078.5	5	5078.5	5	5078.5	5
5079	5	5079	5	5079	5
5079.5	5	5079.5	5	5079.5	5
5080	5	5080	5	5080	5
5080.5	5	5080.5	5	5080.5	5
5081	3	5081	3	5081	3
5081.5	3	5081.5	3	5081.5	3
5082	3	5082	3	5082	3
5082.5	5	5082.5	5	5082.5	5
5083	5	5083	5	5083	5
5083.5	5	5083.5	5	5083.5	5
5084	5	5084	5	5084	5
5084.5	5	5084.5	5	5084.5	5
5085	5	5085	5	5085	5
5085.5	5	5085.5	5	5085.5	5
5086	5	5086	5	5086	5
5086.5	3	5086.5	3	5086.5	3
5087	3	5087	3	5087	3
5087.5	3	5087.5	3	5087.5	3
5088	3	5088	3	5088	3
5088.5	3	5088.5	3	5088.5	3
5089	3	5089	3	5089	3

Table 5 Neural network predictions for wells 15-093-20156, and 20778.

15-093-20156		15-093-20778	
DEPTH	Pred.Facies	DEPTH	Pred.Facies
4840.5	4	4840.5	5
4841	4	4841	5
4841.5	4	4841.5	5
4842	4	4842	5
4842.5	4	4842.5	5
4843	4	4843	5
4843.5	4	4843.5	5
4844	4	4844	5
4844.5	4	4844.5	5
4845	2	4845	5
4845.5	2	4845.5	4
4846	2	4846	4
4846.5	2	4846.5	4
4847	2	4847	4
4847.5	2	4847.5	5
4848	2	4848	5
4848.5	2	4848.5	5
4849	5	4849	5
4849.5	5	4849.5	3
4850	4	4850	5
4850.5	4	4850.5	5
4851	4	4851	5
4851.5	4	4851.5	5
4852	4	4852	5
4852.5	4	4852.5	5
4853	4	4853	4
4853.5	4	4853.5	4
4854	4	4854	4
4854.5	4	4854.5	4
4855	4	4855	4
4855.5	4	4855.5	4
4856	4	4856	4
4856.5	4	4856.5	4
4857	4	4857	4
4857.5	4	4857.5	5
4858	4	4858	5

4858.5	4	4858.5	5
4859	4	4859	5
4859.5	4	4859.5	5
4860	4	4860	5
4860.5	4	4860.5	4
4861	4	4861	4
4861.5	4	4861.5	4
4862	4	4862	5
4862.5	4	4862.5	5
4863	4	4863	5
4863.5	4	4863.5	5
4864	4	4864	3
4864.5	4	4864.5	3
4865	4	4865	3
4865.5	4	4865.5	3
4866	4	4866	3
4866.5	4	4866.5	3
4867	4	4867	3
4867.5	4	4867.5	3
4868	4	4868	3
4868.5	4	4868.5	3
4869	4	4869	4
4869.5	4	4869.5	4
4870	4	4870	4
4870.5	4	4870.5	4
4871	4	4871	4
4871.5	4	4871.5	4
4872	4	4872	4
4872.5	4	4872.5	4
4873	4	4873	4
4873.5	4	4873.5	4
4874	4	4874	4
4874.5	4	4874.5	4
4875	4	4875	2
4875.5	4	4875.5	3
4876	4	4876	3
4876.5	4	4876.5	3
4877	4	4877	3
4877.5	4	4877.5	3

4878	4	4878	3
4878.5	4	4878.5	3
4879	4	4879	3
4879.5	4	4879.5	3
4880	4	4880	3
4880.5	4	4880.5	3
4881	4	4881	2
4881.5	4	4881.5	4
4882	4	4882	4
4882.5	4	4882.5	3
4883	4	4883	3
4883.5	4	4883.5	3
4884	4	4884	3
4884.5	4	4884.5	4
4885	4	4885	4
4885.5	4	4885.5	4
4886	4	4886	4
4886.5	4	4886.5	4
4887	4	4887	4
4887.5	4	4887.5	2
4888	4	4888	2
4888.5	4	4888.5	4
4889	4	4889	4
4889.5	4	4889.5	4
4890	4	4890	4
4890.5	4	4890.5	4
4891	4	4891	4
4891.5	4	4891.5	4
4892	4	4892	4
4892.5	4	4892.5	3
4893	4	4893	3
4893.5	4	4893.5	3
4894	4	4894	3
4894.5	4	4894.5	3
4895	4	4895	3
4895.5	4	4895.5	3
4896	4	4896	3
4896.5	4	4896.5	3
4897	4	4897	3

4897.5	4	4897.5	3
4898	4	4898	3
4898.5	4	4898.5	3
4899	4	4899	3
4899.5	4	4899.5	3
4900	4	4900	4
4900.5	4	4900.5	4
4901	4	4901	2
4901.5	4	4901.5	2
4902	4	4902	2
4902.5	4	4902.5	2
4903	4	4903	3
4903.5	4	4903.5	2
4904	4	4904	2
4904.5	4	4904.5	2
4905	3	4905	2
4905.5	3	4905.5	2
4906	3	4906	4
4906.5	3	4906.5	2
4907	3	4907	2
4907.5	3	4907.5	3
4908	3	4908	2
4908.5	3	4908.5	2
4909	3	4909	2
4909.5	3	4909.5	2
4910	3	4910	2
4910.5	6	4910.5	4
4911	6	4911	4
4911.5	6	4911.5	4
4912	6	4912	4
4912.5	6	4912.5	3
4913	6	4913	3
4913.5	6	4913.5	3
4914	6	4914	3
4914.5	6	4914.5	3
4915	3	4915	3
4915.5	3	4915.5	3
4916	3	4916	4
4916.5	3	4916.5	3

4917	3	4917	3
4917.5	3	4917.5	3
4918	3	4918	3
4918.5	3	4918.5	3
4919	3	4919	3
4919.5	3	4919.5	3
4920	3	4920	3
4920.5	3	4920.5	2
4921	3	4921	4
4921.5	3	4921.5	4
4922	4	4922	4
4922.5	4	4922.5	4
4923	4	4923	4
4923.5	4	4923.5	4
4924	4	4924	4
4924.5	4	4924.5	4
4925	4	4925	4
4925.5	3	4925.5	4
4926	3	4926	4
4926.5	3	4926.5	4
4927	3	4927	4
4927.5	3	4927.5	4
4928	3	4928	4
4928.5	4	4928.5	4
4929	4	4929	4
4929.5	4	4929.5	4
4930	4	4930	4
4930.5	4	4930.5	4
4931	4	4931	3
4931.5	4	4931.5	3
4932	4	4932	3
4932.5	4	4932.5	3
4933	4	4933	3
4933.5	4	4933.5	3
4934	4	4934	3
4934.5	4	4934.5	3
4935	4	4935	3
4935.5	4	4935.5	2
4936	4	4936	2

4936.5	4	4936.5	4
4937	4	4937	4
4937.5	4	4937.5	4
4938	4	4938	3
4938.5	4	4938.5	3
4939	4	4939	3
4939.5	4	4939.5	3
4940	4	4940	3
4940.5	4	4940.5	3
4941	4	4941	3
4941.5	4	4941.5	3
4942	4	4942	3
4942.5	4	4942.5	3
4943	4	4943	3
4943.5	4	4943.5	3
4944	4	4944	3
4944.5	4	4944.5	3
4945	4	4945	2
4945.5	4	4945.5	4
4946	4	4946	3
4946.5	4	4946.5	3
4947	4	4947	3
4947.5	4	4947.5	3
4948	4	4948	3
4948.5	4	4948.5	3
4949	4	4949	3
4949.5	4	4949.5	3
4950	4	4950	3
4950.5	4	4950.5	3
4951	4	4951	3
4951.5	4	4951.5	3
4952	4	4952	3
4952.5	4	4952.5	3
4953	4	4953	2
4953.5	4	4953.5	2
4954	4	4954	2
4954.5	4	4954.5	3
4955	4	4955	3
4955.5	4	4955.5	2

4956	4	4956	4
4956.5	4	4956.5	4
4957	4	4957	4
4957.5	4	4957.5	4
4958	4	4958	3
4958.5	4	4958.5	5
4959	4	4959	5
4959.5	4	4959.5	5
4960	4	4960	5
4960.5	4	4960.5	3
4961	4	4961	3
4961.5	4	4961.5	3
4962	4	4962	3
4962.5	4	4962.5	3
4963	4	4963	3
4963.5	4	4963.5	3
4964	4	4964	3
4964.5	4	4964.5	3
4965	4	4965	3
4965.5	4	4965.5	3
4966	4	4966	3
4966.5	4	4966.5	3
4967	4	4967	4
4967.5	4	4967.5	4
4968	4	4968	4
4968.5	4	4968.5	4
4969	1	4969	4
4969.5	1	4969.5	4
4970	1	4970	4
4970.5	1	4970.5	4
4971	1	4971	3
4971.5	1	4971.5	3
4972	1	4972	3
4972.5	3	4972.5	3
4973	3	4973	3
4973.5	3	4973.5	3
4974	3	4974	3
4974.5	3	4974.5	3
4975	3	4975	3

4975.5	3	4975.5	3
4976	3	4976	2
4976.5	3	4976.5	2
4977	3	4977	2
4977.5	3	4977.5	2
4978	3	4978	2
4978.5	3	4978.5	3
4979	3	4979	3
4979.5	3	4979.5	3
4980	3	4980	3
4980.5	3	4980.5	3
4981	3	4981	3
4981.5	3	4981.5	3
4982	3	4982	3
4982.5	3	4982.5	3
4983	3	4983	3
4983.5	3	4983.5	3
4984	3	4984	3
4984.5	3	4984.5	3
4985	3	4985	3
4985.5	3	4985.5	3
4986	3	4986	3
4986.5	3	4986.5	3
4987	3	4987	3
4987.5	3	4987.5	3
4988	3	4988	3
4988.5	3	4988.5	3
4989	3	4989	3
4989.5	3	4989.5	3
4990	3	4990	3
4990.5	3	4990.5	3
4991	3	4991	3
4991.5	3	4991.5	2
4992	3	4992	2
4992.5	3	4992.5	2
4993	3	4993	2
4993.5	3	4993.5	2
4994	3	4994	2
4994.5	3	4994.5	3

4995	3	4995	3
4995.5	3	4995.5	3
4996	3	4996	3
4996.5	3	4996.5	3
4997	3	4997	3
4997.5	3	4997.5	2
4998	3	4998	2
4998.5	3	4998.5	2
4999	3	4999	3
4999.5	3	4999.5	3
5000	3	5000	3
		5000.5	3
		5001	3
		5001.5	3
		5002	5
		5002.5	5
		5003	3
		5003.5	3
		5004	3
		5004.5	3
		5005	3
		5005.5	3
		5006	3
		5006.5	5
		5007	5
		5007.5	5
		5008	3
		5008.5	3
		5009	3
		5009.5	3
		5010	3
		5010.5	3
		5011	3
		5011.5	3
		5012	3
		5012.5	3
		5013	3
		5013.5	3
		5014	3

5014.5	3
5015	3
5015.5	3
5016	3
5016.5	3
5017	3
5017.5	3
5018	3
5018.5	3
5019	3
5019.5	3
5020	3
5020.5	3
5021	3
5021.5	3
5022	3
5022.5	3
5023	3
5023.5	3
5024	3
5024.5	3
5025	3
5025.5	3
5026	3
5026.5	3
5027	3
5027.5	3
5028	3
5028.5	3
5029	3
5029.5	3
5030	3
5030.5	3
5031	3
5031.5	3
5032	3
5032.5	3
5033	3
5033.5	3

5034	3
5034.5	3
5035	3
5035.5	3
5036	3
5036.5	3
5037	3
5037.5	3
5038	3
5038.5	3
5039	3
5039.5	3
5040	3
5040.5	2
5041	4
5041.5	4
5042	2
5042.5	3
5043	3
5043.5	3
5044	3
5044.5	3
5045	4
5045.5	4
5046	4
5046.5	2
5047	2
5047.5	2
5048	4
5048.5	4
5049	4
5049.5	3
5050	3
5050.5	3
5051	3
5051.5	3
5052	3
5052.5	3
5053	3

5053.5	3
5054	3
5054.5	3
5055	3
5055.5	3
5056	3
5056.5	2
5057	4
5057.5	4
5058	4
5058.5	5
5059	5
5059.5	3
5060	3
5060.5	3
5061	3
5061.5	3
5062	3
5062.5	3
5063	3
5063.5	3
5064	5
5064.5	3
5065	3
5065.5	3
5066	3
5066.5	3
5067	3
5067.5	3
5068	3
5068.5	3
5069	3
5069.5	3
5070	3
5070.5	3
5071	3
5071.5	3
5072	3
5072.5	3

5073	3
5073.5	3
5074	3
5074.5	3
5075	3
5075.5	3
5076	3
5076.5	3
5077	3
5077.5	3
5078	3
5078.5	4
5079	4
5079.5	4
5080	4
5080.5	4